

**REGIONAL DIFFERENCES IN Na^+/K^+ -ATPASE EXPRESSION IN THE
MOUSE AND RAT BRAIN**

by

Michael Golod

A thesis submitted to the Centre for Neuroscience Studies

In conformity with the requirements for
the degree of Master of Science

Queen's University

Kingston, Ontario, Canada

(June, 2018)

Copyright © Michael Golod, 2018

Abstract

Insufficient blood flow to the brain generates widespread neurological damage, yet not all brain regions are similarly vulnerable to ischemic injury. During stroke, failure of the Na⁺/K⁺-ATPase generates a robust anoxic depolarization that silences neurons in higher brain regions such as the neocortex, whereas the brainstem is capable of recovery and is therefore less sensitive to ischemic damage. The alpha subunit of the Na⁺/K⁺-ATPase is primarily responsible for the ion transport rate, particularly the $\alpha 1$ and $\alpha 3$ isoforms which are expressed in neurons. Based on prior evidence that $\alpha 3$ isoform mRNA expression is proportionally greater in the brainstem whereas $\alpha 1$ isoform mRNA expression predominates in higher brain regions such as the neocortex and cerebellum, this study used immunoblotting to investigate the distribution of Na⁺/K⁺-ATPase $\alpha 1$ and $\alpha 3$ isoform proteins in the mouse and rat brain. It was determined that $\alpha 1$ isoform expression is higher in the neocortex and cerebellum, whereas $\alpha 3$ isoform expression is higher in the brainstem. In addition, the striatum and hippocampus express similar amounts of both the $\alpha 1$ and $\alpha 3$ isoforms of the Na⁺/K⁺-ATPase, although this may be due to a heterogeneous isoform distribution pattern as suggested by pilot immunohistochemical experiments. To assess whether elevated oxidative stress generates adaptive changes in Na⁺/K⁺-ATPase expression, isoform distribution was studied in the *Aldh2*^{-/-} mouse model of oxidative stress, as well as in mice subjected to a chronic unpredictable stress protocol. No changes in Na⁺/K⁺-ATPase isoform expression were detected in these cohorts, except for a small but significant decrease in $\alpha 1$ isoform expression in the cerebellum of chronically-stressed *Aldh2*^{-/-} mice compared to unstressed wild-type mice. To assess whether transient ischemia generates adaptive changes in Na⁺/K⁺-ATPase expression, isoform distribution was studied

in rats subjected to 90 minutes of middle cerebral artery occlusion followed by 24 hours of recovery. Pilot immunoblotting experiments suggested an increase in the expression of both $\alpha 1$ and $\alpha 3$ isoforms of the Na^+/K^+ -ATPase in the infarcted striatum, indicating that the Na^+/K^+ -ATPase may be implicated in selective neuronal vulnerability to ischemia, but not oxidative stress. This may help identify molecular targets for improving higher brain survival post stroke.

Co-Authorship

The research presented in this thesis, including experimental work, data analysis, and manuscript preparation, was performed by Michael Golod, under the co-supervision of Dr. R. David Andrew and Dr. Brian M. Bennett.

Acknowledgements

This work was supported by the Heart and Stroke Foundation of Canada and the Canadian Institutes for Health Research. Kathleen A. Harrison performed all rat MCAo surgeries and established stroke model characteristics together with Jesse Kelly. Diane Anderson bred and maintained the mouse colony and Chloe Lowry established the chronic unpredictable stress (CUS) cohort of mice. Contributions to experimental design and interpretation of data were made by Dr. R. David Andrew, Dr. Brian M. Bennett, Dr. Douglas J. Cook, and Dr. Albert Y. Jin.

I am sincerely grateful to all of the following individuals who contributed to the production of this thesis. I would especially like to thank Dr. David Andrew and Dr. Brian Bennett for their continued support and guidance throughout my two years working in their laboratories, as well as Dr. Douglas J. Cook and Dr. Albert Y. Jin for their advice and encouragement when I needed it most. I would also like to thank Chloe Lowry for her collaboration on this project, as well as Kathleen Harrison and Jesse Kelly for welcoming me onto their research team and investing their time to help make this project possible. I am also grateful to Diane Anderson, Lihua Xue, Peter Gagolewicz, Tori Donovan, Ahmed Elharram, and Dr. Yat Tse for their continued advice on my project and technical assistance in the laboratory.

A special thanks to Nicole Czegledy and Alex Platt for sharing in the challenges of graduate school, for brightening late nights in the office, and for helping me keep the big picture in mind. Finally, I would like to thank my parents and siblings for all their love and support during my studies – without you, none of this would have been possible.

Table of Contents

Abstract	ii
Co-Authorship	iv
Acknowledgements	v
List of Figures	viii
List of Tables	x
List of Abbreviations	xi
Chapter 1 Introduction and Literature Review	1
1.1 Brain Ischemia and Stroke	1
1.1.1 Types of Stroke.....	2
1.1.2 Selective Vulnerability to Ischemia.....	3
1.1.3 Ischemic Stroke Pathophysiology	4
1.2 Spreading Depolarization.....	10
1.2.1 Types of Spreading Depolarization	10
1.2.2 Anoxic Depolarization.....	11
1.3 The Na ⁺ /K ⁺ -ATPase	12
1.4 The <i>Aldh2</i> ^{-/-} Mouse Model of Oxidative Stress	18
1.5 Chronic Stress	19
1.6 Objective and Hypotheses.....	21
Chapter 2 Materials and Methods.....	23
2.1 Animals	23
2.1.1 <i>Aldh2</i> ^{-/-} Model of Oxidative Stress	23
2.1.2 Chronic Unpredictable Stress (CUS) Mouse Model	23
2.1.3 Middle Cerebral Artery Occlusion (MCAo) Rat Model of Stroke.....	27
2.2 Tissue Collection.....	31
2.2.1 <i>Aldh2</i> ^{-/-} and CUS Protocol Mice.....	31
2.2.2 MCAo Rats	31
2.3 Biochemical Analysis.....	32
2.3.1 Fluorescent Multiplex Immunoblotting	32
2.3.2 Immunohistochemistry	34
2.4 Statistical Analysis for Immunoblotting	35
Chapter 3 Results	36
3.1 Multiplex Immunoblotting	36
3.2 Total Protein Normalization.....	36
3.3 Na ⁺ /K ⁺ -ATPase α 1 Isoform Expression.....	39

3.3.1 Wild-type Mice Subjected to Chronic Unpredictable Stress	39
3.3.2 <i>Aldh2</i> ^{-/-} Mice Subjected to Chronic Unpredictable Stress	39
3.3.3 Naïve Rats.....	44
3.3.4 Rats Subjected to Transient Middle Cerebral Artery Occlusion	44
3.4 Na ⁺ /K ⁺ -ATPase α3 Isoform Expression.....	48
3.4.1 Wild-type Mice Subjected to Chronic Unpredictable Stress.....	48
3.4.2 <i>Aldh2</i> ^{-/-} Mice Subjected to Chronic Unpredictable Stress	48
3.4.3 Naïve Rats.....	53
3.4.4 Rats Subjected to Transient Middle Cerebral Artery Occlusion	53
3.5 Na ⁺ /K ⁺ -ATPase α1/α3 Isoform Expression Ratio.....	57
3.5.1 Wild-type Mice Subjected to Chronic Unpredictable Stress.....	57
3.5.2 <i>Aldh2</i> ^{-/-} Mice Subjected to Chronic Unpredictable Stress	57
3.5.3 Naïve Rats.....	62
3.5.4 Rats Subjected to Transient Middle Cerebral Artery Occlusion	62
3.5.5 Pilot Immunohistochemistry of Naïve Rats.....	66
Chapter 4 Discussion	68
4.1 Expression in Naïve Mice and Rats	68
4.1.1 The Striatum	69
4.1.2 The Hippocampus.....	70
4.2 Oxidative Stress Cohorts	73
4.3 Ischemic Cohort	75
4.3.1 Infarction in the striatum	75
4.3.2 Infarction in the neocortex.....	76
4.3.3 Neuroprotective effect of altered Na ⁺ /K ⁺ -ATPase alpha isoform expression..	76
4.4 Study Assumptions.....	77
4.5 Study Limitations	78
4.5.1 Study Design.....	78
4.5.2 Animal Housing.....	79
4.5.3 Dissection Technique	80
4.5.4 Animal Models	81
4.6 Future Directions.....	82
Chapter 5 Conclusion.....	84
References.....	86
Appendix.....	95

List of Figures

Figure 1. Regional Na ⁺ /K ⁺ -ATPase α1 isoform mRNA expression in the mouse brain. .	16
Figure 2. Regional Na ⁺ /K ⁺ -ATPase α3 isoform mRNA expression in the mouse brain ..	17
Figure 3. Correlation of stroke volume and behavioural deficits 24 hours after reperfusion in rats undergoing transient MCAo.....	30
Figure 4. Multiplex immunoblot of Na ⁺ /K ⁺ -ATPase α1 and α3 isoform expression in the naïve mouse brain.	37
Figure 5. Total protein normalization using a UV302-activated non-protein moiety within TGX Stain-Free Gels.	38
Figure 6. Regional protein expression of the Na ⁺ /K ⁺ -ATPase α1 isoform in naïve and stressed wild-type mice.	40
Figure 7. Regional protein expression of the Na ⁺ /K ⁺ -ATPase α1 isoform in naïve and stressed <i>Aldh2</i> ^{-/-} mice.	41
Figure 8. Regional protein expression of the Na ⁺ /K ⁺ -ATPase α1 isoform in stressed wild-type and <i>Aldh2</i> ^{-/-} mice.	42
Figure 9. Regional protein expression of the Na ⁺ /K ⁺ -ATPase α1 isoform in unstressed wild-type and stressed <i>Aldh2</i> ^{-/-} mice.	43
Figure 10. Regional expression of the Na ⁺ /K ⁺ -ATPase α1 isoform in naïve rats.....	45
Figure 11. Regional protein expression of the Na ⁺ /K ⁺ -ATPase α1 isoform in control and infarcted tissue.	46
Figure 12. Regional protein expression of the Na ⁺ /K ⁺ -ATPase α1 isoform in non-infarcted and infarcted hemispheres of rats subjected to transient MCAo.	47
Figure 13. Regional protein expression of the Na ⁺ /K ⁺ -ATPase α3 isoform in naïve and stressed wild-type mice.....	49
Figure 14. Regional protein expression of the Na ⁺ /K ⁺ -ATPase α3 isoform in naïve and stressed <i>Aldh2</i> ^{-/-} mice.	50
Figure 15. Regional protein expression of the Na ⁺ /K ⁺ -ATPase α3 isoform in stressed wild-type and <i>Aldh2</i> ^{-/-} mice.....	51

Figure 16. Regional protein expression of the Na ⁺ /K ⁺ -ATPase α3 isoform in unstressed wild-type and stressed <i>Aldh2</i> ^{-/-} mice.	52
Figure 17. Regional protein expression of the Na ⁺ /K ⁺ -ATPase α3 isoform in the left and right hemispheres of naïve rats.	54
Figure 18. Regional protein expression of the Na ⁺ /K ⁺ -ATPase α3 isoform in control and infarcted tissue.	55
Figure 19. Regional protein expression of the Na ⁺ /K ⁺ -ATPase α3 isoform in non-infarcted and infarcted hemispheres of rats subjected to transient MCAo.	56
Figure 20. Regional Na ⁺ /K ⁺ -ATPase α1/α3 isoform ratios in naïve and stressed male (top) and female (bottom) wild-type mice.	58
Figure 21. Regional Na ⁺ /K ⁺ -ATPase α1/α3 isoform ratios in naïve and stressed male (top) and female (bottom) <i>Aldh2</i> ^{-/-} mice.	59
Figure 22. Regional Na ⁺ /K ⁺ -ATPase α1/α3 isoform ratios in male (top) and female (bottom) stressed wild-type and <i>Aldh2</i> ^{-/-} mice.	60
Figure 23. Regional Na ⁺ /K ⁺ -ATPase α1/α3 isoform ratios in male (top) and female (bottom) unstressed wild-type and stressed <i>Aldh2</i> ^{-/-} mice.	61
Figure 24. Regional Na ⁺ /K ⁺ -ATPase α1/α3 isoform ratios in naïve rats.	63
Figure 25. Regional Na ⁺ /K ⁺ -ATPase α1/α3 isoform ratios in naïve rats and rats subjected to transient MCA occlusion.	64
Figure 26. Regional Na ⁺ /K ⁺ -ATPase α1/α3 isoform ratios in infarcted and non-infarcted hemispheres of rats subjected to transient MCA occlusion.	65
Figure 27. Regional Na ⁺ /K ⁺ -ATPase α1 and α3 isoform expression in naïve rats.	67
Figure 28. Total protein activation showing loss of distinct bands in infarcted tissue.	95

List of Tables

Table 1. Stressors used in the Chronic Unpredictable Stress (CUS) protocol.....	25
Table 2. Schedule of the 28-day Chronic Unpredictable Stress (CUS) protocol.....	26
Table 3. The Bederson scale of ischemia-induced neurological impairment.	29

List of Abbreviations

aCSF	Artificial cerebrospinal fluid
AD	Anoxic depolarization
ALDH2, <i>Aldh2</i>	Aldehyde dehydrogenase 2
ANOVA	Analysis of variance
ATP	Adenosine triphosphate
BBB	Blood-brain barrier
BSA	Bovine serum albumin
CBF	Cerebral blood flow
CNS	Central nervous system
CSD	Cortical spreading depression
CUS	Chronic unpredictable stress
DNA	Deoxyribonucleic acid
DTT	Dithiothreitol
EDTA	Ethylenediaminetetraacetic acid
ETC	Electron transport chain
H ₂ O ₂	Hydrogen peroxide
ICP	Intracranial pressure
MCA	Middle cerebral artery
MCAo	Middle cerebral artery occlusion
MDA	Malondialdehyde
MELAS	Mitochondrial encephalomyopathy, lactic acidosis, and stroke-like episodes

MMP	Matrix metalloproteinase
mRNA	Messenger ribonucleic acid
Na ⁺ /K ⁺ pump	Na ⁺ /K ⁺ -ATPase
NADPH	Nicotinamide adenine dinucleotide phosphate
OGD	Oxygen-glucose deprivation
PBS	Phosphate-buffered saline
PCR	Polymerase chain reaction
PID	Peri-infarct depolarization
PMSF	Phenylmethylsulfonyl fluoride
pO ₂	Partial pressure of oxygen
PVDF	Polyvinylidene fluoride
ROS	Reactive oxygen species
RNS	Reactive nitrogen species
SD	Spreading depolarization
SDS	Sodium dodecyl sulfate
TBS	Tris-buffered saline
TIA	Transient ischemic attack
TSPP	Tetrasodium pyrophosphate
TTC	Tetrazolium chloride
UCP2	Uncoupling protein 2
UV	Ultraviolet
UV302	Ultraviolet light, 302 nm
4-HNE	4-hydroxy-2-nonenal

Chapter 1

Introduction and Literature Review

1.1 Brain Ischemia and Stroke

Stroke is a serious neurological condition characterized by disrupted blood flow to the brain, resulting in brain ischemia – an inadequate supply of oxygen and nutrients needed to meet the metabolic demands of cellular survival. Stroke is among the leading causes of long-term disability in North America, yet available treatments are often ineffective because they only address the restoration of cerebral blood flow, rather than the pathophysiological sequelae initiated by brain ischemia (Mozaffarian et al., 2016). Treatment is limited by a narrow time window of 3-4.5 hours after symptom onset, and requires exclusion of multiple confounding factors (Hacke et al., 2008). The prognosis of stroke largely depends on how quickly treatment is administered. Untreated patients lose an estimated 1.9 million neurons every minute, equivalent to 3.6 years of age-related neurodegeneration each hour (Saver, 2006). The heterogeneity of stroke location and severity as well as genetic differences between patients play a significant role in survival and give rise to a multitude of clinical outcomes.

Brain ischemia leads to pathophysiological changes at the cellular level, promoting neuronal death and the development of lesions within brain tissue. Such lesions have long-term consequences and may produce serious neurological deficits. Pathophysiological consequences begin at ischemic onset, persist after reperfusion, and can exacerbate damage in a process known as secondary ischemic injury (Siesjö and Siesjö, 1996). Secondary injury can arise from excitotoxicity, oxidative stress, inflammation, and blood-brain barrier dysfunction, as well as recruitment of neuroimmune and peripheral immune systems.

1.1.1 Types of Stroke

Occlusive stroke encompasses approximately 87% of stroke cases, and refers to an occlusion within the vasculature that deprives the brain of blood, and therefore oxygen and glucose (Beal, 2010). On the other hand, hemorrhagic stroke occurs from the rupture of a blood vessel, aneurysm, or arteriovenous malformation in the brain, leading to a rise in intracranial pressure (ICP) which also restricts blood flow to the brain. Below a threshold level, diminished blood supply is insufficient to meet metabolic demands, leading to cerebral infarction (Bandera et al., 2006). Stroke symptoms can be mimicked by transient ischemic attack (TIA), which temporarily decreases brain perfusion without causing widespread infarction but may eventually develop into a more severe ischemic stroke (Johnston, 2002). Although all categories of stroke lead to loss of neuronal tissue, it is of vital importance to diagnose stroke quickly for optimal treatment.

Ischemic stroke is further subdivided based on the amount of the brain impacted. Global ischemia affects the entire brain and is usually a consequence of hypoperfusion from cardiac arrest, while focal ischemia is most commonly triggered by an occlusion within a specific region of the cerebral vasculature, often from thromboembolism (Woodruff et al., 2011). The clinical syndrome of stroke varies greatly depending on occlusion location. Large-vessel stroke, such as middle cerebral artery occlusion (MCAo), impacts vast regions of the striatum and neocortex and can involve deep cerebral structures through branching arteries (Maas et al., 2009). This typically leads to neurological deficits in multiple modalities of brain function.

During stroke, the infarct core suffers the greatest loss of blood supply and undergoes rapid necrotic death, while the surrounding penumbral region receives some collateral blood supply, rendering it functionally silent but metabolically active (Woodruff

et al., 2011). Stroke must be treated within a few hours of symptom onset, with hyperacute treatments aiming to remove the vessel occlusion using endovascular therapy or thrombolysis. To reduce the risk of another stroke, stroke patients typically undergo secondary prevention with prophylactic anticoagulant or antithrombotic medications such as low-dose Aspirin. Even with reperfusion, secondary ischemic damage occurs over the hours and days following stroke, so the peri-infarct penumbra is a therapeutic target to mitigate damage following stroke (Siesjö and Siesjö, 1996).

Hemorrhagic stroke is considered more dangerous than ischemic stroke because vessel rupture allows arterial blood to leak into brain tissue or into the subarachnoid space, creating a space-occupying lesion that displaces venous blood and cerebrospinal fluid. This ‘mass effect’ increases intracranial pressure, which can cause a midline shift, brain herniation, or prevent blood flow to the brain. The devastating nature of intracranial hemorrhage causes widespread injury and pathophysiological changes in the brain that are challenging to assess.

1.1.2 Selective Vulnerability to Ischemia

Variations in neuronal phenotype generate a phenomenon known as selective vulnerability, which refers to intrinsic differences in sensitivity to ischemic insult among brain regions and neuronal populations (Schmidt-Kastner and Freund, 1991). Selectively vulnerable regions include ‘higher’ brain regions such as the neocortex and striatum as well as the cerebellum and thalamus, which readily succumb to ischemic damage both *in vivo* and in live brain slices (Pulsinelli et al., 1982; Kawai et al., 1992; Jarvis et al., 2001; Jiang et al., 1992). Despite uniform reductions in blood flow throughout the brain during global ischemia, these regions exhibit greater susceptibility to injury compared to ‘lower’ brain

regions such as the hypothalamus and brainstem (Sieber et al., 1995). Similarly, neurons of the hippocampal CA1 subfield differ drastically in their sensitivity to ischemia compared to other regions of the brain, including the adjacent CA3 subfield of the hippocampus (Schmidt-Kastner and Freund, 1991).

Studies of cerebral neurons subjected to ischemia have demonstrated a rapid and near-complete depolarization which electrically silences neurons and shuts down cerebral function. In contrast, brainstem neurons undergo a milder, recoverable depolarization which preserves vital respiratory, cardiac, and autonomic functions (Brisson and Andrew, 2012; Brisson et al., 2013). This poorly understood paradox can lead to an ‘awake but not aware’ condition termed the persistent vegetative state, in which global ischemia patients exhibit a lack of conscious awareness but maintain brainstem and hypothalamus-mediated autonomic functions (Wytrzes et al., 1989). The preservation of sleep-wake cycles differentiates this syndrome from coma and brain death, the latter of which involves irreversible damage to the brainstem.

Selectively vulnerable regions of the brain are readily overwhelmed by both ischemia and secondary ischemic injury mechanisms, and continue to degenerate days after ischemia-reperfusion. Discovering how brainstem neurons are naturally ischemia-resilient would help identify molecular targets for improving higher brain survival post stroke.

1.1.3 Ischemic Stroke Pathophysiology

A considerable portion of ischemic damage is dependent on the activation of multiple complex pathophysiological processes that promote cellular death and lead to maladaptive exacerbation of ischemic injury. In the absence of oxygen and glucose, adenosine triphosphate (ATP) cannot be generated by oxidative phosphorylation. Within

minutes, this prevents the ATP-dependent Na^+/K^+ -ATPase (or Na^+/K^+ 'pump') from maintaining the transmembrane electrochemical potential in neurons, leading to increased membrane permeability and loss of ion homeostasis (Holm and Lykke-Hartmann, 2016). The subsequent influx of ionic species leads to the phenomenon known as anoxic depolarization (AD) which shuts down neuronal function and leads to cellular swelling and dendritic beading (Jarvis et al., 2011). AD is the initial damaging event of stroke and eventually generates the infarct core. Peri-infarct depolarizations (PIDs) in the surrounding ischemic penumbra are recurring AD-like events; however, neurons in the penumbra may recover from PIDs if adequate metabolic substrates are available. In conjunction with AD-enhanced glutamate release, AD promotes toxic increases in intracellular calcium, activating a multitude of signaling pathways responsible for reacting to severe cell stress such as caspase-dependent apoptosis (Rizzuto et al., 2003). This process is known as excitotoxicity.

Another signaling pathway activated by elevated intracellular calcium is the calmodulin-dependent activation of neuronal nitric oxide synthase, which produces nitric oxide. This is a free radical that readily diffuses across membranes and reacts with other free radicals to form highly reactive oxygen and nitrogen species (ROS/RNS) (Dawson and Dawson, 1998). Under normal circumstances, ROS are involved in signaling pathways and maintaining cellular homeostasis; however, elevated levels can exceed the antioxidant capacity of cells, resulting in significant damage to cell structures and biomolecules. In fact, ROS can interact with calcium pumps and channels to further increase intracellular calcium levels, promoting additional ROS formation as well as mitochondrial dysfunction (Rizzuto et al., 2003). This imbalance between the production of ROS and cellular antioxidant defenses is known as oxidative stress.

Oxidative stress is among the biggest drivers of ischemia-induced apoptosis and is also relevant in the context of other conditions, particularly neurodegenerative disorders such as Alzheimer's and Parkinson's disease, as well as cardiovascular diseases such as atherosclerosis. During ischemia, oxygen becomes depleted before glucose, promoting anaerobic glycolysis as a means of ATP production (Liu et al., 2004). The resultant accumulation of lactic acid causes acidosis, which reduces the activity of antioxidant enzymes and liberates sequestered iron stores (Ying et al., 1999). Iron metabolism is tightly controlled to avoid the production of superoxide and hydroxyl radicals from molecular oxygen and H_2O_2 . The mitochondrial disorder known as Friedreich's ataxia is a particularly good example of the consequences of dysfunctional iron metabolism, where insufficient levels of the iron-processing protein frataxin lead to abnormalities in iron biochemistry as well as alterations in lipid and energy metabolism. The resultant escalation in oxidative stress causes severe damage to body systems most susceptible to degeneration, particularly the nervous, cardiovascular, and skeletal systems (Rotig et al., 1997).

The mitochondrial electron transport chain (ETC) generates reactive oxygen species such as superoxide during the reduction of molecular oxygen to water by the ETC complexes (Liu et al., 2002). Oxygen deprivation prevents cellular respiration at complex IV of the ETC, causing accumulation of reduced ETC intermediates and ROS during the first few minutes of hypoxia while the mitochondrial membrane potential dissipates (Abramov et al., 2007). Subsequent ATP depletion leads to the conversion of adenine nucleotides into xanthine and hypoxanthine, which react with xanthine oxidase to produce H_2O_2 . Remarkably, restoring blood flow following ischemia can further exacerbate oxidative stress through the generation of superoxide by NADPH oxidase, much of which

is supplied by activated microglia and infiltrating peripheral leukocytes (Abramov et al., 2007; Stoll et al., 1998).

Lipid peroxidation is the process by which ROS react with the fatty acids of lipids, initiating a chain reaction that results in fatty acid oxidation. Polyunsaturated fatty acids are particularly prone to this reaction by virtue of the reactive hydrogen atoms in methylene bridges that lie between double bonds (termed bis-allylic hydrogen atoms), leading to the destruction of membrane lipids and the generation of lipid peroxidation products that are exceptionally deleterious to cell survival (Dexter et al, 1989; Adibhatla and Hatcher, 2010). Lipid peroxidation generally occurs at a low rate in normal conditions; however, when antioxidant defense mechanisms are insufficient to mitigate the production of ROS and terminate the chain-reaction, the self-propagating nature of lipid peroxidation can lead to extensive tissue damage. Moreover, the products of lipid peroxidation are considerably more stable than ROS, extending the impact of oxidative damage by generating cytotoxicity, protein and DNA damage, and selective alterations in cell signaling. Lipid peroxidation frequently leads to the deregulation of molecular mechanisms and has been implicated in a variety of disorders including Alzheimer's disease, atherosclerosis, and cancer (Adibhatla and Hatcher, 2010).

Lipid peroxidation products are prevalent in ischemic brains, particularly malondialdehyde (MDA) and 4-hydroxy-2-nonenal (4-HNE), which are detectable in the plasma of stroke patients (Nanetti et al., 2011; Lee et al, 2012). In the absence of adequate antioxidant defenses, these highly toxic reactive aldehydes form adducts with proteins and impair their function, provoking pathological consequences such as inflammation and apoptosis. MDA is strongly implicated in DNA damage, leading to mutation, strand breaks, cell cycle arrest, and apoptosis (Ji et al, 1998; Niedernhofer et al, 2003). On the other hand,

4-HNE can initiate apoptosis both as a cytotoxic compound and as a signaling molecule. In addition to covalently modifying biomolecules through interactions with amino and thiol residues, 4-HNE modifies the activity of many transcription factors involved in cell proliferation, differentiation, and survival, as well as apoptosis and necrosis (Schaur, 2003; Siow et al., 2007). 4-HNE also increases mitochondrial calcium uptake and alters antioxidant metabolism, impairing mitochondrial function and promoting cell death (Kruman and Mattson, 1999). Overall, the myriad of cellular mechanisms modulated by MDA and 4-HNE as well as their biomolecular adducts highlights the devastating impact of excessive lipid peroxidation in ischemia.

Activation of transcription factors by elevated oxidative stress and lipid peroxidation products increases the production of neuroprotective factors, as well as pro-inflammatory cytokines and chemokines, in neurons, microglia, and astrocytes (Tuttolomondo et al., 2008). This promotes membrane expression of adhesion molecules and rapid recruitment of peripheral leukocytes, particularly neutrophils, to the site of injury. In addition, damage-associated molecular patterns released by injured cells are recognized by pattern-recognition receptors, further promoting immune system activation (Okun et al., 2009). Recruitment of T-lymphocytes to the boundary of the infarct core occurs 24 hours after reperfusion, and plays a critical role in amplifying reperfusion injury following cerebral ischemia (Shichita et al., 2009). This mixed inflammatory response typically leads to secondary injury of the salvageable penumbra; however, inflammation is an important process for recovery and repair following stroke and may be beneficial beyond the acute stage of ischemic insult (Wang et al., 2007).

An especially pervasive consequence of any stroke is dysfunction of the blood-brain barrier (BBB), which increases in permeability following ischemia. Swelling of the

microvascular endothelium shortly after ischemia onset causes degradation of the basal lamina and loss of tight junction integrity, while swelling of the astrocytes causes detachment of end-feet processes that provide biochemical support to the BBB (Del Zoppo and Hallenbeck, 2000). In addition, oxidative stress promotes activity of matrix metalloproteinases (MMPs) within hours of ischemia, which further degrade the microvascular endothelium and extracellular matrix of the BBB (Lakhan et al., 2013). In conjunction with the rapid cellular swelling generated by anoxic depolarization, BBB breakdown promotes brain edema through the accumulation of interstitial fluid (Del Zoppo and Hallenbeck, 2000). This increases intracranial pressure (ICP) which further limits cerebral blood flow and can cause severe complications such as brain herniation. BBB disruption is a serious issue that can potentiate secondary ischemic damage through exposure of the brain to systemic blood pressure and leakage of systemic blood components such as serum proteins and platelets into the brain. These components, along with infiltrating leukocytes, can cause obstructions within the cerebral microvasculature that prevent restoration of cerebral blood flow after reperfusion – a process known as the no-reflow phenomenon (Rezkalla and Kloner, 2002). One of the most severe complications of BBB dysfunction is the incidence of hemorrhagic transformation, in which an ischemic stroke develops into a hemorrhagic stroke due to microvascular and BBB damage from edema, oxidative stress, inflammation, and immune activation (Toni et al., 1996). This occurs most frequently following reperfusion of ischemic tissue – a consequence of the sudden resurgence of blood flow to severely compromised tissue.

This overview of stroke pathophysiology and secondary ischemic injury is by no means comprehensive, but serves as an outline of the major pathophysiological

mechanisms that promote exacerbation of ischemia-reperfusion injury, particularly in selectively vulnerable brain regions.

1.2 Spreading Depolarization

Spreading depolarization (SD), first described by Leão (1944), is an umbrella term that refers to a wave of near-complete sustained depolarizations in neurons and glia that propagates across gray matter at a rate of 2-5 mm/min. Due to the dissipation of transmembrane ionic gradients, affected neurons become unexcitable and may be permanently impaired in the absence of proper metabolic function. SD has been induced both *in vivo* and *in vitro* in many different organisms such as insects, amphibians, and mammals, and has also been observed clinically in humans (Hartings et al., 2017; Church and Andrew, 2005; Dreier et al., 2011). Experimentally, SD can be evoked using ischemia, mechanical perturbation, elevated potassium concentrations, hyperthermia or hypothermia, and inhibition of the Na⁺/K⁺-ATPase with ouabain (Chen et al., 1993; Dreier, 2011; Hartings et al., 2017). Rodent studies have also reported SD caused by metabolic stress, focal ischemia, global ischemia, and traumatic brain injury. As described earlier, ‘higher’ brain regions of mammals such as the neocortex undergo a more robust spreading depolarization than the brainstem, which is resistant to electrical silencing by SD (Brisson and Andrew, 2012).

1.2.1 Types of Spreading Depolarization

Although not well understood, all forms of spreading depolarization share a common cause involving impairment or failure of the Na⁺/K⁺-ATPase. SD then leads to loss of ion homeostasis. Under normal metabolic conditions, a mild form of SD known as

cortical spreading depression (CSD) causes focal inactivation of neurons and glia for 1-2 minutes. CSD is not thought to cause lasting damage in the brain, and generates an increase in regional cerebral blood flow (CBF) upon neuronal recovery (Dreier, 2011). CSD is implicated in migraine aura and visual scintillating scotomas, possibly causing transient sensory deficits associated with migraine pain (Dreier, 2011). On the other hand, anoxic depolarization (AD) is a much more severe form of SD that originates in oxygen and glucose-deprived neurons during ischemia or traumatic brain injury, causing permanent injury to vulnerable neurons and glia unless reperfusion is achieved within minutes (Brisson and Andrew, 2012). At the edge of the ischemic core, neurons receiving some collateral blood supply undergo recurring depolarizations and repolarizations known as peri-infarct depolarizations (PIDs), leading to depletion of energy reserves as neurons and glia attempt to restore transmembrane ionic gradients (Fabricius et al., 2005). Although milder than AD, PIDs persist in the penumbra over the hours and days following stroke, promoting expansion of the infarct core. Since the penumbra continues to receive some supply of oxygen and glucose from collateral blood flow, the penumbra represents a salvageable area of tissue and is therefore an important therapeutic target to mitigate the spread of ischemic damage.

1.2.2 Anoxic Depolarization

Within minutes of AD, pyramidal cells of the neocortex exhibit neuronal swelling as well as dendritic spine loss and ‘beading,’ representing permanent neuronal damage (Davies et al., 2007; Jarvis et al., 2001). Selectively vulnerable regions of the neocortex, striatum, cerebellum, and hippocampus do not recover from prolonged AD and undergo permanent morphological changes. Cellular architecture does not account for a region’s

susceptibility or resistance to AD (Carpenter, 1981; Brisson and Andrew, 2012). In contrast to CSD, anoxic depolarization promotes vasoconstriction of local blood vessels and reduces CBF in a maladaptive manner. This paradoxical ‘inverse neurovascular coupling’ leads to hypoperfusion of compromised tissue and may exacerbate ischemic injury, especially in the penumbra (Hinzman et al., 2014). Importantly, inducing spreading depolarization in the neocortex prior to focal ischemia reduces infarct volume in rodents, indicating the existence of adaptive neuroprotective changes in vulnerable brain regions (Kawahara et al., 1995; Kobayashi et al., 1995; Yanamoto et al., 1998). Determining the mechanisms underlying resilience to anoxic depolarization in the brainstem and in SD-treated neurons would help identify molecular targets for improving survival of selectively vulnerable regions after stroke. One possible candidate may be differences in the kinetic properties of the Na⁺/K⁺-ATPase between brain regions, as suggested by several studies showing differences in Na⁺/K⁺ pump efficiency and distribution in different brain regions and neuronal populations (Gottron and Lo, 2009; Munzer et al., 1994).

1.3 The Na⁺/K⁺-ATPase

The Na⁺/K⁺-ATPase is a ubiquitous plasma membrane protein responsible for regulating transmembrane ionic gradients via ATP-driven exchange of three cytosolic Na⁺ ions for two extracellular K⁺ ions. The Na⁺/K⁺-ATPase is the primary consumer of ATP in the brain and plays a critical role in promoting proper neuronal signalling and excitability by maintaining low intracellular sodium and high intracellular potassium concentrations (Boldyrev, 2000). Maintenance of the transmembrane sodium gradient by the Na⁺/K⁺-ATPase is also important for sodium-coupled transport of molecules such as glucose across

the plasma membrane (Blanco and Mercer, 1998). The Na⁺/K⁺-ATPase is a heteromeric protein composed of two alpha (α) and two beta (β) subunits, and may also contain an accessory gamma (γ) subunit which is thought to modulate the pump's kinetic properties by increasing its affinity for ATP, but is not necessary for its function (Gottron and Lo, 2010, Therien et al., 1999). The alpha subunit is a 112kDa polypeptide and represents the catalytic domain of the protein, and therefore is primarily responsible for the ion transport rate. Moreover, the alpha subunit contains binding sites for Na⁺, K⁺, ATP, and molecular inhibitors of the pump such as ouabain (Blanco et al., 1995; Kim et al., 1995). The beta subunit is a 35kDa polypeptide and promotes proper insertion and stability of the protein in the plasma membrane, and may also modulate cation affinity of the pump (Blanco et al., 1995). Neurons primarily express the β1 isoform of the beta subunit (Clausen et al., 2017). One complete conformational cycle of the Na⁺/K⁺ pump transports two K⁺ ions in and three Na⁺ ions out of the cell, allowing each pump to transport approximately 100 ions per second (Gadsby et al., 2012).

There are four distinct isoforms of the Na⁺/K⁺-ATPase alpha subunit which are expressed in a tissue-specific manner (Blanco, 2005). The α1 isoform is ubiquitously expressed in the body and mediates ion homeostasis under basal conditions. The α2 isoform is found in muscle, adipocytes, and mature glia, as well as in developing, but not mature, neurons of the central nervous system. The α3 isoform is predominantly expressed in mature neurons of the central nervous system, but is also found in peripheral systems such as γ-motor neurons and skeletal muscle stretch receptor afferents. The α4 isoform is expressed exclusively in sperm cells (Gottron and Lo, 2009; Crambert et al., 2000). Importantly, Na⁺/K⁺-ATPase alpha subunit sequence is highly conserved among different species, with 92% homology of the α1 and α2 isoforms and 96% homology of the α3

isoform (Blanco, 2005; Blanco and Mercer, 1998). These isoforms differ in their kinetic and catalytic properties, with certain isoforms pumping at higher rates during depolarization or ischemia. For example, the pump functions under near-anoxic conditions in adrenal medullary cells, in contrast to neocortical neurons where it quickly fails (Dobretsov and Stimers, 2005).

Mature neurons of the central nervous system primarily express the $\alpha 1$ and $\alpha 3$ isoforms of the Na^+/K^+ -ATPase (Cameron et al., 1994). The $\alpha 1$ isoform has a steep voltage dependence, allowing quick activation following short action potential bursts, and therefore mediates the majority of active transport under basal conditions (Brines and Robbins, 1993). In contrast, the voltage-independent $\alpha 3$ isoform continues to function during prolonged depolarization and low-energy conditions, and is therefore considered more ischemia-resistant. These two isoforms share 87% sequence homology and differ in their affinities for cations, ATP, and inhibitors such as ouabain (Blanco and Mercer, 1998; Blanco, 2005). It is suspected that the $\alpha 3$ isoform may act as a reserve pump under low-energy conditions due to its low affinity for sodium, allowing it to restore membrane potential during prolonged depolarization in spite of $\alpha 1$ isoform failure. The heterogeneity of Na^+/K^+ -ATPase alpha isoform distribution in different tissues suggests an important functional role for each isoform, although the significance of pump isoform distribution is poorly understood. Detecting consistent pump differences amongst brain regions may identify resilient isoform combinations which are normally present and act in reserve to enhance neuronal survival under low-energy or ischemic conditions.

The laboratory of R. David Andrew has proposed that expression of the $\alpha 3$ isoform is proportionally higher in ischemia-resistant neurons such as those found in the brainstem. This is supported by in-situ hybridization data mined from the Allen Mouse Brain Atlas

(R.D. Andrew, unpublished), which shows higher mRNA expression of the $\alpha 1$ isoform in the neocortex and striatum (**Figure 1**), and higher proportional mRNA expression of the $\alpha 3$ isoform in the brainstem (**Figure 2**). It is important to reproduce these findings with $\alpha 1$ and $\alpha 3$ isoform protein expression in different regions of the brain, since mRNA expression does not necessarily translate proportionally to protein expression. This is the main focus of this thesis.

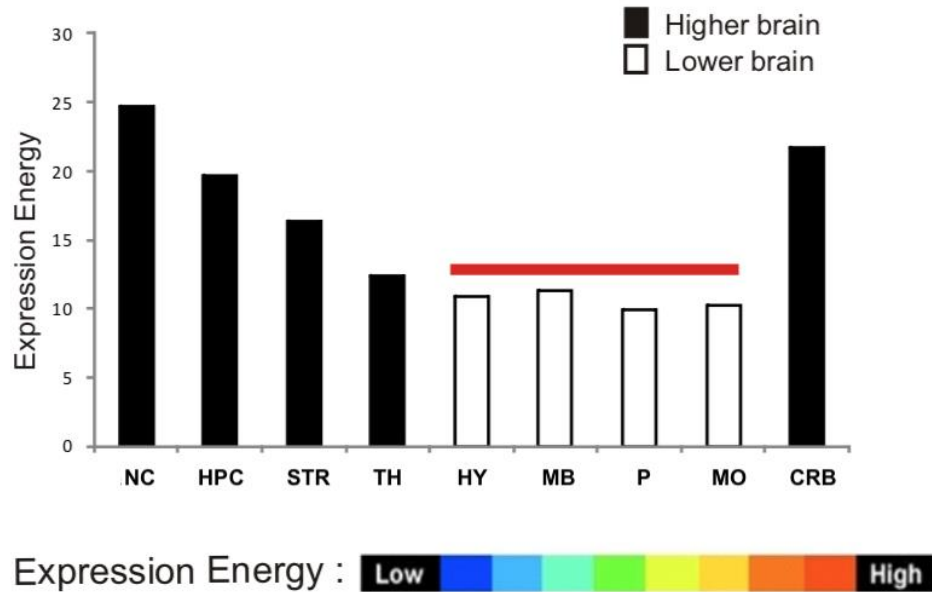
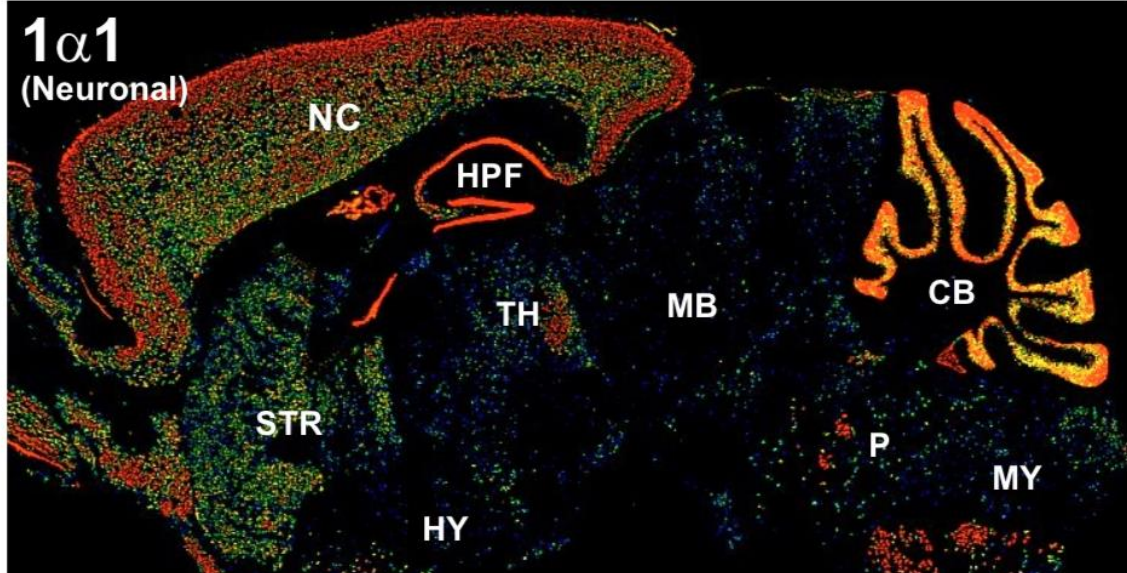


Figure 1. Regional Na⁺/K⁺-ATPase α 1 isoform mRNA expression in the mouse brain.

In-situ hybridization data mined from the Allen Mouse Brain Atlas by R.D. Andrew (n=3, error bars not shown but very small). Na⁺/K⁺-ATPase α 1 isoform mRNA is primarily expressed in the neocortex (NC), hippocampus (HPC), striatum (STR), thalamus (TH), and cerebellum (CRB). The hypothalamus (HY), midbrain (MB), pons (P), and medulla (MO/MY) express lower levels of Na⁺/K⁺-ATPase α 1 isoform mRNA. Courtesy of R. D. Andrew.

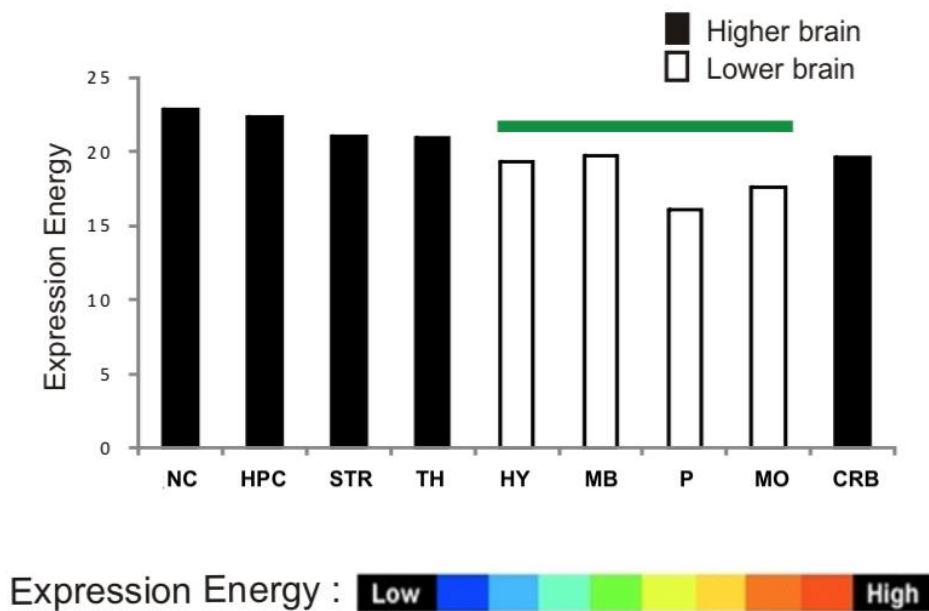
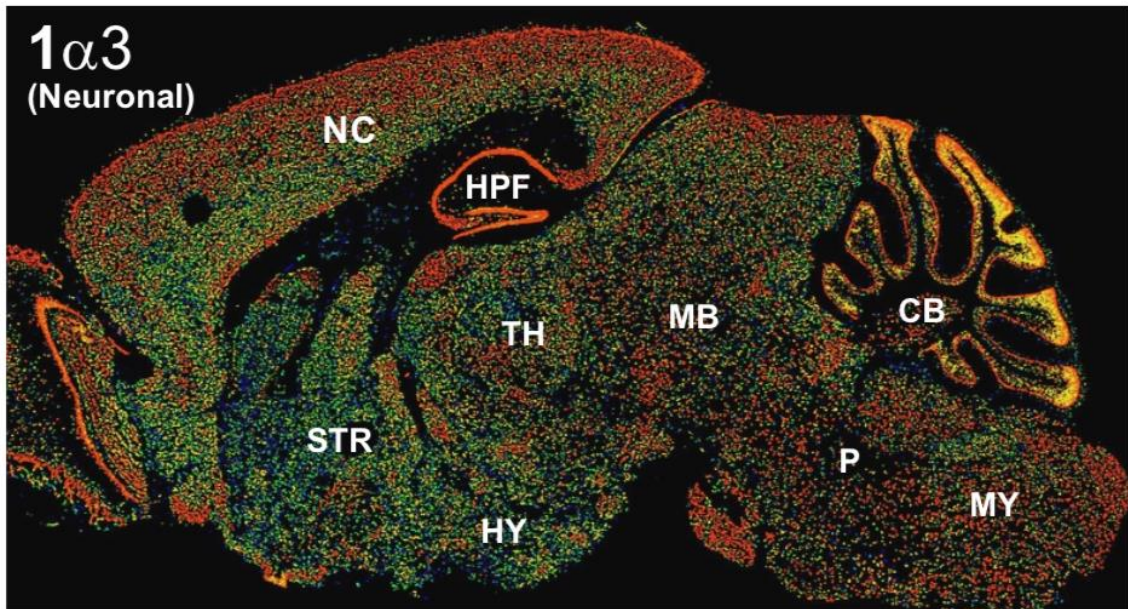


Figure 2. Regional Na^+/K^+ -ATPase $\alpha 3$ isoform mRNA expression in the mouse brain.

In-situ hybridization data mined from the Allen Mouse Brain Atlas by R.D. Andrew (n=3, error bars not shown but very small). Na^+/K^+ -ATPase $\alpha 3$ isoform mRNA is fairly consistent throughout the brain, although lower brain regions such as the hypothalamus (HY), midbrain (MB), pons (P) and medulla (MO/MY) exhibit proportionally higher $\alpha 3$ isoform mRNA than $\alpha 1$ isoform mRNA expression (see Figure 1). Courtesy of R. D. Andrew.

1.4 The *Aldh2*^{-/-} Mouse Model of Oxidative Stress

Aldehyde dehydrogenase 2 (ALDH2) is a critical enzyme for the detoxification of highly cytotoxic aldehydes such as 4-hydroxy-2-nonenal (4-HNE), which are generated by lipid peroxidation during oxidative stress (Wang et al., 2011). It is also the second enzyme of oxidative alcohol metabolism. Polymorphisms of the ALDH2 gene are linked to inflammatory processes in disorders such as cancer and cardiovascular disease, and ALDH2 deficiency leads to elevated oxidative stress (Hashimoto, 2002; Zhao and Wang, 2015; D'Souza et al., 2015).

The *Aldh2*^{-/-} mouse model exhibits age-related cognitive impairment and neurodegeneration associated with a toxic increase in oxidative stress and lipid peroxidation products such as 4-HNE, as well as elevated levels of F₂-isoprostanes and prostaglandin F_{2α} (D'Souza et al., 2015; Elharram et al., 2017). These mice also exhibit morphological abnormalities in the brain such as cerebrovascular pathology, endothelial dysfunction, and brain atrophy (D'Souza et al., 2015). Although currently being studied as a model for age-related cognitive impairment and Alzheimer's disease, these mice may resemble another rare and untreatable human syndrome known as mitochondrial encephalomyopathy, lactic acidosis, and stroke-like episodes (MELAS). MELAS occurs due to mutations in mitochondrial DNA and is therefore maternally inherited, resulting in a progressive neurodegeneration as well as pathological changes in other tissues, particularly muscle (Ciafaloni et al., 1992; Testai et al., 2010). Patients with MELAS exhibit early symptoms such as recurrent headaches and seizures that develop into stroke-like symptoms such as hemiparesis and altered consciousness in middle age. Recurring episodes of stroke-like symptoms cause permanent damage to the brain, such as motor abnormalities and loss of cognitive function. MELAS involves significant defects in

neuronal oxidative metabolism due to dysfunction in the electron-transport chain, which severely limits ATP production and can lead to neuronal death (Beal et al., 1993). Electron transport chain impairment is also correlated with a rise in oxidative stress – reactive nitrogen species such as nitric oxide can bind cerebral blood vessels via cytochrome *c* oxidase-positive sites, displacing heme-bound oxygen and reducing neuronal access to oxygen (Pavlakakis et al., 1984; Ciafaloni et al., 1992).

As a result of mitochondrial dysfunction, MELAS patients exhibit abnormal coupling of neural activity and cerebral blood flow (CBF) (Betts et al., 2006). This is especially detrimental during migraine episodes – cortical spreading depression, a usually benign phenomenon, can lead to the development of isolated infarcts in the posterior cortex in the absence of an adaptive cerebral blood flow response. Similarly, seizures associated with stroke-like episodes in MELAS patients may also promote development of infarcts within the brain due to the maladaptive coupling of CBF to seizure activity (Montagna et al., 1988). This suggests a strong association between mitochondrial impairment and susceptibility to injury from spreading depolarization.

1.5 Chronic Stress

Stress is an evolved response to distressing stimuli involving a ‘fight or flight’ response through activation of the sympathetic nervous system and the hypothalamic-pituitary-adrenal axis. The resultant release of stress hormones such as glucocorticoids promotes an adaptive response to acute exposure to real or perceived threats; however, prolonged activation of the stress response is maladaptive and can increase the risk of psychiatric and physical abnormalities. Glucocorticoids are normally present under

homeostatic conditions and help maintain energy homeostasis by promoting gluconeogenesis and glycogenolysis under stressful conditions.

Elevated levels of glucocorticoids from prolonged exposure to stress can result in cytotoxicity and morphological alterations in the brain, particularly in vulnerable regions such as the hippocampus, neocortex, and striatum (Sapolsky and Pulsinelli, 1985). Studies employing behavioural stress protocols in rodents have demonstrated increased glucocorticoid levels and oxidative stress in the brain as well as increased neurodegeneration and atrophy in animal models of Alzheimer's disease (Sapolsky et al., 1986; Lee et al., 2009). This is due in part to the induction of nitric oxide production, which impairs mitochondrial function, depletes antioxidant defenses, and initiates lipid peroxidation (Madrigal et al., 2001). Glucocorticoid-mediated disruptions in energy metabolism involve reduced glucose uptake and utilization in neurons, increasing susceptibility to oxidative stress (Sapolsky et al, 1986). This is particularly apparent in mouse models of neurological disorders involving elevated oxidative stress such as Alzheimer's disease, in which glucocorticoids are thought to lower neuronal resistance to oxidative stress and promote neurodegeneration. Similarly, glucocorticoids exacerbate ischemic damage in rodents by lowering the metabolic threshold for neurodegeneration, while glucocorticoid-deficient rodents (subject to adrenalectomy) exhibit significantly reduced infarct volume (Sapolsky and Pulsinelli, 1985). Glucocorticoids further promote ischemic damage by promoting calcium influx into cells and the release of excitatory neurotransmitters, potentiating excitotoxicity in neurons.

1.6 Objective and Hypotheses

Based on previous evidence that inhibition of the Na⁺/K⁺-ATPase using O₂-glucose deprivation (OGD) or the specific blocker ouabain resembles ischemia-induced anoxic depolarization, this project proposes that selective vulnerability of different brain regions to spreading depolarization may be explained, at least in part, by a heterogeneous distribution of the α1 and α3 isoforms of the Na⁺/K⁺-ATPase (Tanaka et al., 1997; Jarvis et al., 2001; Gottron and Lo, 2009). Previous mRNA expression data from the Allen Mouse Brain Atlas (R.D. Andrew, unpublished) shows proportionally greater expression of the α3 isoform in the brainstem and proportionally greater expression of the α1 isoform in higher brain structures such as the neocortex, striatum, and cerebellum (Lein et al., 2007). It is hypothesized that protein translation of these two isoforms follows a similar distribution, with the ischemia-efficient α3 isoform highest in the brainstem and the vulnerable α1 isoform prevailing in higher brain regions.

In order to assess whether mitochondrial dysfunction and elevated oxidative stress promote changes in Na⁺/K⁺-ATPase alpha isoform expression in the absence of ischemia, wild-type and *Aldh2*^{-/-} mice were subjected to a 28-day chronic unpredictable stress protocol. The combined use of two models of oxidative stress may reveal expression changes that are not apparent in either model in isolation. It is hypothesized that elevated oxidative stress in the brain may promote a neuroprotective response to mitochondrial dysfunction and low-energy conditions by increasing expression of the more resilient α3 isoform in vulnerable brain regions such as the neocortex and striatum.

The mechanisms underlying the differential sensitivity of different brain regions to spreading depolarization and ischemia are poorly understood. Since failure of the Na⁺/K⁺-ATPase is the initiating event of spreading depolarization, it is plausible that brain regions

may alter their Na⁺/K⁺-ATPase isoform expression following an ischemic event in order to improve recovery under low energy conditions. In this study, naïve rats were subjected to 90-minute transient unilateral middle cerebral artery occlusion (MCAo) followed by a 24 hour reperfusion period in order to assess alterations in Na⁺/K⁺-ATPase alpha isoform expression in infarcted tissue. Due to delays in establishing a rat stroke model, this phase of the study is limited by a small sample size and is therefore considered pilot experimental data for future studies. It is hypothesized that the multitude of pathophysiological sequelae initiated by ischemia may increase expression of the ischemia-efficient $\alpha 3$ isoform in infarcted regions such as the striatum and neocortex. The devastating nature of stroke may induce changes in Na⁺/K⁺-ATPase isoform expression that are more substantial than those generated by elevated oxidative stress from ALDH2 deficiency and/or chronic environmental stress.

Chapter 2

Materials and Methods

2.1 Animals

2.1.1 *Aldh2*^{-/-} Model of Oxidative Stress

The *Aldh2*^{-/-} mouse colony was generated using a gene-targeting knockout approach as described by Kitagawa and colleagues (2000) and kindly provided by Dr. T. Kawamoto (University of Occupational and Environmental Health, Kitakyushu, Japan). Wild-type male C57BL/6 mice (20-30 g) were obtained from Jackson Laboratory (Bar Harbor, ME) and backcrossed with *Aldh2*^{-/-} mice for more than 10 generations. The cohort of *Aldh2*^{-/-} mice used in this study was generated by mating heterozygotes, with the progeny genotyped by PCR analysis of genomic DNA extracted from ear punch samples collected at weaning (21 days) using the primers as reported (Isse et al., 2002). These animals were used and cared for under experimental protocols approved by the Queen's University Animal Care Committee (Kingston, Ontario, Canada) and in accordance with the Canadian Council on Animal Care guidelines. Animals were maintained under a 12 hour light/dark cycle, with free access to food and water. Wild-type and *Aldh2*^{-/-} C57BL/6 mice were studied at an approximate age of four months (25-30g weight, n=5 per group).

2.1.2 Chronic Unpredictable Stress (CUS) Mouse Model

The chronic unpredictable stress (CUS) protocol was modified from Barnum et al. (2012), lasted 28 days, and involved a randomized rotation of seven different stressors to avoid habituation. Excluding 36-hour periods of continuous light, stressors were performed twice daily: at the beginning of the dark cycle (10:00 hrs) and at the beginning of the light cycle (22:00 hrs). Mice were divided into two groups, with the second group beginning the

CUS protocol three days after the first group to facilitate tissue collection. All mice were subjected to each stressor the same number of times, and were sacrificed 24 hours after completion of the 28-day CUS protocol. A detailed description of the stressors used and the schedule of the 28-day CUS protocol can be found in **Table 1** and **Table 2**, respectively. Control mice included both wild-type and *Aldh2*^{-/-} C57BL/6 mice that did not undergo the CUS protocol (n=5 per group).

Table 1. Stressors used in the Chronic Unpredictable Stress (CUS) protocol.

Stressor	Description	Duration
Tail suspension	Tail suspension over an empty cage	6 min
Novel environment	Each mouse was placed into an empty 40x50x20cm box	30 min
Confinement	Confinement in an open-ended upright cylindrical tube (8cm diameter, 15cm height) with limited motion possible	2 hours
Slanted cage*	Home cage tilted sideways at a 45° angle	12 hours
No bedding*	Mice were placed into clean, empty cages without bedding	12 hours
Saturated bedding*	Home cage bedding flooded with 300mL room temperature water to ensure complete saturation	12 hours
Continuous light	Mice (in their home cages) were exposed to constant light	36 hours

*Stressors only performed during dark cycle (1000 – 2200 hrs)

Table 2. Schedule of the 28-day Chronic Unpredictable Stress (CUS) protocol.

		Sunday	Monday	Tuesday	Wednesday	Thursday	Friday	Saturday
Week 1	<i>am</i>	Restraint	Slanted cage	No bedding	Slanted cage	Saturated bedding	Tail suspension	
	<i>pm</i>	Tail suspension	Tail suspension	Novel environment*	Restraint	Novel environment	Continuous light	
Week 2	<i>am</i>	No bedding	Slanted cage	Saturated bedding	No bedding	Slanted cage	Saturated bedding	
	<i>pm</i>	Tail suspension	Novel environment	Tail suspension	Restraint	Tail suspension	Continuous light	
Week 3	<i>am</i>	Saturated bedding	No bedding		Saturated bedding	No bedding	Slanted cage	
	<i>pm</i>	Novel environment	Continuous light		Tail suspension	Restraint	Continuous light	
Week 4	<i>am</i>	No bedding	Saturated bedding		Slanted cage	Slanted cage	No bedding	Saturated bedding
	<i>pm</i>	Tail suspension	Continuous light		Novel environment	Restraint	Tail suspension	Novel environment**
Week 5	<i>am</i>	No bedding	Slanted cage	Restraint				
	<i>pm</i>	Tail suspension	Tail suspension					

*Beginning of protocol, cohort #2 **End of protocol, cohort #1

2.1.3 Middle Cerebral Artery Occlusion (MCAo) Rat Model of Stroke

All MCAo surgeries were performed by Kathleen Harrison with assistance from Michael Golod. These animals were used and cared for under experimental protocols approved by the Queen's University Animal Care Committee (Kingston, Ontario, Canada) and in accordance with the Canadian Council on Animal Care guidelines. Rats were subjected to a 90-minute transient occlusion of the left middle cerebral artery as performed by Longa et al. (1989).

Animals were anesthetized with isoflurane (Fresenius Kabi, Bad Homburg, Germany) until the righting reflex was absent, then prepared for surgery with eye lubrication, shaving of the incision area, and a three-step disinfection of the incision site with soap, 70% isopropyl alcohol, and povidone iodine (Betadyne). Surgical level of anesthesia was confirmed with eye blink reflex and the toe pinch test. The local anesthetic Bupivacaine (7 mg/kg) was injected into the subcutaneous space at the location of incision, and the anesthetic/analgesic Medetomidine (0.3 mg/kg) was injected intraperitoneally. An incision was made above the sternocleidomastoid muscle and the common carotid artery was isolated from the vagus nerve, with a silk suture placed under it. The external carotid artery was sutured at two adjacent sites and cut between the sutures to allow intraluminal access to the cerebral vasculature. A silicon rubber-coated monofilament (L23, Docol Corporation, Massachusetts, USA, size 4-0, diameter 0.185mm, length 30mm, diameter with coating 0.41 \pm 0.02mm, coating length 2-3mm) was maneuvered into the MCA (~20mm insertion) to occlude blood flow for 90 minutes. With the suture in place, the incision in the neck was closed and animals were placed in a heated incubation chamber at 35°C. After 80 minutes of MCA occlusion, animals were anesthetized with isoflurane until

a surgical level of anesthesia was reached. The incision in the neck was re-opened and the monofilament was removed after 90 minutes of MCA occlusion. The incision in the neck was sutured and animals were treated with Meloxicam (1 mg/kg) subcutaneously and Tramadol (20 mg/kg) intraperitoneally.

Animals were monitored and rotated side to side every five minutes until righting reflex was observed, then allowed to recover on a sheet of paper in a dry clean cage on a heated pad for three hours. Temperature of animals was monitored using a rectal thermometer, and animals were provided with unlimited water and food (moist chow).

Animals were allowed to recover for 24 hours after MCA occlusion was terminated. Neurological deficits such as forelimb flexion, lateral gait weakness, and circling were recorded at 24 hours by placing the animal in an open field for two minutes and by holding the animal by the base of its tail for 30 seconds. Neurological deficits were assessed using the Bederson Stroke Deficit Scale (**Table 3**) (Bederson et al., 1986). **Figure 3** is a representative cohort of the transient MCAo rat stroke model established by the Cook laboratory, and indicates a correlation between behavioural deficits and stroke volume as a percentage of total brain tissue as determined by tetrazolium chloride (TTC) staining of 2mm coronal brain sections (Spearman's $r=0.84$). Stroke volume of infarcted brains used in this study was not assessed by TTC staining to avoid confounding biochemical analyses. Control rats did not undergo surgery, and did not present with any neurological impairments (Bederson Score of 0).

Table 3. The Bederson scale of ischemia-induced neurological impairment.

Degree of deficit	Description	Score
Normal	Both forepaws reach out, no lateral weakness or circling	0
Mild	Flexion of limbs contralateral to infarcted hemisphere	1
Moderate	Decreased resistance to lateral push without circling	2
Severe	Decreased resistance to lateral push with circling	3

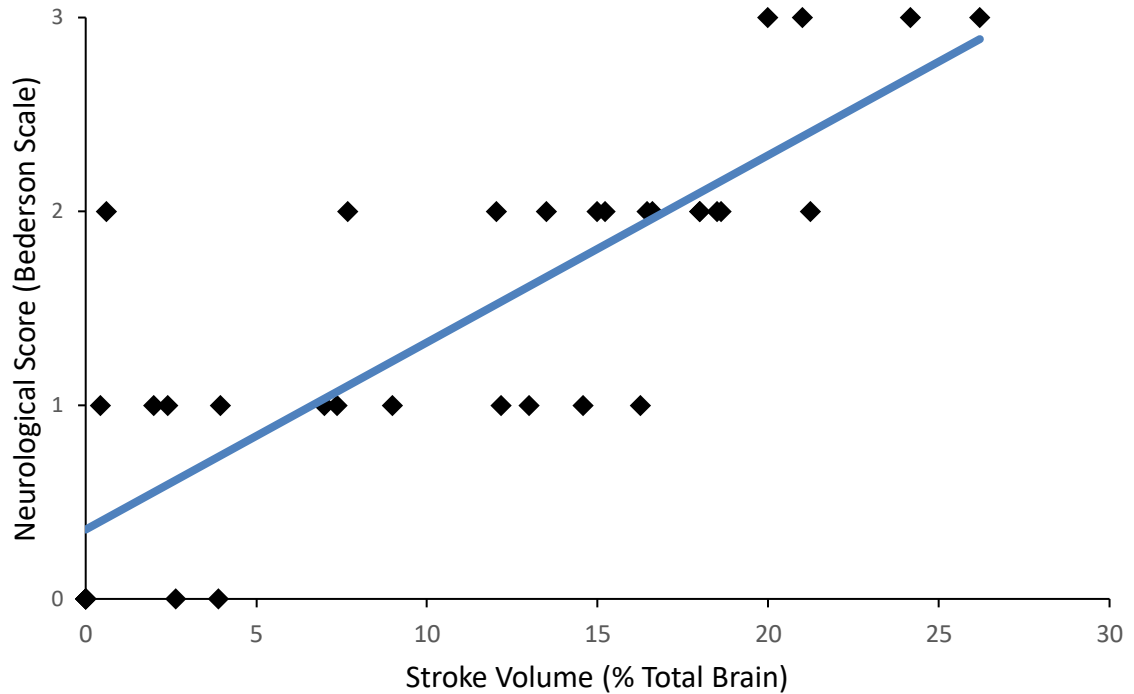


Figure 3. Correlation of stroke volume and behavioural deficits 24 hours after reperfusion in rats undergoing transient MCAo.

Rats were subjected to a 90-minute occlusion of the left MCA, followed by 24 hours of recovery. Prior to termination, animals were placed in an open field for two minutes and held by the tail for 30 seconds to assess neurological deficits. Stroke volume was assessed by TTC staining of 2mm thick coronal brain sections. The linear regression (blue line) indicates a correlation between stroke volume and neurological score (n=35, Spearman's $r=0.84$). Courtesy of Kathleen A. Harrison.

2.2 Tissue Collection

2.2.1 *Aldh2*^{-/-} and CUS Protocol Mice

Mice were deeply anesthetized with isofluorane, followed by intracardial perfusion with 0.1 M phosphate-buffered saline (PBS). After decapitation, the hippocampus, overlying neocortex, brainstem, and cerebellum from one hemisphere were dissected. The entire hippocampal formation, as well as similarly sized blocks of the other regions were homogenized in cell lysis buffer (50 mM Tris, pH 7.4, 50 mM TSP, 1 mM EDTA, 100 mM DTT, 100 mM PMSF, 100 mM NaF, 100 mM Na₃VO₄, 1.0 M sodium β-glycerophosphate, Roche protease inhibitor cocktail), centrifuged at 10,000 rpm for 10 minutes, and the supernatant frozen at -80°C.

2.2.2 MCAo Rats

Infarcted and control rats were deeply anesthetized with isofluorane followed by intracardiac perfusion with artificial cerebrospinal fluid (aCSF).

Rats intended for immunoblotting analysis were decapitated and the hippocampal formation, neocortex, brainstem, cerebellum, and striatum were collected. Tissue from the neocortex and striatum was collected between bregma +2.0mm and -1.0mm to incorporate infarcted tissue supplied by the MCA. Tissues were stored at -80°C before homogenization in cell lysis buffer (50 mM Tris, pH 7.4, 50 mM TSP, 1 mM EDTA, 100 mM DTT, 100 mM PMSF, 100 mM NaF, 100 mM Na₃VO₄, 1.0 M sodium β-glycerophosphate, Roche protease inhibitor cocktail), centrifuged at 10,000 rpm for 10 minutes, and the supernatant frozen at -80°C.

Rats intended for immunohistochemical analysis underwent additional intracardiac perfusion-fixation with 10% neutral-buffered formalin. The entire brain was then removed and stored in 10% neutral-buffered formalin until tissue processing.

2.3 Biochemical Analysis

2.3.1 Fluorescent Multiplex Immunoblotting

Protein content of brain homogenates was determined using the Bradford Protein Assay (Bio-Rad, Mississauga, ON, #5000006). Equivalent amounts of protein (30µg) were loaded in each lane of a 10% Mini-PROTEAN[®] TGX Stain-Free[™] Precast Gel (12 well, 20µl, Bio-Rad #4568035), using Precision Plus Protein[™] All Blue Prestained Protein Standards (Bio-Rad #1610373) for the marker lane. Gel electrophoresis was performed at 175V for 1 hour under reducing and denaturing conditions (4x Laemmli Sample Buffer, Bio-Rad #1610747) using Tris/Glycine/SDS Running Electrophoresis Buffer (Bio-Rad #1610732) in a Mini-PROTEAN[®] Tetra Vertical Electrophoresis Cell for Mini Precast Gels (Bio-Rad #1658004). Gels were activated in UV light at 302nm for 5 minutes using the Azure Biosystems c600 Gel Imaging System (Azure Biosystems, Dublin, California) and the cSeries Capture Software, allowing imaging of total protein in each lane by UV-induced fluorescence. Transfer electrophoresis was performed at 0.2A for 1 hour in a Mini Trans-Blot[®] Cell (Bio-Rad #1703930) onto an Immun-Blot[®] PVDF Membrane (Bio-Rad #1620177). Membranes were imaged in UV light at 302nm using the Azure Biosystems c600 Gel Imaging System and the cSeries Capture Software, allowing imaging of total protein in each lane by UV-induced fluorescence to ensure proper protein transfer onto the PVDF membrane.

After washing in TBS-T (Tris-buffered saline, 0.05% Tween20, 3x5min), membranes were incubated in blocking buffer (5% skim milk in TBS-T) for 1.5 hours at room temperature. After washing in TBS-T (3x5min), membranes were incubated in a primary antibody solution containing anti- $\alpha 1$ Na⁺/K⁺-ATPase (Mouse monoclonal, 1:4000, Abcam, Toronto, ON, ab7671) and anti- $\alpha 3$ Na⁺/K⁺-ATPase (Rabbit monoclonal, 1:4000, Abcam, ab182572) in TBS-T overnight at 4°C. After washing in TBS-T (3x5min), membranes were incubated in a fluorescent secondary antibody solution containing Goat Anti-Mouse IgG H&L preadsorbed (Alexa Fluor[®] 790, Abcam, ab186695 for mice or Cy5[®], Abcam, ab6563 for rats) and Goat Anti-Rabbit IgG H&L preadsorbed (Alexa Fluor[®] 680, Abcam, ab186696 for mice or Cy3[®], Abcam, ab6939 for rats) in blocking buffer (5% skim milk in TBS-T) for 1.5 hours at room temperature in the dark.

After washing in TBS-T, membranes were imaged using the NIR (AlexaFluor secondary antibodies for mice) or RGB (Cy3/5 secondary antibodies for rats) function (multi-channel detection, IR700/IR800 or Cy3/Cy5) of the Azure Biosystems c600 Gel Imaging System and the cSeries Capture Software. The apparent molecular masses of the separated proteins were determined using the marker lane (Precision Plus Protein[™] All Blue Prestained Protein Standards, Bio-Rad #1610373). The Band Analysis tools of the AzureSpot Analysis Software were used to select and determine the density of the protein bands on the membranes in order to determine the relative abundance of $\alpha 1$ and $\alpha 3$ isoforms of the Na⁺/K⁺-ATPase as well as total protein content per lane, to allow for total protein normalization between different lanes.

2.3.2 Immunohistochemistry

Whole rat brains were cryoprotected in a 15% sucrose solution until sinking was observed (~24 hours), followed by a 30% sucrose solution until sinking was observed (~3 days). Whole brains were embedded in frozen section compound (VWR, 95057-838) and flash-frozen in methyl butane at -50°C. Frozen brains were sectioned at 40µm using a Leica CM1950 cryostat at -20°C and stored in 0.1M PBS. Brain sections were plated onto positively-charged microscope slides and allowed to dry for one hour. Plated sections were immersed in an antigen retrieval solution in a Copling Jar (10mM sodium citrate, 0.05% Tween20, pH 6.0) at 95°C for 20 minutes, followed by immersion in 0.1M PBS at 4°C until cool. Plated sections were allowed to dry for one hour and a hydrophobic pen was used outline each brain section. After washing in 0.1M PBS (3x5min), sections were incubated in blocking buffer (3% bovine-serum albumin in 0.1M PBS, 100µl per section) for three hours at room temperature. After washing in 0.1M PBS (3x5min), sections were incubated in a primary antibody solution containing anti- α 1 Na⁺/K⁺-ATPase (Mouse monoclonal, 1:4000, Abcam, Toronto, ON, ab7671) and anti- α 3 Na⁺/K⁺-ATPase (Rabbit monoclonal, 1:4000, Abcam, ab182572) in blocking buffer (3% BSA, 100µl per section) overnight (~18 hours) at 4°C. After washing in 0.1M PBS (3x5min), sections were incubated in a fluorescent secondary antibody solution containing Goat Anti-Mouse IgG H&L preadsorbed (Alexa Fluor[®] 488, Invitrogen by Thermo Fisher Scientific, Eugene, OR, A-11001) and Goat Anti-Rabbit IgG H&L preadsorbed (Cy3[®], Abcam, ab6563) in blocking buffer (3% BSA in 0.1M PBS) for three hours at room temperature in the dark.

After washing in 0.1M PBS (3x5min), sections were allowed to dry in the dark for one hour. A small drop of mounting media with DAPI stain (Abcam, ab104139) was placed

onto each tissue section and a cover slip was applied to the microscope slide. Mounted slides were left to cure for 24 hours in the dark. Sections were imaged at 10x magnification and stitched together using a Leica DM5500 B fluorescence microscope with DAPI, RHO and Y3 filter blocks.

2.4 Statistical Analysis for Immunoblotting

Statistical data analysis was carried out on normalized band densitometry values using two-way analysis of variance (ANOVA) and Prism 7 by GraphPad. Since the TGX Gels used only contained 12 protein lanes each, a maximum of three cohorts with four brain regions each (mice) or two cohorts with five brain regions each (rats) could be analyzed simultaneously. Separate graphs were generated for relative $\alpha 1$ and $\alpha 3$ isoform expression between brain regions, normalized to total protein content in each lane. Additionally, a graph of the ratio of $\alpha 1$ and $\alpha 3$ isoform expression was generated to illustrate proportional differences between brain regions.

Correction for multiple comparisons was achieved with Bonferroni post hoc analysis, allowing comparison between brain regions in each cohort to determine regional differences in isoform expression. Similarly, multiple comparisons were used to compare between cohorts in each brain region to illustrate changes in isoform expression induced by oxidative stress, environmental stress, or ischemia. Statistical significance was determined using a p value < 0.05.

Chapter 3

Results

3.1 Multiplex Immunoblotting

Fluorescent multiplex immunoblotting allows the simultaneous detection of multiple proteins without the need for stripping and re-probing of membranes, even if they are of similar molecular weight. It is more selective and specific for the proteins of interest than traditional enhanced chemiluminescence (ECL) immunoblotting. **Figure 4** shows the raw data, in which green bands represent the $\alpha 1$ isoform of the Na^+/K^+ -ATPase, whereas red bands represent the $\alpha 3$ isoform. The bands representing $\alpha 1$ and $\alpha 3$ isoforms of the Na^+/K^+ -ATPase were detected at their expected molecular size of 112 kDa as determined by a marker lane, with high expression of the Na^+/K^+ -ATPase $\alpha 1$ isoform in the neocortex and cerebellum and slightly higher expression of the $\alpha 3$ isoform in the brainstem and hippocampus.

3.2 Total Protein Normalization

Normalization of total protein in each lane was achieved by UV302-activation of a non-protein moiety within Mini-PROTEAN[®] TGX Stain-Free[™] Precast Gels, which allows visualization of total protein in each lane by UV302 imaging without the need for additional probing for a housekeeping protein. **Figure 5** shows an activated gel and membrane to demonstrate consistent transfer of bound protein to a PVDF membrane as well as fairly uniform loading of protein in each lane. This ensures accurate analysis of the target proteins during immunoblotting not confounded by variations in protein concentrations within each sample.

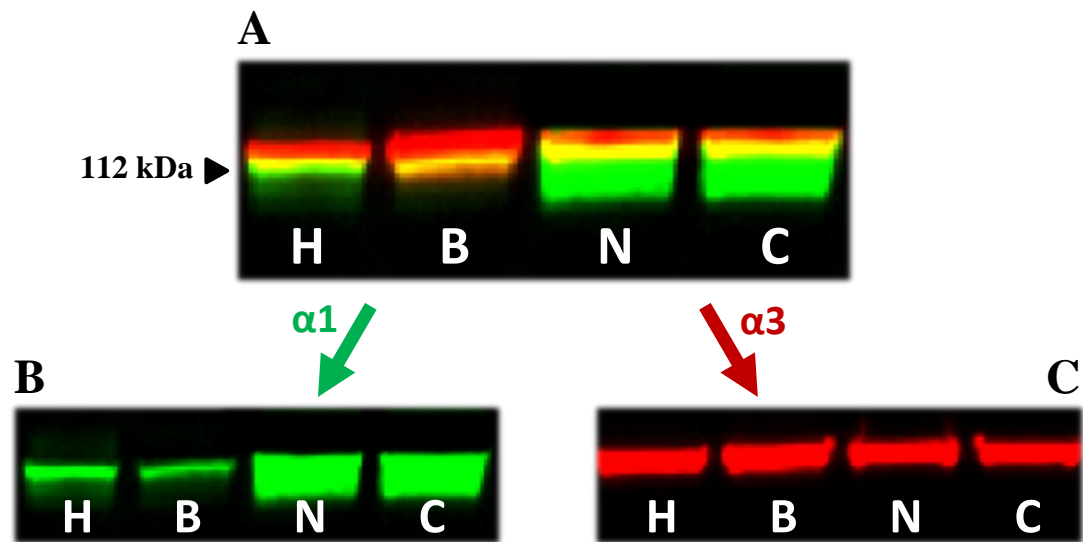


Figure 4. Multiplex immunoblot of Na⁺/K⁺-ATPase α 1 and α 3 isoform expression in the naïve mouse brain.

H=hippocampus, B=brainstem, N=neocortex, C=cerebellum. The use of fluorescent secondary antibodies allows the simultaneous detection of two proteins with separate analysis of α 1 (B, green bands) and α 3 (C, red bands) isoforms of the Na⁺/K⁺-ATPase. Density of bands indicates the relative abundance of each protein.

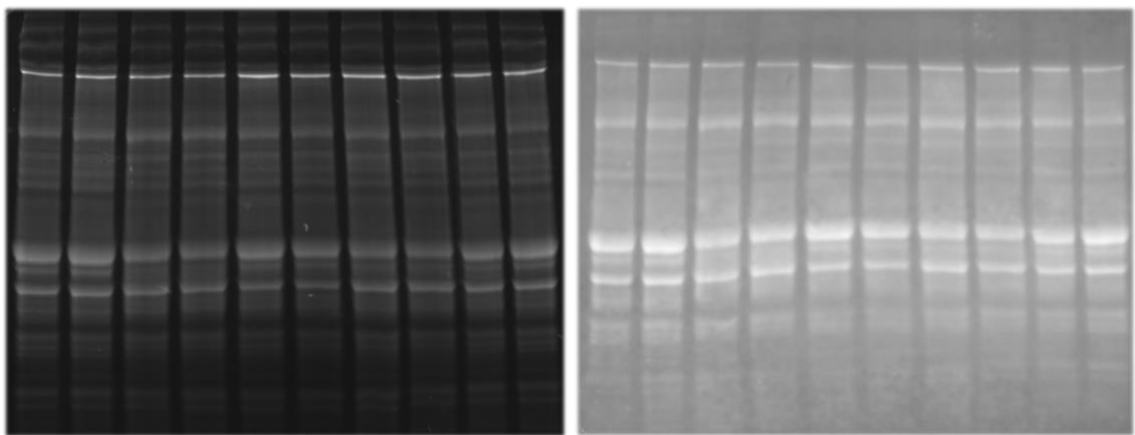


Figure 5. Total protein normalization using a UV302-activated non-protein moiety within TGX Stain-Free Gels.

Visualization of total protein in each lane of the gel (left) and PVDF membrane (right) allows for a more robust normalization of loaded protein per lane than traditional housekeeping proteins. White bands represent protein bound with a UV302-activated non-protein moiety, with total lane density indicating the relative abundance of total protein within each sample.

3.3 Na⁺/K⁺-ATPase α 1 Isoform Expression

3.3.1 Wild-type Mice Subjected to Chronic Unpredictable Stress

Protein expression of the Na⁺/K⁺-ATPase α 1 isoform was investigated across four brain regions in 5-7 month old male wild-type mice subjected to a chronic unpredictable stress (CUS) protocol for 28 days. Na⁺/K⁺-ATPase α 1 isoform expression was highest in the cerebellum and the neocortex, and lowest in the hippocampus and brainstem. Significant differences were found in α 1 isoform expression between all brain regions, except when comparing the hippocampus and brainstem (**Figure 6**). However, no significant differences were found in α 1 isoform expression between naïve mice and mice subjected to a 28-day CUS protocol.

3.3.2 *Aldh2*^{-/-} Mice Subjected to Chronic Unpredictable Stress

Protein expression of the Na⁺/K⁺-ATPase α 1 isoform was investigated across four brain regions in 5-7 month old male *Aldh2*^{-/-} mice subjected to a chronic unpredictable stress (CUS) protocol for 28 days. Na⁺/K⁺-ATPase α 1 isoform expression was highest in the cerebellum and the neocortex, and lowest in the hippocampus and brainstem (**Figures 7-9**). Significant differences were found in α 1 isoform expression between all brain regions, except when comparing the hippocampus and brainstem as well as the neocortex and cerebellum. No significant differences were found in α 1 isoform expression between naïve mice and mice subjected to a 28-day CUS protocol, except a small but statistically significant decrease in α 1 isoform expression when comparing the cerebellum of stressed *Aldh2*^{-/-} mice to unstressed wild-type mice (**Figure 9**).

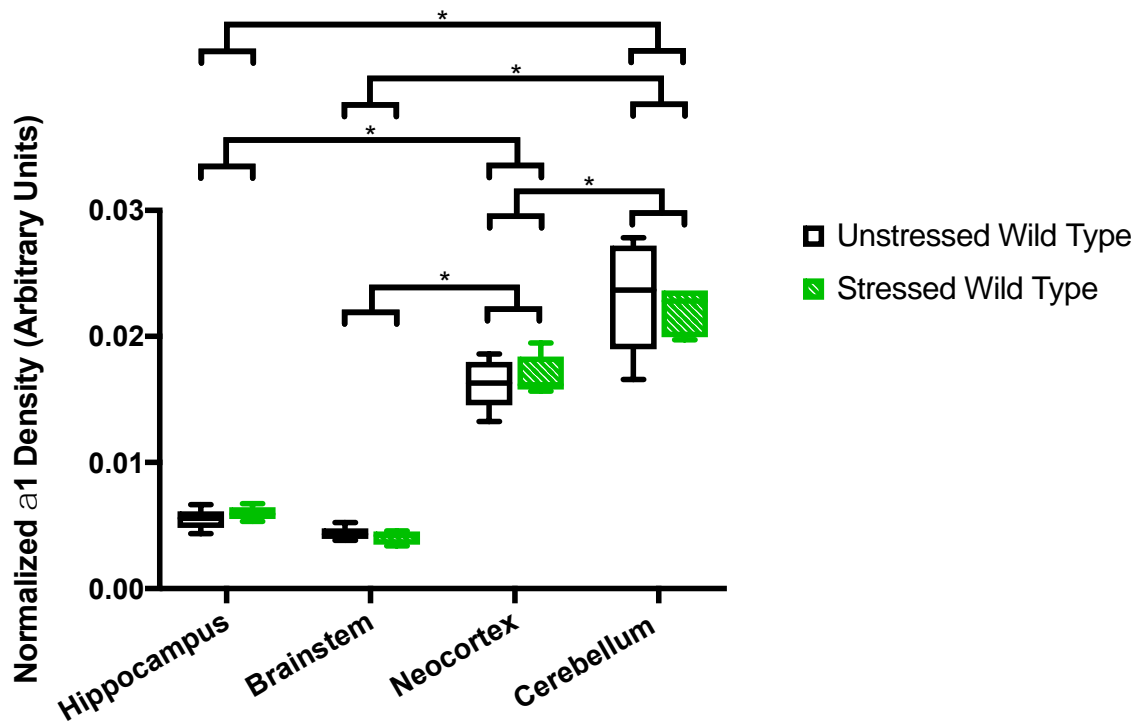


Figure 6. Regional protein expression of the Na⁺/K⁺-ATPase α 1 isoform in naïve and stressed wild-type mice.

Protein expression of the Na⁺/K⁺-ATPase α 1 isoform was normalized to total protein in each lane. Na⁺/K⁺-ATPase α 1 isoform expression is highest in the cerebellum and the neocortex, and lowest in the hippocampus and brainstem. A 28-day chronic unpredictable stress protocol did not significantly alter α 1 isoform protein expression in any of the brain regions studied. Data are presented as median with interquartile range (n=5 per group), analyzed by two-way ANOVA with correction for multiple comparisons achieved with Bonferroni post-hoc analysis (p>0.05 for statistical significance).

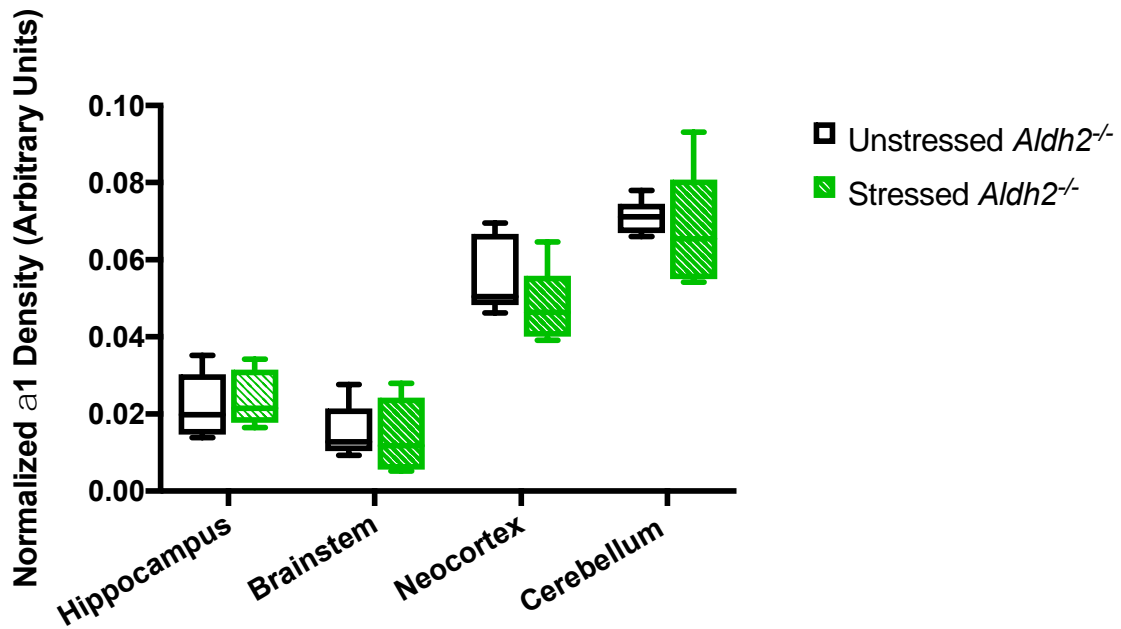


Figure 7. Regional protein expression of the Na⁺/K⁺-ATPase α1 isoform in naïve and stressed *Aldh2*^{-/-} mice.

Protein expression of the Na⁺/K⁺-ATPase α1 isoform was normalized to total protein in each lane. A 28-day chronic unpredictable stress protocol did not significantly alter α1 isoform protein expression. Data are presented as median with interquartile range (n=5 per group), analyzed by two-way ANOVA with correction for multiple comparisons achieved with Bonferroni post-hoc analysis (p>0.05 for statistical significance).

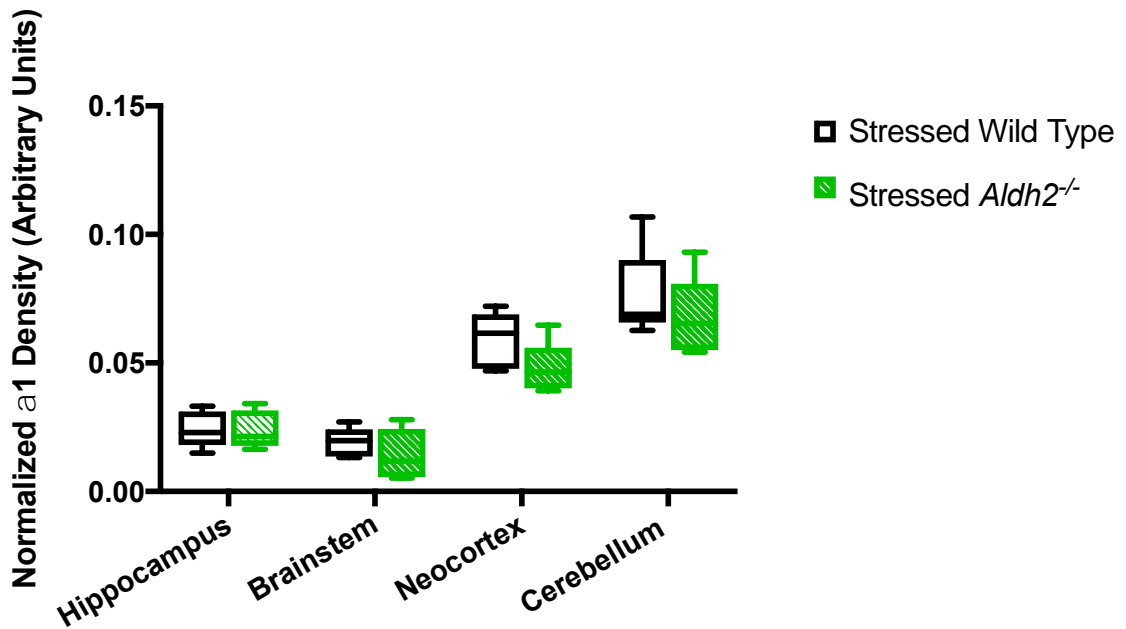


Figure 8. Regional protein expression of the Na⁺/K⁺-ATPase α1 isoform in stressed wild-type and *Aldh2*^{-/-} mice.

Protein expression of the Na⁺/K⁺-ATPase α1 isoform was normalized to total protein in each lane. No significant differences in α1 isoform protein expression were found between wild-type and *Aldh2*^{-/-} mice. Data are presented as median with interquartile range (n=5 per group), analyzed by two-way ANOVA with correction for multiple comparisons achieved with Bonferroni post-hoc analysis (p>0.05 for statistical significance).

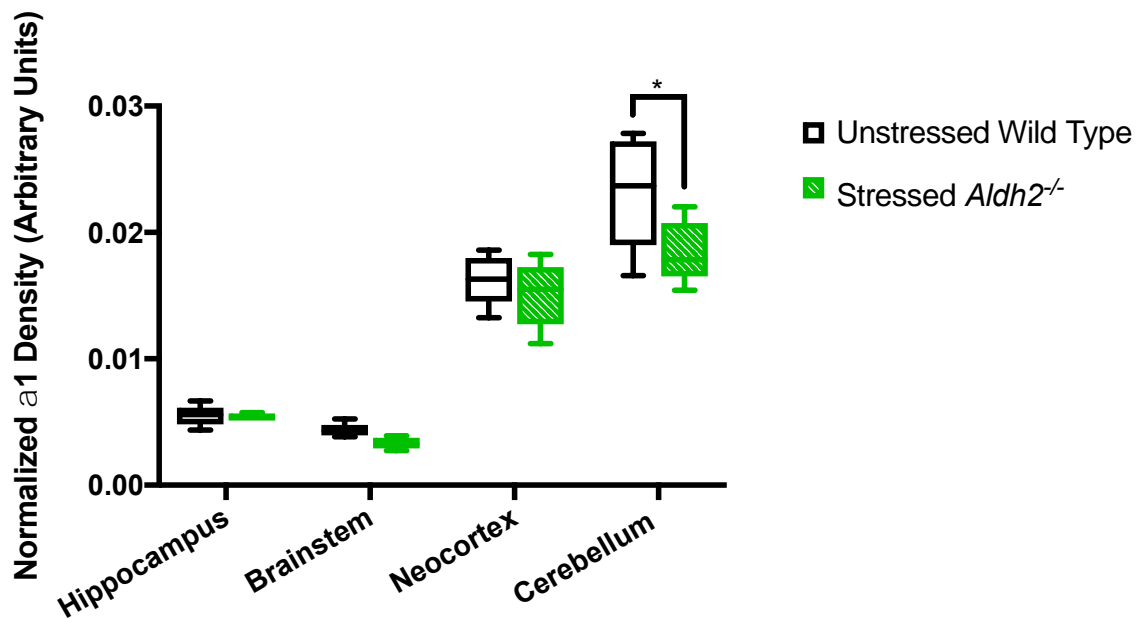


Figure 9. Regional protein expression of the Na⁺/K⁺-ATPase α1 isoform in unstressed wild-type and stressed *Aldh2*^{-/-} mice.

Protein expression of the Na⁺/K⁺-ATPase α1 isoform was normalized to total protein in each lane. A 28-day chronic unpredictable stress protocol significantly decreased α1 isoform protein expression in the cerebellum of *Aldh2*^{-/-} mice compared to unstressed wild-type mice. Data are presented as median with interquartile range (n=5 per group), analyzed by two-way ANOVA with correction for multiple comparisons with Bonferroni post-hoc analysis (p>0.05 for statistical significance).

3.3.3 Naïve Rats

Protein expression of the Na⁺/K⁺-ATPase α1 isoform was investigated across five brain regions in naïve male 450-600g Sprague Dawley rats. Mean Na⁺/K⁺-ATPase α1 isoform expression was highest in the cerebellum and neocortex, and lowest in the hippocampus, striatum, and brainstem, although differences were not significant due to small sample size (**Figure 10**). No differences were found in α1 isoform expression between left and right hemispheres.

3.3.4 Rats Subjected to Transient Middle Cerebral Artery Occlusion

Protein expression of the Na⁺/K⁺-ATPase α1 isoform was investigated across five brain regions in 450-600g Sprague Dawley rats subjected to a 90-minute occlusion of the left middle cerebral artery followed by 24 hours of recovery. Mean Na⁺/K⁺-ATPase α1 isoform expression was highest in the cerebellum and neocortex, and lowest in the hippocampus, striatum, and brainstem, although differences were not significant due to small sample size (**Figures 11-12**). No differences were observed in α1 isoform expression within brain regions when comparing the infarcted hemisphere of rats subjected to transient left MCAo to the left hemisphere of naïve rats (**Figure 11**), or to the non-infarcted hemisphere of infarcted rats (**Figure 12**). However, an increase in α1 isoform expression was noted in the infarcted striatum of rats subjected to left MCAo when compared to non-infarcted striatum.

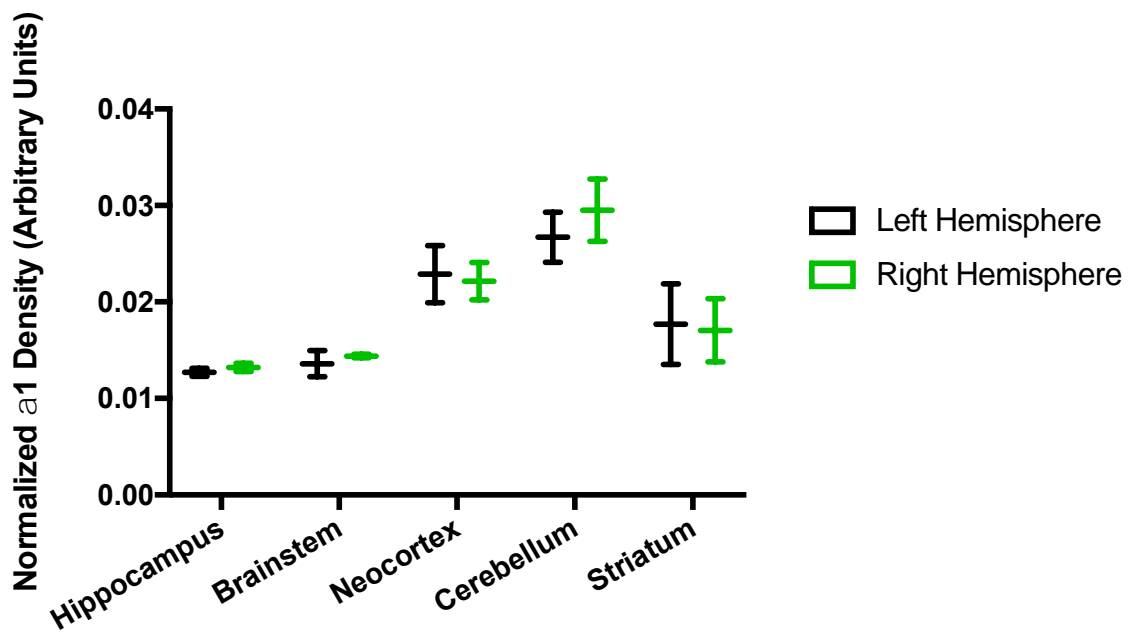


Figure 10. Regional expression of the Na⁺/K⁺-ATPase α1 isoform in naïve rats.

Protein expression of the Na⁺/K⁺-ATPase α1 isoform was normalized to total protein in each lane. No differences in α1 protein expression were found between the same brain regions in left and right hemispheres. Data are presented as mean with total range (n=2 per group).

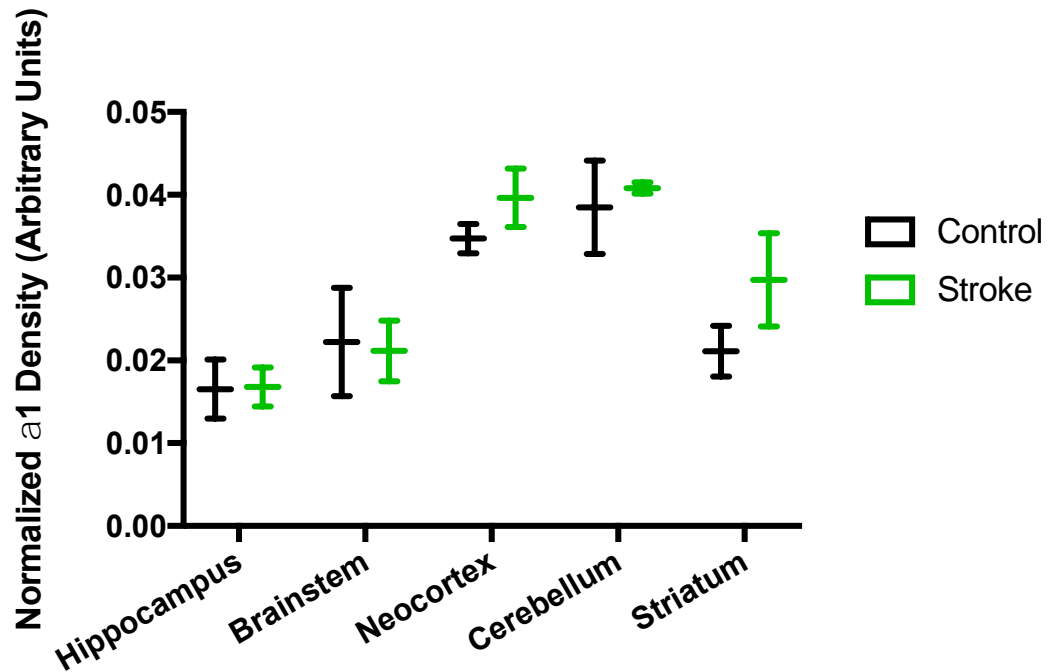


Figure 11. Regional protein expression of the Na⁺/K⁺-ATPase α1 isoform in control and infarcted tissue.

Protein expression of the Na⁺/K⁺-ATPase α1 isoform was normalized to total protein in each lane. An increase in α1 expression was noted in the infarcted striatum when compared to the striatum of naïve rats. Data are presented as mean with total range (n=2 per group).

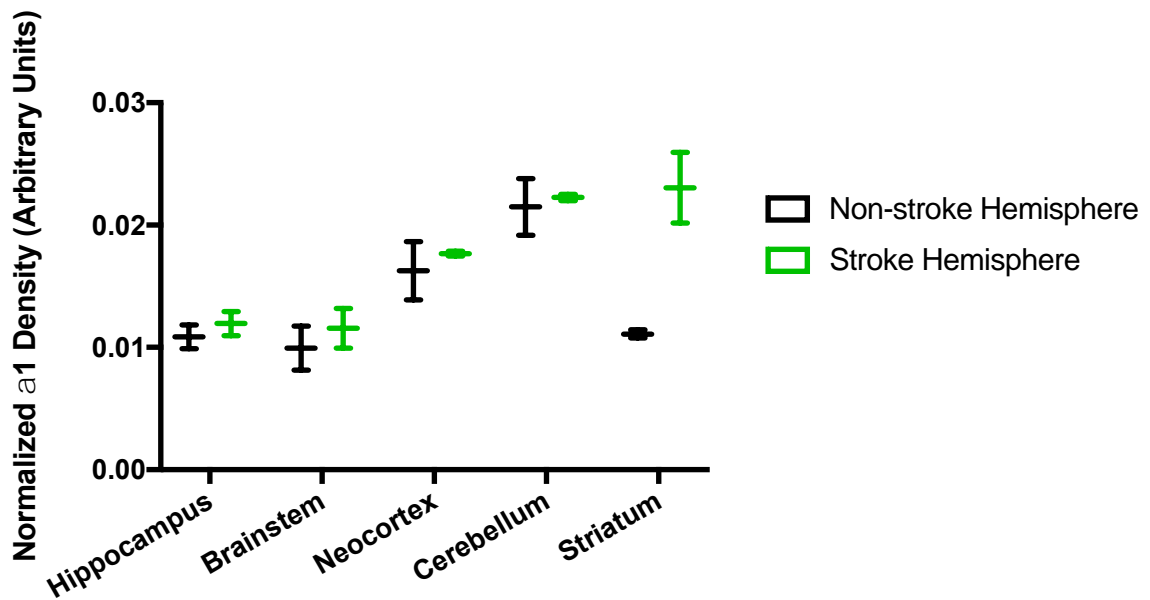


Figure 12. Regional protein expression of the Na⁺/K⁺-ATPase α1 isoform in non-infarcted and infarcted hemispheres of rats subjected to transient MCAo.

Protein expression of the Na⁺/K⁺-ATPase α1 isoform was normalized to total protein in each lane. An increase in α1 expression was noted in the infarcted striatum when compared to the non-infarcted striatum in the same rats. Data are presented as mean with total range (n=2 per group).

3.4 Na⁺/K⁺-ATPase α 3 Isoform Expression

3.4.1 Wild-type Mice Subjected to Chronic Unpredictable Stress

Protein expression of the Na⁺/K⁺-ATPase α 3 isoform was investigated across four brain regions in 5-7 month old wild-type male mice subjected to a chronic unpredictable stress (CUS) protocol for 28 days. Na⁺/K⁺-ATPase α 3 isoform expression was highest in the brainstem, and lowest in the neocortex and cerebellum. Significant differences were found in α 3 isoform expression between the brainstem and all other brain regions (**Figure 13**). However, no significant differences were found in α 3 isoform expression between naïve mice and mice subjected to a 28-day CUS protocol.

3.4.2 *Aldh2*^{-/-} Mice Subjected to Chronic Unpredictable Stress

Protein expression of the Na⁺/K⁺-ATPase α 3 isoform was investigated across four brain regions in 5-7 month old male *Aldh2*^{-/-} mice subjected to a chronic unpredictable stress (CUS) protocol for 28 days. Na⁺/K⁺-ATPase α 3 isoform expression was highest in the brainstem, and lowest in the neocortex and cerebellum. Significant differences were found in α 3 isoform expression between the brainstem and all other brain regions (**Figures 14-16**). No significant differences were found in α 3 isoform expression between naïve mice and mice subjected to a 28-day CUS protocol, regardless of genotype.

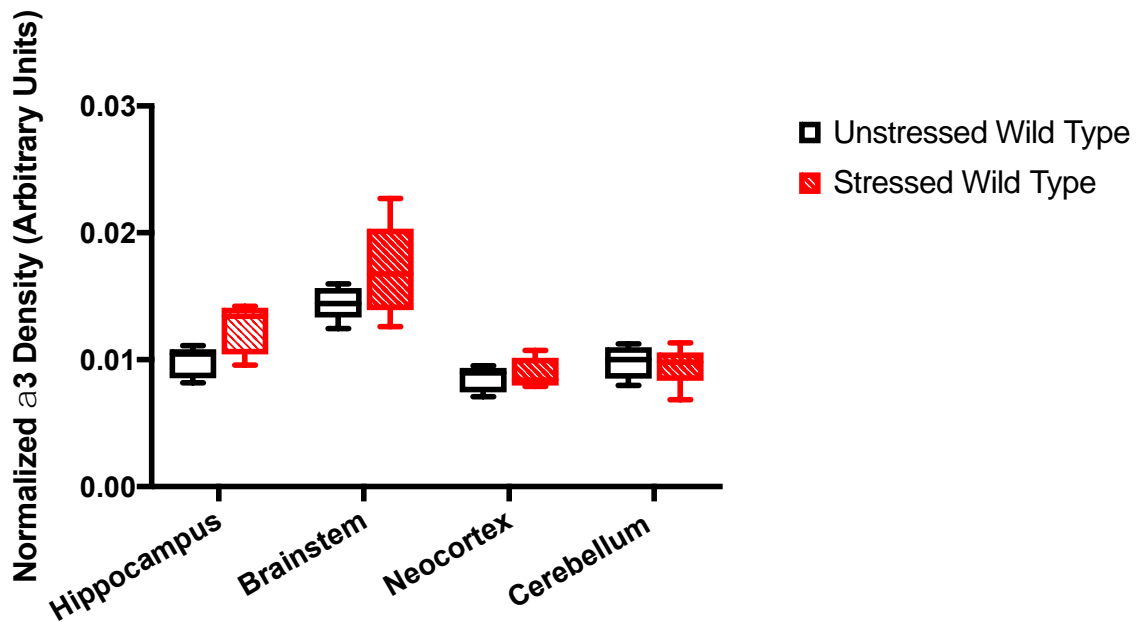


Figure 13. Regional protein expression of the Na⁺/K⁺-ATPase α 3 isoform in naïve and stressed wild-type mice.

Protein expression of the Na⁺/K⁺-ATPase α 3 isoform was normalized to total protein in each lane. A 28-day chronic unpredictable stress protocol did not significantly alter α 3 isoform expression in any of the brain regions studied. Data are presented as median with interquartile range (n=5 per group), analyzed by two-way ANOVA with correction for multiple comparisons achieved with Bonferroni post-hoc analysis (p>0.05 for statistical significance).

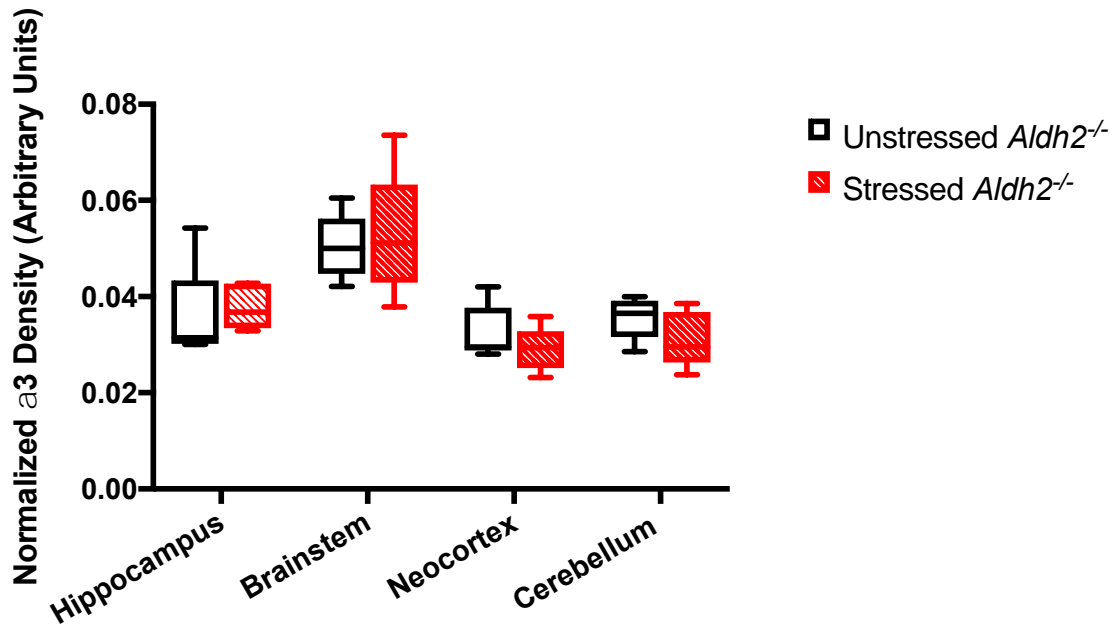


Figure 14. Regional protein expression of the Na⁺/K⁺-ATPase α 3 isoform in naïve and stressed *Aldh2*^{-/-} mice.

Protein expression of the Na⁺/K⁺-ATPase α 3 isoform was normalized to total protein in each lane. A 28-day chronic unpredictable stress protocol did not significantly alter α 3 protein expression. Data are presented as median with interquartile range (n=5 per group), analyzed by two-way ANOVA with correction for multiple comparisons achieved with Bonferroni post-hoc analysis (p>0.05 for statistical significance).

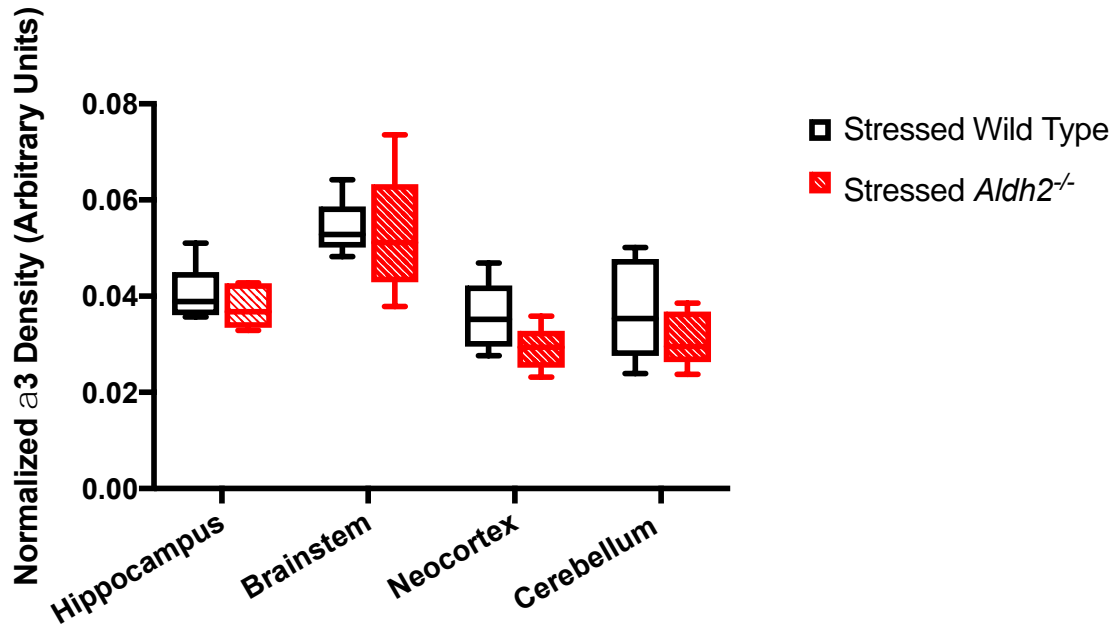


Figure 15. Regional protein expression of the Na⁺/K⁺-ATPase α3 isoform in stressed wild-type and *Aldh2*^{-/-} mice.

Protein expression of the Na⁺/K⁺-ATPase α3 isoform was normalized to total protein in each lane. No significant differences in α3 isoform protein expression were found between wild-type and *Aldh2*^{-/-} mice. Data are presented as median with interquartile range (n=5 per group), analyzed by two-way ANOVA with correction for multiple comparisons achieved with Bonferroni post-hoc analysis (p>0.05 for statistical significance).

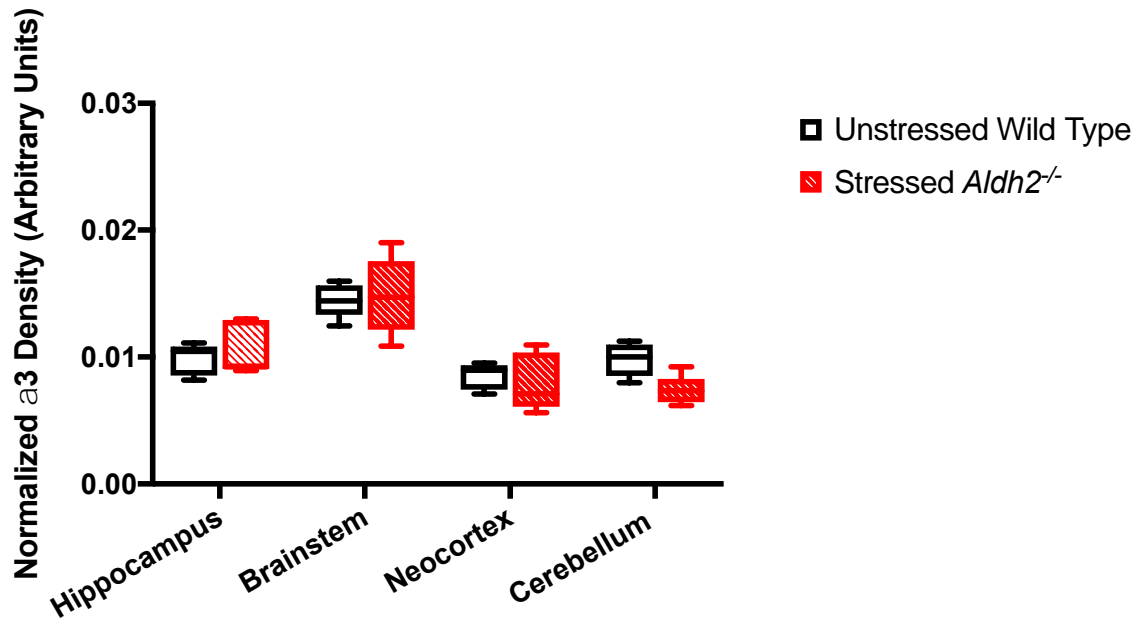


Figure 16. Regional protein expression of the Na⁺/K⁺-ATPase α3 isoform in unstressed wild-type and stressed *Aldh2*^{-/-} mice.

Protein expression of the Na⁺/K⁺-ATPase α3 isoform was normalized to total protein in each lane. A 28-day chronic unpredictable stress protocol did not significantly alter α3 protein expression. Data are presented as median with interquartile range (n=5 per group), analyzed by two-way ANOVA with correction for multiple comparisons with Bonferroni post-hoc analysis (p>0.05 for statistical significance).

3.4.3 Naïve Rats

Protein expression of the Na⁺/K⁺-ATPase α3 isoform was investigated across five brain regions in naïve male 450-600g Sprague Dawley rats. Mean Na⁺/K⁺-ATPase α3 isoform expression was higher in the brainstem compared to other brain regions, although differences were not significant due to small sample size (**Figure 17**). No differences were found in α3 isoform expression between left and right hemispheres.

3.4.4 Rats Subjected to Transient Middle Cerebral Artery Occlusion

Protein expression of the Na⁺/K⁺-ATPase α3 isoform was investigated across five brain regions in 450-600g Sprague Dawley rats subjected to a 90-minute occlusion of the left middle cerebral artery followed by 24 hours of recovery. Mean Na⁺/K⁺-ATPase α3 isoform expression was highest in the brainstem, although differences were not significant due to small sample size (**Figures 18-19**). No differences were observed in α3 isoform expression within brain regions when comparing the infarcted hemisphere of rats subjected to transient left MCAo to the left hemisphere of naïve rats (**Figure 18**), or to the non-infarcted hemisphere of infarcted rats (**Figure 19**). However, an increase in α3 isoform expression was noted in the infarcted striatum and neocortex of rats subjected to left MCAo when compared to non-infarcted striatum and neocortex.

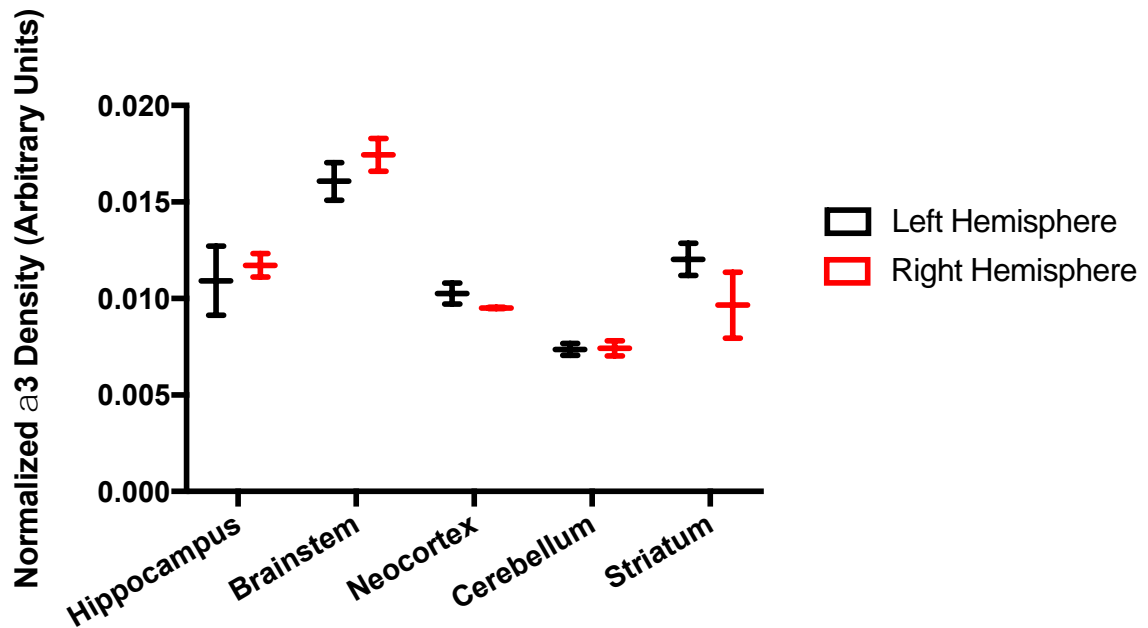


Figure 17. Regional protein expression of the Na⁺/K⁺-ATPase $\alpha 3$ isoform in the left and right hemispheres of naïve rats.

Protein expression of the Na⁺/K⁺-ATPase $\alpha 3$ isoform was normalized to total protein in each lane. Expression of the $\alpha 3$ isoform is highest in the brainstem when compared to other brain regions. No differences in $\alpha 3$ protein expression were found between left and right hemispheres. Data are presented as mean with total range (n=2 per group).

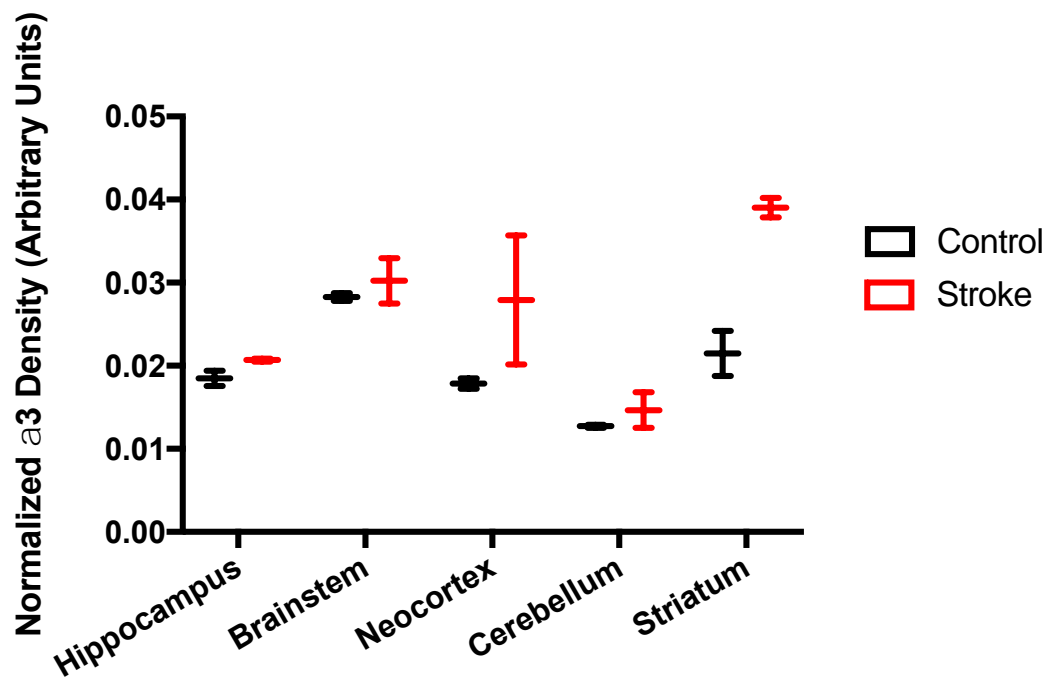


Figure 18. Regional protein expression of the Na⁺/K⁺-ATPase α 3 isoform in control and infarcted tissue.

Protein expression of the Na⁺/K⁺-ATPase α 3 isoform was normalized to total protein in each lane. An increase in α 3 expression was noted in the infarcted striatum and neocortex when compared to the left striatum and neocortex of naïve rats. Data are presented as mean with total range (n=2 per group).

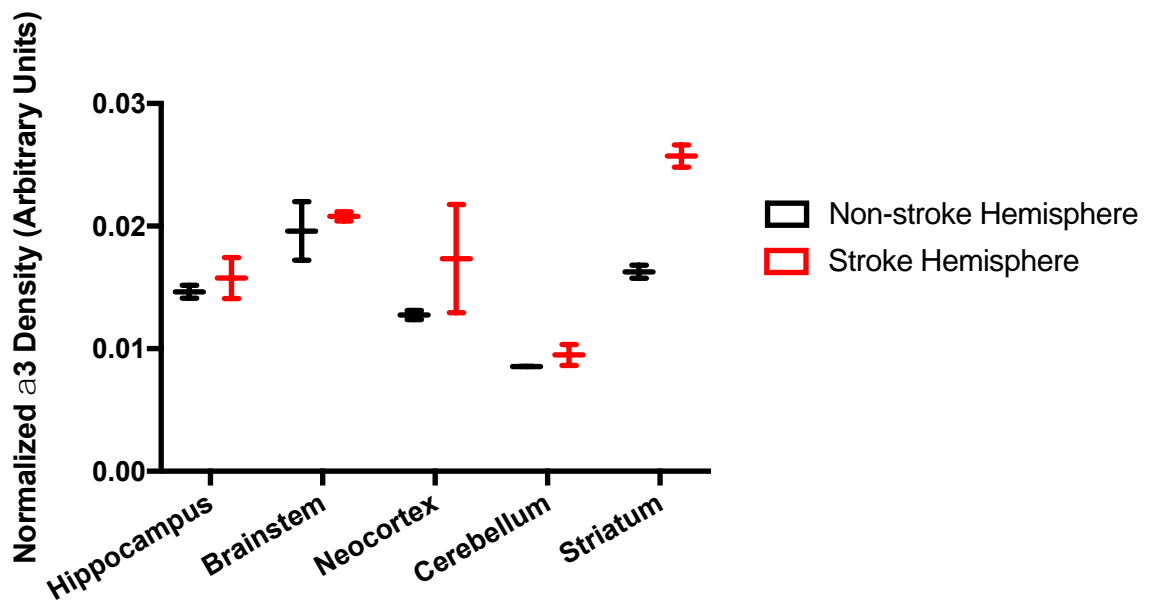


Figure 19. Regional protein expression of the Na⁺/K⁺-ATPase α3 isoform in non-infarcted and infarcted hemispheres of rats subjected to transient MCAo.

Protein expression of the Na⁺/K⁺-ATPase α3 isoform was normalized to total protein in each lane. An increase in α3 expression was noted in the infarcted striatum and neocortex when compared to the non-infarcted right striatum and neocortex. Data are presented as mean with total range (n=2 per group).

3.5 Na⁺/K⁺-ATPase α 1/ α 3 Isoform Expression Ratio

3.5.1 Wild-type Mice Subjected to Chronic Unpredictable Stress

The ratio of α 1/ α 3 isoform expression is indicative of the relative abundance of Na⁺/K⁺-ATPase alpha isoforms in different brain regions. Protein expression of the Na⁺/K⁺-ATPase α 1 and α 3 isoforms was investigated across four brain regions in 5-7 month old male and female wild-type mice subjected to a chronic unpredictable stress (CUS) protocol for 28 days. Based on the α 1/ α 3 isoform ratio, α 1 isoform expression was higher in the neocortex and cerebellum, whereas expression of the α 3 isoform was higher in the hippocampus and brainstem of both male and female mice. Significant differences were found in the α 1/ α 3 isoform expression ratio between all brain regions, except when comparing the hippocampus and brainstem (**Figure 20**). The α 1/ α 3 isoform expression ratio also appears to be lower in the brainstem than in the hippocampus, although this was not found to be statistically significant. However, no significant differences were found in the α 1/ α 3 isoform ratio between naïve mice and mice subjected to a 28-day CUS protocol.

3.5.2 *Aldh2*^{-/-} Mice Subjected to Chronic Unpredictable Stress

Protein expression of the Na⁺/K⁺-ATPase α 1 and α 3 isoforms was investigated across four brain regions in 5-7 month old male *Aldh2*^{-/-} mice subjected to a chronic unpredictable stress (CUS) protocol for 28 days. Based on the α 1/ α 3 isoform ratio, α 1 isoform expression was higher in the neocortex and cerebellum, whereas expression of the α 3 isoform was higher in the hippocampus and brainstem of both male and female mice (**Figures 21-23**). No significant differences were found in the α 1/ α 3 isoform ratio between naïve mice and mice subjected to a 28-day CUS protocol.

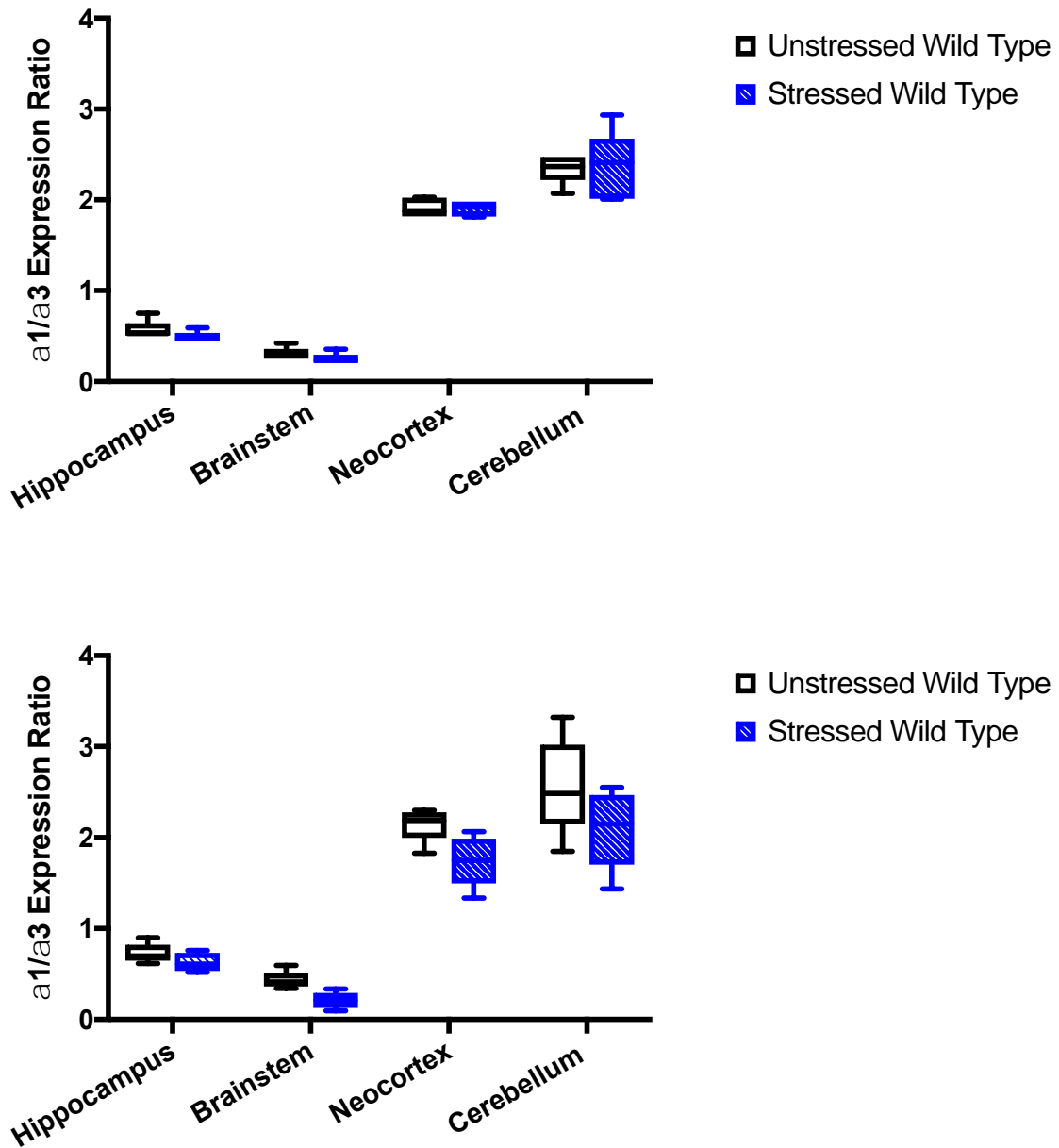


Figure 20. Regional Na⁺/K⁺-ATPase α1/α3 isoform ratios in naïve and stressed male (top) and female (bottom) wild-type mice.

Na⁺/K⁺-ATPase α3 isoform expression is higher in the hippocampus and brainstem whereas α1 isoform expression is higher in the neocortex and the cerebellum. A 28-day chronic unpredictable stress protocol did not significantly alter the α1/α3 expression ratio in any of the brain regions studied. Data are presented as median with interquartile range (n=5 per group), analyzed by two-way ANOVA with correction for multiple comparisons achieved with Bonferroni post-hoc analysis (p>0.05 for statistical significance).

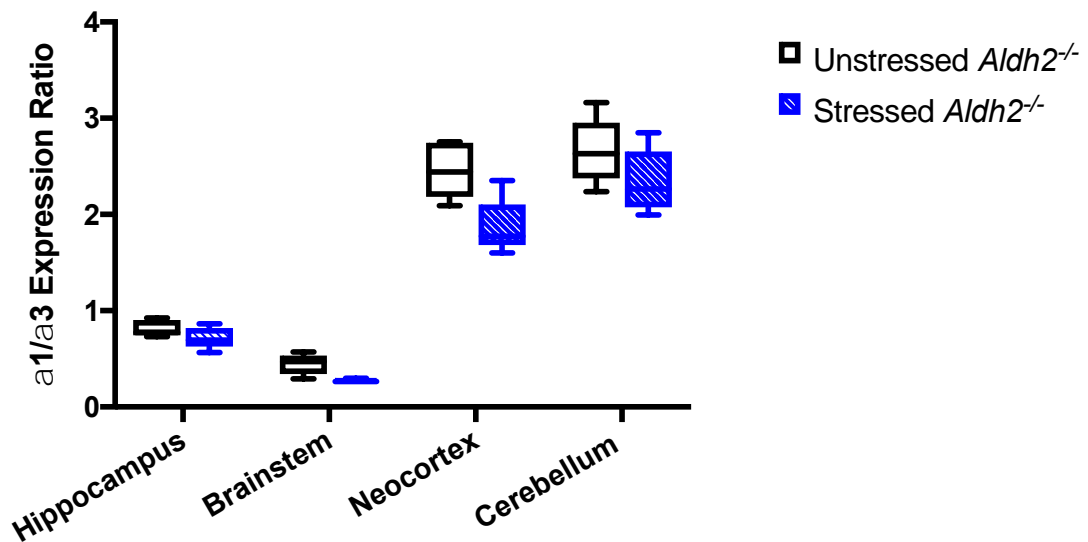
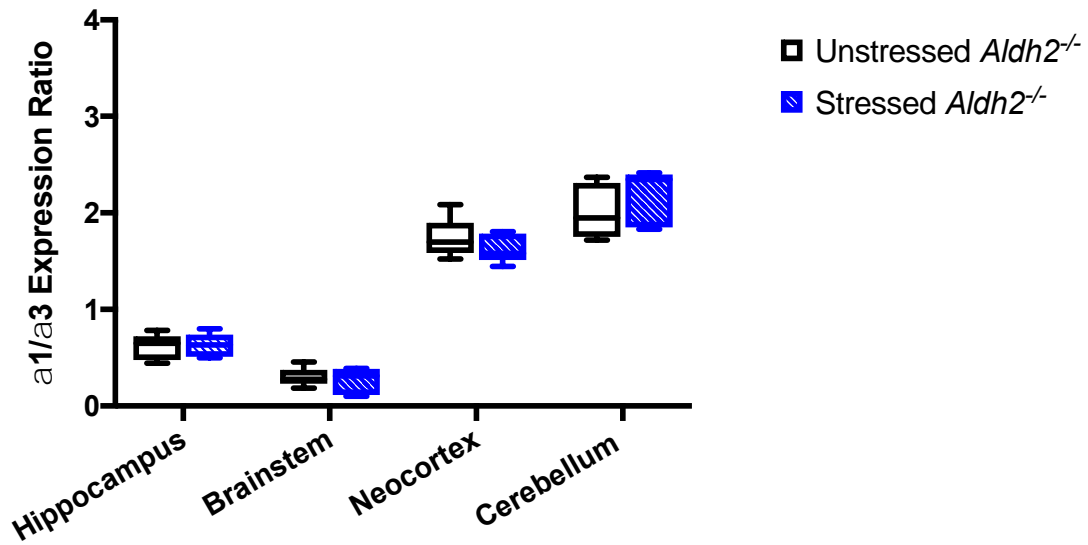


Figure 21. Regional Na⁺/K⁺-ATPase $\alpha 1/\alpha 3$ isoform ratios in naïve and stressed male (top) and female (bottom) *Aldh2*^{-/-} mice.

Na⁺/K⁺-ATPase $\alpha 3$ isoform expression is higher in the hippocampus and brainstem whereas $\alpha 1$ isoform expression is higher in the neocortex and the cerebellum. A 28-day chronic unpredictable stress protocol did not significantly alter the $\alpha 1/\alpha 3$ isoform expression ratio. Data are presented as median with interquartile range (n=5 per group), analyzed by two-way ANOVA with correction for multiple comparisons achieved with Bonferroni post-hoc analysis (p>0.05 for statistical significance).

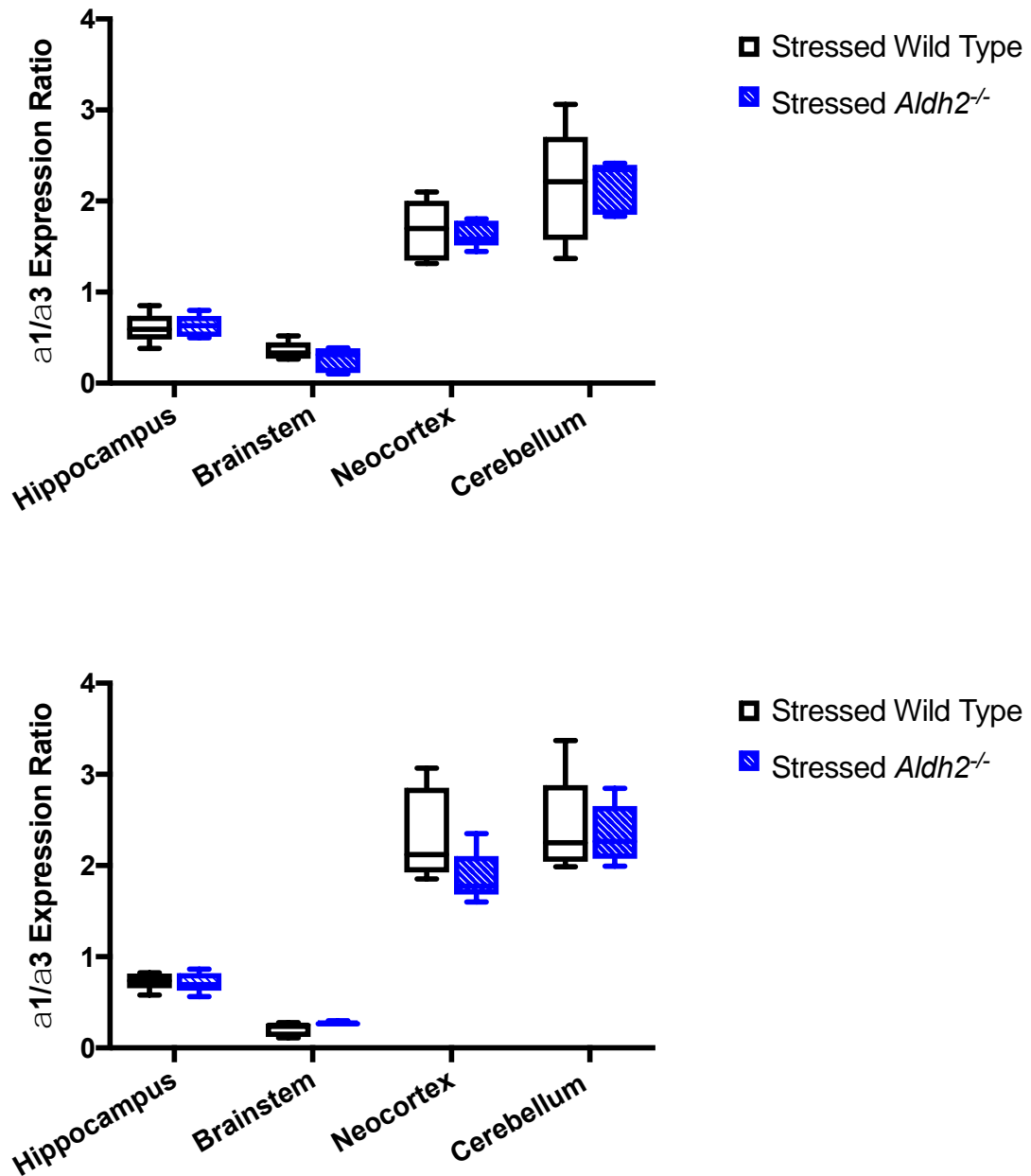


Figure 22. Regional Na⁺/K⁺-ATPase α 1/ α 3 isoform ratios in male (top) and female (bottom) stressed wild-type and *Aldh2*^{-/-} mice.

Na⁺/K⁺-ATPase α 3 isoform expression is higher in the hippocampus and brainstem whereas α 1 isoform expression is higher in the neocortex and the cerebellum. No significant differences in the α 1/ α 3 expression ratio were found between wild-type and *Aldh2*^{-/-} mice. Data are presented as median with interquartile range (n=5 per group), analyzed by two-way ANOVA with correction for multiple comparisons achieved with Bonferroni post-hoc analysis (p>0.05 for statistical significance).

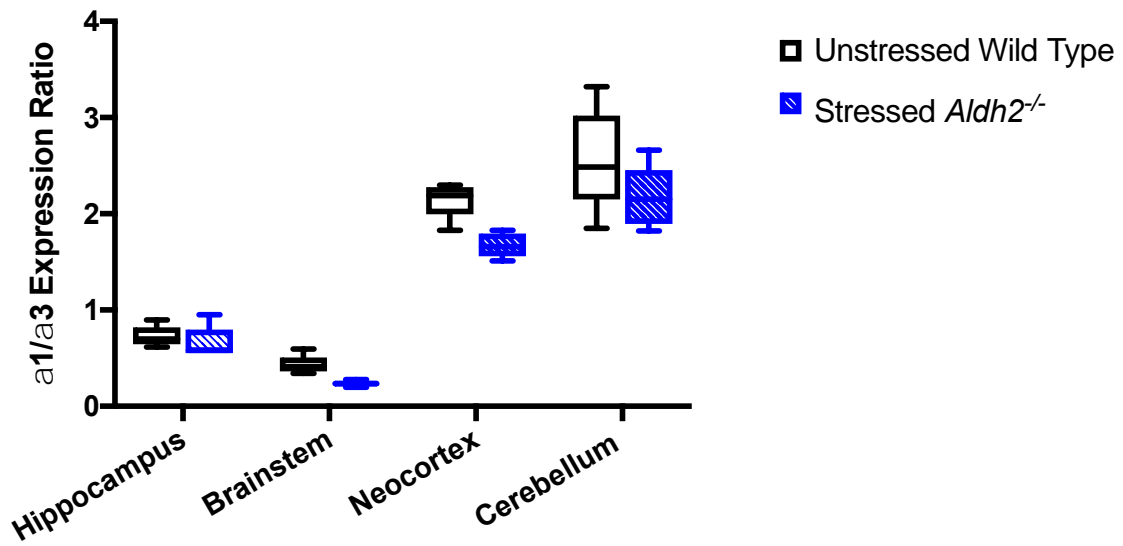
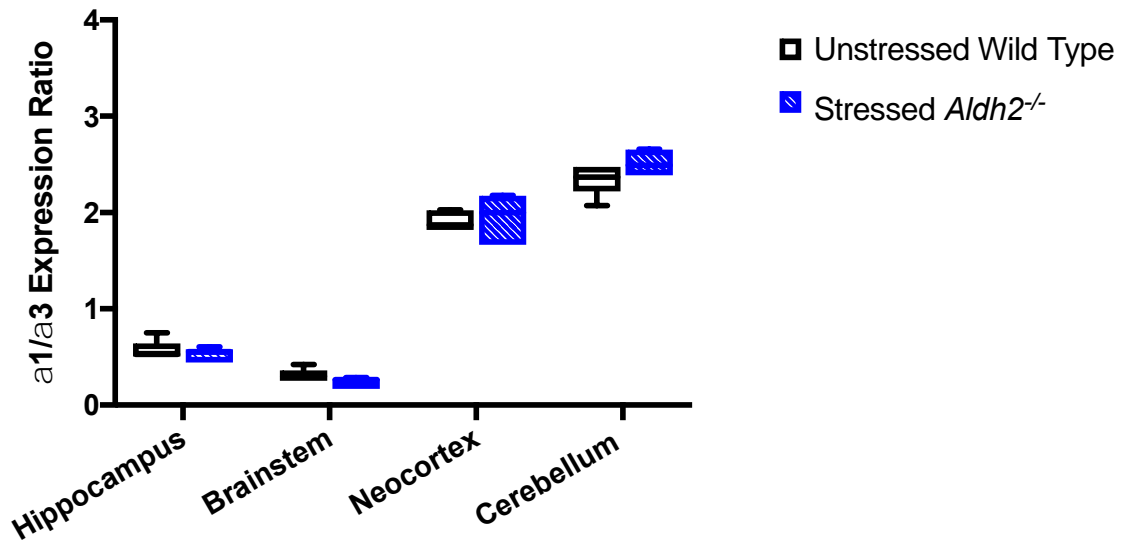


Figure 23. Regional Na⁺/K⁺-ATPase α 1/ α 3 isoform ratios in male (top) and female (bottom) unstressed wild-type and stressed *Aldh2*^{-/-} mice.

Na⁺/K⁺-ATPase α 3 isoform expression is higher in the hippocampus and brainstem whereas α 1 isoform expression is higher in the neocortex and the cerebellum. A 28-day chronic unpredictable stress protocol did not significantly alter the α 1/ α 3 expression ratio in any of the brain regions studied. Data are presented as median with interquartile range (n=5 per group), analyzed by two-way ANOVA with correction for multiple comparisons achieved with Bonferroni post-hoc analysis (p>0.05 for statistical significance).

3.5.3 Naïve Rats

Protein expression of the Na⁺/K⁺-ATPase α 1 and α 3 isoforms was investigated across five brain regions in naïve male 450-600g Sprague Dawley rats. Based on the α 1/ α 3 isoform ratio, α 1 isoform expression was higher in the neocortex and cerebellum, whereas expression of the α 3 isoform was higher in the brainstem. The hippocampus and striatum expressed comparable levels of both the α 1 and α 3 isoforms (**Figure 24**). No differences were observed in the α 1/ α 3 isoform expression ratio between left and right hemispheres.

3.5.4 Rats Subjected to Transient Middle Cerebral Artery Occlusion

Protein expression of the Na⁺/K⁺-ATPase α 1 and α 3 isoforms was investigated across five brain regions in 450-600g Sprague Dawley rats subjected to a 90-minute occlusion of the left middle cerebral artery followed by 24 hours of recovery. Based on the α 1/ α 3 isoform ratio, α 1 isoform expression was higher in the neocortex and cerebellum, whereas expression of the α 3 isoform was higher in the brainstem. The hippocampus and striatum expressed comparable levels of both the α 1 and α 3 isoforms (**Figures 25-26**). A decrease in the α 1/ α 3 isoform expression ratio was noted in the infarcted neocortex when compared to the left neocortex of naïve rats (**Figure 25**), but not when compared to the non-infarcted neocortex of rats subjected to transient MCAo (**Figure 26**). No other differences in the α 1/ α 3 isoform expression ratio were observed within brain regions when comparing infarcted and non-infarcted tissue.

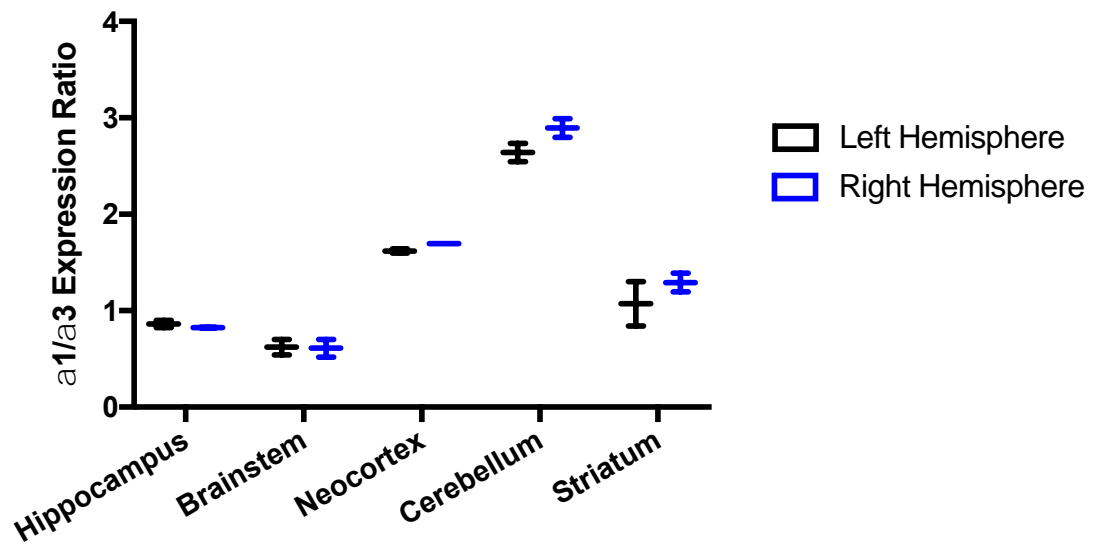


Figure 24. Regional Na⁺/K⁺-ATPase α 1/ α 3 isoform ratios in naïve rats.

Na⁺/K⁺-ATPase α 3 isoform expression is higher in the brainstem whereas α 1 isoform expression is higher in the neocortex and the cerebellum. The hippocampus and striatum exhibit comparable levels of both α 1 and α 3 isoform expression. No differences in the α 1/ α 3 expression ratio were found between the same brain regions in left and right hemispheres. Data are presented as mean with total range (n=2 per group).

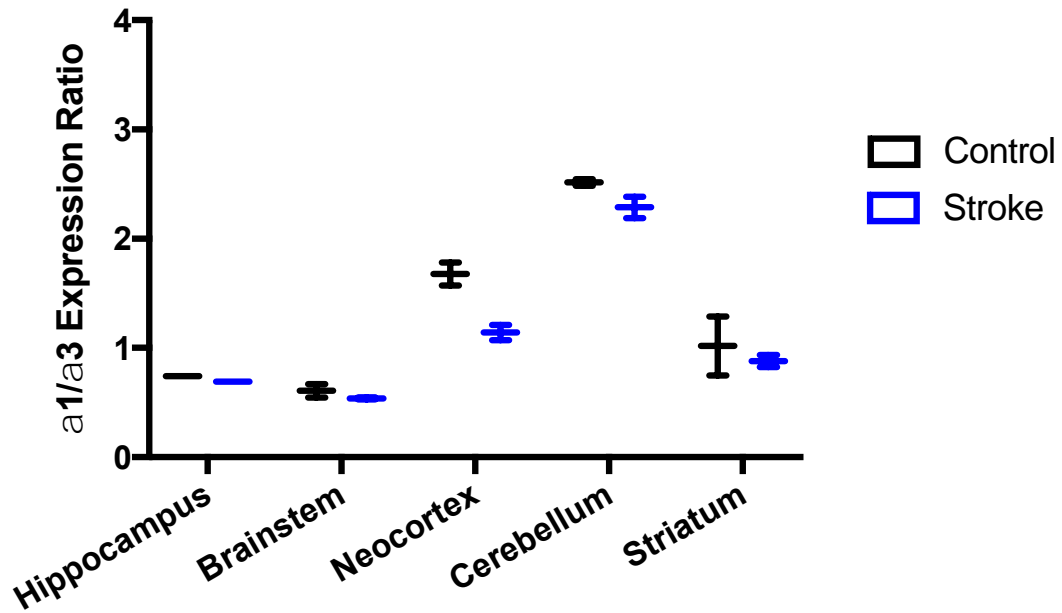


Figure 25. Regional Na⁺/K⁺-ATPase α 1/ α 3 isoform ratios in naïve rats and rats subjected to transient MCA occlusion.

Na⁺/K⁺-ATPase α 3 isoform expression is higher in the brainstem whereas α 1 isoform expression is higher in the neocortex and the cerebellum. The hippocampus and striatum exhibit comparable levels of both α 1 and α 3 isoforms. A decrease in the α 1/ α 3 isoform expression ratio was noted in the infarcted neocortex when compared to the left neocortex of naïve rats. Data are presented as mean with total range (n=2 per group).

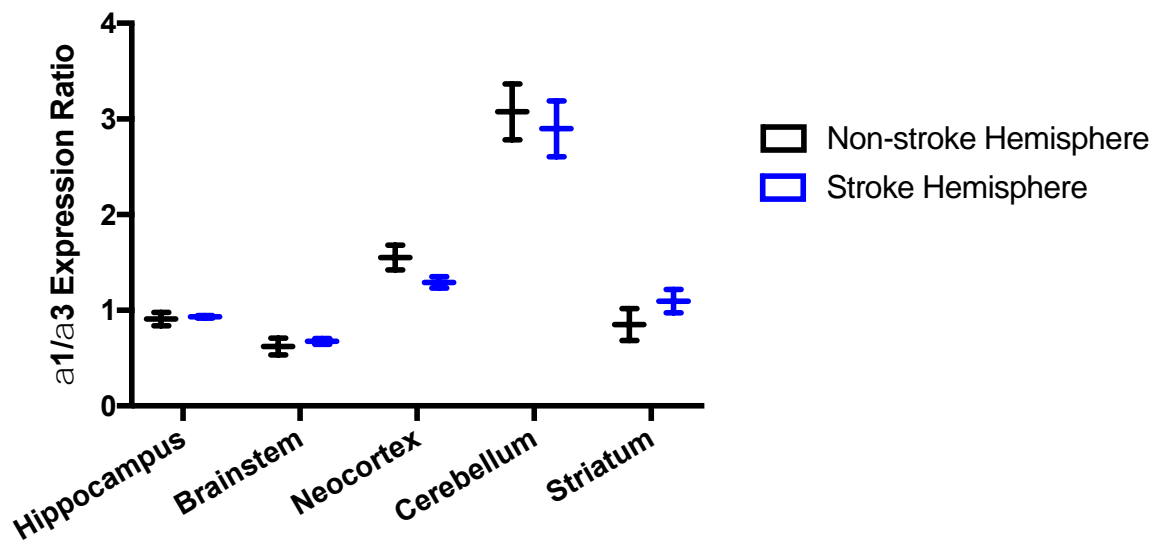


Figure 26. Regional Na⁺/K⁺-ATPase α 1/ α 3 isoform ratios in infarcted and non-infarcted hemispheres of rats subjected to transient MCA occlusion.

Na⁺/K⁺-ATPase α 3 isoform expression is higher in the brainstem whereas α 1 isoform expression is higher in the neocortex and the cerebellum. The hippocampus and striatum exhibit comparable levels of both α 1 and α 3 isoforms. No differences in the α 1/ α 3 expression ratio were observed between the same brain regions in infarcted and non-infarcted tissue. Data are presented as mean with total range (n=2 per group).

3.5.5 Pilot Immunohistochemistry of Naïve Rats

Protein expression of the Na⁺/K⁺-ATPase α 1 and α 3 isoforms was investigated in 40 μ m brain slices of naïve male 450-600g Sprague Dawley rats using an immunohistochemical approach. Slices were taken from bregma +0.70 mm, -2.00 mm, and -5.00 mm.

The Na⁺/K⁺-ATPase α 1 isoform exhibited greater binding in the neocortex, striatum, and thalamus, as well as in the molecular and polymorphonuclear layers of the hippocampus. The Na⁺/K⁺-ATPase α 3 isoform exhibited greatest binding in white matter tracts such as the internal and external capsules, the corpus callosum, the fimbria, the fornix, and the anterior commissure. Moreover, α 3 isoform binding co-localized with DAPI binding in the cell bodies of pyramidal and dentate gyrus neurons within the hippocampus (**Figure 27**). No apparent differences in Na⁺/K⁺-ATPase alpha isoform binding were observed in the CA1, CA2, and CA3 subfields of the hippocampus.

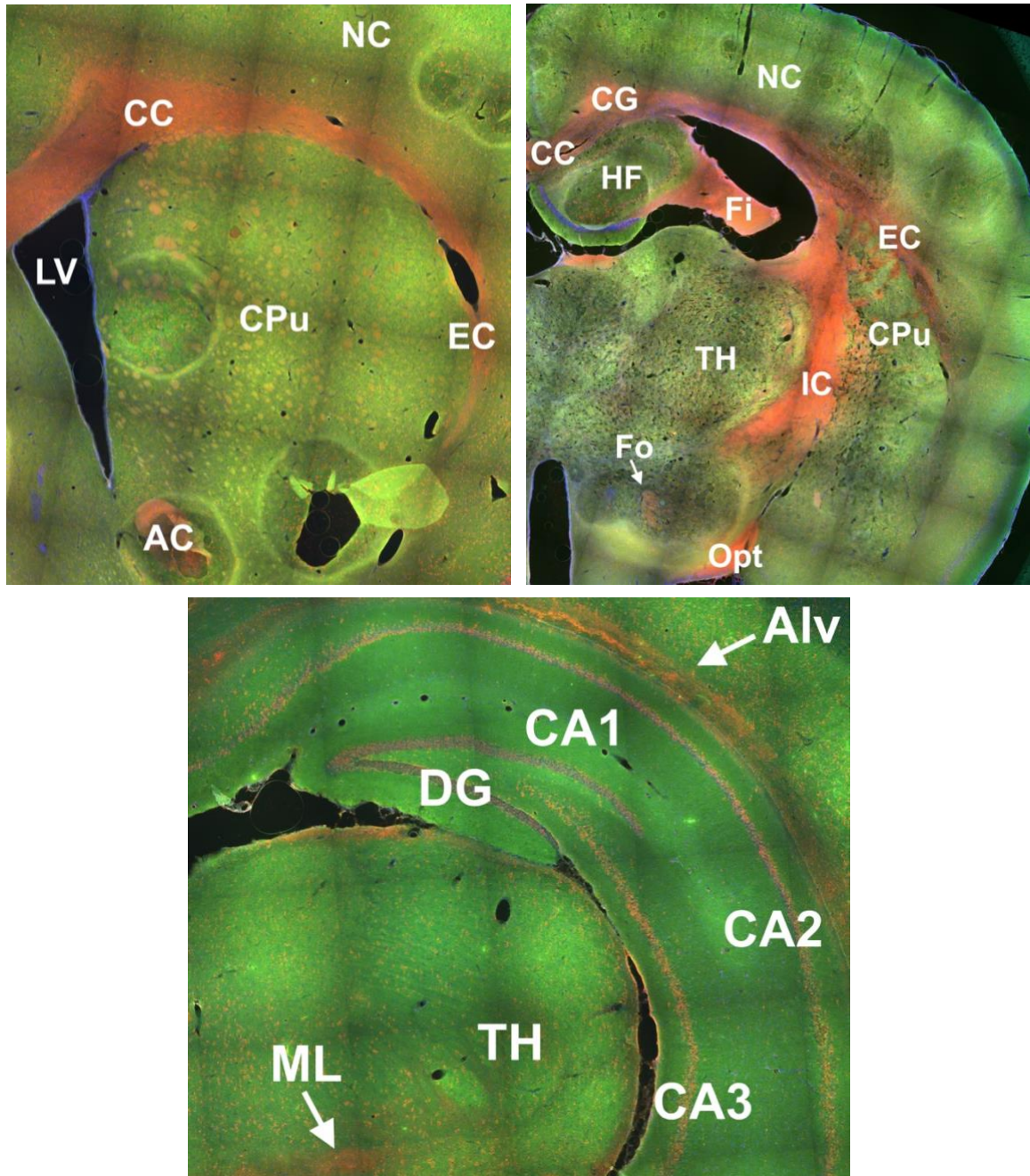


Figure 27. Regional Na⁺/K⁺-ATPase α 1 and α 3 isoform expression in naïve rats.

Na⁺/K⁺-ATPase α 1 (green) isoform binding predominated in grey matter structures including the caudate-putamen (CPu), neocortex (NC), and thalamus (TH), as well as in the CA1, CA2, and CA3 subfields of the hippocampal formation (HF). Na⁺/K⁺-ATPase α 3 (red) isoform binding predominated in white matter tracts including the corpus callosum (CC), cingulum (CG), external capsule (EC), internal capsule (IC), optic tract (Opt), anterior commissure (AC), fimbria (Fi), fornix (Fo), medial lemniscus (ML), and alveus of the hippocampus (Alv), as well as in the cell body layers of the hippocampus containing pyramidal and dentate gyrus neurons.

Chapter 4

Discussion

Selective vulnerability of the central nervous system to ischemia-induced injury is a noteworthy phenomenon that has been demonstrated both clinically and experimentally. However, the differential sensitivity of ‘higher’ and ‘lower’ brain regions to anoxic depolarization is poorly understood and has been a focus of the Andrew laboratory since they found that hypothalamic and brainstem neurons resist the same oxygen-glucose deprivation conditions under which cortical neurons perish (Brisson and Andrew, 2012; Brisson et al., 2013). Failure of the Na⁺/K⁺-ATPase is considered to initiate anoxic depolarization (AD) in neurons; thus, this study investigated whether neuronal susceptibility to AD could be correlated with differential regional expression of known neuronal Na⁺/K⁺-ATPase isozymes.

4.1 Expression in Naïve Mice and Rats

Data from the Allen Mouse Brain Bank showed proportionally greater Na⁺/K⁺-ATPase α 1 isoform mRNA expression in the neocortex and proportionally greater α 3 isoform mRNA in the brainstem. Therefore, the present study aimed to determine if a similar pattern of protein expression can be detected experimentally. The Na⁺/K⁺-ATPase α 1/ α 3 isoform expression ratio, as determined by immunoblotting of mouse and rat brain homogenates, demonstrated that α 1 isoform expression predominates in ischemia-vulnerable brain regions such as the neocortex and cerebellum, while α 3 isoform expression is proportionally higher in the ischemia-resistant brainstem. This is consistent

with parallel regional mRNA studies of Na⁺/K⁺-ATPase α 1 and α 3 isoforms in the mouse brain performed in the Andrew laboratory (C. Lowry, data not shown). These results support the hypothesis that the ischemia-resistant brainstem predominantly expresses the α 3 isoform, which may confer a neuroprotective advantage under energetically unfavorable conditions such as brain ischemia or mitochondrial dysfunction.

Other ischemia-vulnerable regions such as the hippocampus and striatum exhibited comparable expression of both α 1 and α 3 isoforms of the Na⁺/K⁺-ATPase, which may be due in part to a heterogeneous pattern of expression as suggested by pilot immunohistochemical studies in naïve rat brain slices.

4.1.1 The Striatum

Based on pilot immunoblotting experiments conducted in rats, it appears that the striatum expresses nearly equivalent amounts of both isoforms: α 1 isoform expression in the striatum was lower than the neocortex and cerebellum, while α 3 isoform expression was more consistent among these regions. Additional data from both mice and rats is necessary to confirm these findings; however, pilot immunohistochemistry experiments also indicate a heterogeneous pattern of Na⁺/K⁺-ATPase alpha isoform expression in the striatum and adjacent regions. In rat brain slices, it was observed that α 1 isoform binding predominated in the caudate-putamen while α 3 isoform binding predominated in white matter tracts such as the anterior commissure, the internal and external capsule, the cingulum, and the corpus callosum. Numerous studies have suggested that brain grey matter has a higher metabolic rate and consumes more energy than brain white matter, likely rendering it more sensitive to metabolic dysfunction (Reivich et al., 1979; Sokoloff, 1977). Moreover, clinical studies of infarction thresholds based on cerebral blood flow

(CBF) have shown that grey matter is more vulnerable to ischemia than white matter (Arakawa et al., 2006). The regional distribution of $\alpha 1$ and $\alpha 3$ isoforms of the Na^+/K^+ -ATPase shown by immunohistochemistry in this study offers one potential explanation for the differential vulnerability of white and grey matter to ischemia, and warrants further experiments to determine if $\alpha 3$ -dominant neurons are more resistant to anoxic depolarization than $\alpha 1$ isoform-dominant neurons in adjacent regions of the brain.

4.1.2 The Hippocampus

In both mouse and rat immunoblotting experiments, hippocampal expression of the Na^+/K^+ -ATPase seemed to slightly favour $\alpha 3$ isoform over $\alpha 1$ isoform expression, although to a lesser extent than in the brainstem. Importantly, $\alpha 3$ isoform expression was not found to be significantly different between the hippocampus, neocortex, and cerebellum, suggesting that the lower $\alpha 1/\alpha 3$ expression ratio detected in the hippocampus occurs due to lower overall $\alpha 1$ isoform expression. This was confirmed by significantly greater expression of the $\alpha 1$ isoform in the neocortex and cerebellum when compared to the hippocampus. In immunohistochemistry experiments, $\alpha 3$ isoform binding was largely restricted to the fornix and fimbria of the hippocampus, which represent major nerve fibre bundles that connect the hippocampus to subcortical structures (Witter, 2009). This binding pattern resembles the differential binding of $\alpha 1$ and $\alpha 3$ isoforms in grey and white matter observed in the striatum, and lends support to the $\alpha 1$ isoform-mediated theory of gray matter vulnerability to ischemia described earlier.

Within the hippocampal layers, $\alpha 3$ isoform binding predominated in the cell bodies of pyramidal and dentate gyrus neurons, and co-localized with DAPI, which binds to adenine-thymine rich regions in DNA. The polymorphic and molecular layers of the

hippocampus containing nerve fibers, dendrites, and interneurons predominantly bound the $\alpha 1$ isoform of the Na^+/K^+ -ATPase. This may provide a rationale for the high vulnerability of the hippocampus to anoxic depolarization despite the low $\alpha 1/\alpha 3$ isoform ratio observed in immunoblotting results.

The hippocampus is composed of several interconnected sub-regions which comprise molecularly distinct neuronal populations (Duvernoy, 2005). No apparent differences were observed in Na^+/K^+ -ATPase alpha isoform expression between differentially vulnerable regions of the hippocampus, such as the CA1 and CA3 subfields. Numerous studies have established the hippocampal CA1 subfield to be especially vulnerable to secondary ischemic injury, as evidenced by delayed injury 24 hours after global ischemia (Schmidt-Kastner and Freund, 1991). Other regions of the hippocampus, such as the adjacent CA3 subfield, are more resilient to secondary ischemic injury; however, the cellular properties underlying this disparity are poorly understood. Based on pilot immunohistochemical experiments, the delayed selective vulnerability of the CA1 hippocampal subfield to ischemic damage is not likely related to differential Na^+/K^+ -ATPase alpha isoform expression. This suggests that delayed selective vulnerability of the CA1 hippocampal subfield to ischemia is mediated by a different mechanism than that of selective susceptibility to anoxic depolarization.

The mechanisms underlying the selective vulnerability of the hippocampal CA1 region to delayed ischemic injury are poorly understood, particularly since regional susceptibility to ischemia varies based on the animal model studied. One potential explanation is that endogenous levels of oxidative stress within different neuronal populations of the hippocampus are not equivalent – CA1 neurons and their mitochondria

contain significantly higher levels of reactive oxygen species (ROS) than CA3 neurons under normal conditions (Wang and Michaelis, 2010). Furthermore, CA1 neurons have significantly higher expression of both anti-oxidant and ROS-producing genes than CA3 neurons, suggesting higher levels of basal oxidative stress. This finding is consistent among other ischemia-vulnerable neurons of the brain, including cerebellar granule neurons and dopaminergic neurons in the midbrain (Chung et al., 2005; Wang et al., 2009). High endogenous oxidative stress within the CA1 region may be attributed to the functional role of ROS as signalling molecules – superoxide is required for long-term potentiation in the CA1 region but not the CA3 region (Klann, 1998; Thiels et al., 2000). High intrinsic oxidative stress leads to increased generation of free radicals and ROS within the mitochondrial ETC which can damage nearby mitochondrial DNA and impair mitochondrial enzyme function. Due to the limited repair capacity of mitochondrial DNA and the importance of mitochondrial enzymes for ATP production, even minor disruptions can lead to dysfunctional mitochondria. An important mechanism by which mitochondria reduce ROS production and protect themselves from oxidative stress is through the uncoupling of oxidative phosphorylation and ATP synthesis, which is mediated by the mitochondrial protein uncoupling protein 2 (UCP2) (Mattiasson et al., 2003). Neurons in the CA1 region express lower basal levels of UCP2 than neurons in the CA3 region (Richard et al., 2001). This causes further accumulation of ROS, resulting in a vicious cycle of oxidative damage and mitochondrial impairment. Based on all of these factors, CA1 neurons encountering additional oxidative stress may be more easily overwhelmed than CA3 neurons, accelerating the impact of secondary ischemic damage.

Selective vulnerability of the CA1 region may also be attributed in part to glial cells. Under ischemic conditions, CA1 astrocytes exhibit decreased glutamate uptake compared to dentate gyrus astrocytes, while CA1 microglia are activated earlier and to a greater extent than CA3 and DG microglia (Bernaudin et al., 1998; Ouyang et al., 2007;). Activation of microglia releases large amounts of ROS and promotes inflammation, which further damages the vulnerable CA1 region. In addition to high intrinsic oxidative stress, CA1 neurons have high intrinsic transcriptional activity of genes responsible for inflammation as well as cytokine and chemokine production (Wang et al., 2007). This is suggestive of chronic inflammatory stress in the CA1 region, which would render it more vulnerable to ischemia-induced inflammation.

Lastly, the protein hamartin is selectively upregulated by ischemia in neurons of the hippocampal CA3 subfield, but not in the CA1 subfield (Papadakis et al., 2013). Hamartin promotes efficient autophagy, which is thought to be neuroprotective following cerebral ischemia. The inability of hippocampal CA1 neurons to upregulate hamartin may contribute to their vulnerability to delayed ischemic injury. Although not comprehensive, intrinsic characteristics of the hippocampal CA1 field such as the ones described above are plausible candidates underlying a selective vulnerability to ischemic damage not mediated by differential Na^+/K^+ -ATPase alpha isoform expression.

4.2 Oxidative Stress Cohorts

In addition to demonstrating regional differences in Na^+/K^+ -ATPase alpha isoforms in naïve rodent brains, this study proposed that heightened oxidative stress may lead to changes in alpha isoform expression. To investigate whether chronic mitochondrial

dysfunction and impaired metabolic function induce alterations in Na⁺/K⁺-ATPase alpha isoform expression in vulnerable brain regions, we used two mouse models of elevated metabolic and oxidative stress: the *Aldh2*^{-/-} mouse model and the environmental stress model of chronic unpredictable stress (CUS). These mice exhibited similar trends in regional $\alpha 1$ and $\alpha 3$ isoform expression to naïve mice, with $\alpha 1$ isoform expression predominating in the neocortex and cerebellum, $\alpha 3$ isoform expression prevailing in the brainstem, and slightly higher $\alpha 3$ than $\alpha 1$ isoform expression in the hippocampus. Expression of the $\alpha 3$ isoform was highest in the brainstem and fairly consistent between the neocortex, cerebellum, and hippocampus, while expression of the $\alpha 1$ isoform was highest in the neocortex and cerebellum and lowest in the hippocampus and brainstem.

Elevated oxidative stress from ALDH2 deficiency, chronic unpredictable stress, or a combination of the two did not have a significant impact on protein expression of the Na⁺/K⁺-ATPase alpha isoforms in either the male or female mouse brain, with the exception of a small but significant decrease in $\alpha 1$ isoform expression in the cerebellum of chronically stressed male *Aldh2*^{-/-} mice when compared to unstressed wild-type mice. We had hypothesized that expression of the Na⁺/K⁺-ATPase $\alpha 3$ isoform would increase in vulnerable brain regions as a neuroprotective response to oxidative stress and chronic metabolic impairment, but this negative result indicated that our elevated oxidative stress models did not modulate Na⁺/K⁺-ATPase alpha isoform expression in the brain. Importantly, this does not contradict the possibility of altered Na⁺/K⁺-ATPase alpha isoform expression following anoxic depolarization and ischemia, but potentially excludes elevated environmental and oxidative stress as confounding factors for the results observed in rats subjected to transient middle artery occlusion.

4.3 Ischemic Cohort

The final phase of this study proposed that transient ischemic insult followed by a recovery period may induce alterations in Na⁺/K⁺-ATPase alpha isoform expression in vulnerable brain regions as a neuroprotective response to anoxic depolarization. To test the hypothesis that vulnerable brain regions would upregulate $\alpha 3$ isoform expression following ischemia, we used a transient MCAo rat model of stroke with a 24 hour recovery period. Pilot immunoblotting results showed similar trends in regional Na⁺/K⁺-ATPase $\alpha 1$ and $\alpha 3$ isoform expression to naïve rats in brain regions not supplied by the middle cerebral artery, with $\alpha 1$ expression predominating in the cerebellum, $\alpha 3$ expression prevailing in the brainstem, and slightly higher $\alpha 3$ than $\alpha 1$ isoform expression in the hippocampus. The lack of changes in Na⁺/K⁺-ATPase alpha isoform expression in these areas supports earlier results of this study indicating that elevated oxidative stress (from secondary ischemic injury mechanisms) does not alter Na⁺/K⁺-ATPase alpha isoform expression. On the other hand, the neocortex and striatum receive the majority of their blood supply from the middle cerebral artery, with preliminary results suggesting increased Na⁺/K⁺-ATPase alpha isoform expression in infarcted brain regions following ischemia-reperfusion.

4.3.1 Infarction in the striatum

Although additional experiments are needed to confirm these findings, the striatum was most affected by ischemia-reperfusion, with an increase in both $\alpha 1$ and $\alpha 3$ isoform expression in infarcted tissue when compared to both naïve rats and the non-infarcted hemisphere of rats subjected to transient MCAo. Most notably, the $\alpha 1/\alpha 3$ isoform expression ratio was not different in infarcted striatum samples, despite large increases in the expression of both isoforms. This suggests the possibility of an overall increase in

Na⁺/K⁺-ATPase density in the striatum 24 hours after infarction, and may represent an adaptive response to ischemia wherein the Na⁺/K⁺-ATPase is overexpressed in an attempt to mitigate severe disruptions in metabolic function and ion homeostasis.

4.3.2 Infarction in the neocortex

Interestingly, the neocortex exhibited an increase in $\alpha 3$, but not $\alpha 1$ isoform expression, although this was only observed in one of two rats studied. This may be due to differences in infarct volume inherent to the transient MCAo rat model of stroke – rats with a confirmed stroke typically sustain infarct in the striatum, with variable involvement of the neocortex (Longa et al., 1989). Consistent with increased $\alpha 3$ isoform expression and unaltered $\alpha 1$ isoform expression, the $\alpha 1/\alpha 3$ expression ratio was lower in infarcted neocortex samples, although this was most apparent when compared to naïve neocortex samples. Additional studies are needed to increase statistical power and verify these ischemia-induced changes in Na⁺/K⁺-ATPase alpha isoform expression. Infarcted rats with and without cortical involvement should be analyzed as separate cohorts to reduce variability in neocortical Na⁺/K⁺-ATPase alpha isoform expression.

4.3.3 Neuroprotective effect of altered Na⁺/K⁺-ATPase alpha isoform expression

Perhaps the most significant finding of this study is that regional Na⁺/K⁺-ATPase alpha isoform protein expression is consistent with previous mRNA data, with high $\alpha 1$ expression in higher brain structures such as the neocortex and cerebellum and proportionally greater $\alpha 3$ expression in the brainstem. Additionally, elevated oxidative and environmental stress did not impact alpha isoform expression in any of the brain regions studied. This establishes a good baseline for future studies with infarcted animals, since changes in regional Na⁺/K⁺-ATPase alpha isoform expression are not likely confounded

by the stressful environmental conditions implicated in surgery, nor by secondary ischemic injury mechanisms underlying the selective vulnerability of brain regions such as the hippocampal CA1 subfield. Rather, it appears that anoxic depolarization may elicit altered Na⁺/K⁺-ATPase alpha isoform expression in infarcted regions of the brain, which suggests a possible mechanism underlying the ischemia-protective effect of induced spreading depolarization prior to focal ischemia (Kawahara et al., 1995; Kobayashi et al., 1995; Yanamoto et al., 1998). Nonetheless, these results should be treated with caution due to the small sample size analyzed. This phenomenon warrants further investigation to determine if preconditioning rodents with induced spreading depolarization may modulate Na⁺/K⁺-ATPase alpha isoform expression in a neuroprotective manner.

4.4 Study Assumptions

The results obtained in this study were based on several assumptions. Firstly, that neurological impairment in rats subjected to transient MCAo correlates with infarction volume. In rats used for biochemical studies, infarction volume was not assessed, since earlier experiments in this study suggested that increased tissue manipulation during TTC staining of brain tissue reduced its viability and may have confounded biochemical analyses. This was addressed by prior experiments in our laboratory indicating that rats exhibiting higher neurological impairment also suffered larger infarcts with a Spearman's rank correlation coefficient of 0.84.

For immunoblotting experiments, we assumed that binding of antibodies to the PVDF membrane is similar for α 1 and α 3 isoforms, allowing a direct comparison between the abundance of these proteins based on band densitometry values. It was also assumed

that all proteins are transferred equally from the gel to the PVDF membrane during transfer electrophoresis. This was addressed by normalizing protein band densities to total protein in each lane of TGX Stain-Free™ Precast Gels, which contain a non-protein moiety that binds to protein in response to UV302-activation. Once activated, this non-protein moiety transfers together with protein to the PVDF membrane and can be imaged with the UV302 function of the Azure Biosystems c600 Gel Imaging System and the cSeries Capture Software. Numerous studies have indicated this method of protein normalization is more effective and reliable than traditional housekeeping proteins such as beta-actin (Colella et al., 2012; Gilda and Gomes, 2015).

4.5 Study Limitations

4.5.1 Study Design

Limitations of this study include a small sample size (n=5 per group for mice, n=2 per group for rats). To increase the statistical power of results from rat brain tissue, this study will involve another phase in the near future in which the number of control and infarcted rats is increased. Additional immunoblotting and immunohistochemical experiments will provide insight into the similar levels of $\alpha 1$ and $\alpha 3$ isoform expression observed in the hippocampus and striatum, with the subregions of these areas independently analyzed to account for heterogeneous expression of the Na⁺/K⁺-ATPase alpha isoforms within brain regions.

The number of brain regions investigated from each mouse rendered it impossible to measure pump isoform expression in all four cohorts on one gel. Since each immunoblotting gel contained only 12 protein lanes, only 3 of the cohorts were compared

at once, using either wild-type or *Aldh2*^{-/-} mice as unstressed controls. Similarly, the number of brain regions investigated from each rat limited the comparison of infarcted tissue to either the non-infarcted hemisphere or to naïve rat tissue on each gel. Future experiments should make use of gels with more than 12 lanes to increase the number of directly comparable samples and reduce the number of experiments required.

Total lane protein images revealed a distinct pattern of total protein expression in infarcted tissue samples, in which several prominent bands found in non-infarcted tissue were missing (**Figure 28, Appendix**). This likely reflects degradation of several abundant proteins by hydrolytic enzymes released from lysosomes in infarcted tissue, and may represent a potential confound of this study if the Na⁺/K⁺-ATPase alpha isoforms were over-represented in infarcted protein samples. Future studies should compare total lane protein results with a reliable housekeeping protein which is expressed consistently in all brain regions regardless of infarct status.

4.5.2 Animal Housing

The results presented above were based on the assumption that different cohorts of animals were subject to similar housing conditions. However, housing of mice that underwent the chronic unpredictable stress (CUS) protocol was slightly different than that of their naïve counterparts: CUS mice were singly housed on a reverse 12-hour light-dark cycle, while naïve mice were housed with littermates on a standard 12-hour light-dark cycle. Tissue for both cohorts was collected at the same time, thus the possibility exists that differences in circadian rhythm between cohorts impacted Na⁺/K⁺-ATPase alpha isoform expression. mRNA expression of both alpha isoforms of the Na⁺/K⁺-ATPase has been shown to exhibit a circadian rhythm in non-brain tissues of mice, although no

evidence exists to support a similar relationship in the brain. Nevertheless, this potential confound cannot be completely overlooked (Zhang et al., 2014).

Another possible limitation of the animal housing conditions in this study included an ongoing construction project adjacent to the animal care facility, which may have confounded results by promoting a chronic stress response in animals frightened by loud, abrupt noise. While this may have dampened the effect of the CUS protocol on mice, the presence of significant changes in Na⁺/K⁺-ATPase alpha isoform expression in infarcted rats (housed in the same facility) suggests that alterations in alpha isoform expression are not likely confounded by stressful environmental conditions.

4.5.3 Dissection Technique

The results presented in this study were somewhat divergent between immunoblotting and immunohistochemical experiments. While immunoblotting of hippocampal and striatal homogenates revealed fairly proportionate expression of both alpha isoforms of the Na⁺/K⁺-ATPase, immunohistochemistry of brain slices revealed a heterogeneous pattern of binding wherein $\alpha 1$ isoform binding was primarily localized to grey matter while $\alpha 3$ isoform binding was predominantly observed in white matter tracts. Although the immunohistochemical results of this study are preliminary and not quantitative, these differing results may be explained in part by the dissection technique, which did not necessarily exclude white matter tracts such as the fimbria-fornix pathway of the hippocampus or the internal capsule adjacent to the striatum. In future experiments, white and grey matter tracts of the hippocampus and striatum should be divided and analyzed separately in order to conduct a more robust evaluation of Na⁺/K⁺-ATPase alpha isoform expression in ischemia-vulnerable brain regions.

4.5.4 Animal Models

The animal models used in this study are also subject to several limitations. All mice used were of the common C57BL/6 strain which is known to be particularly resistant to chronic environmental stress conditions. Chronic unpredictable stress (CUS) protocols for C57BL/6 mice are recommended to last a minimum of eight weeks (Monteiro et al., 2015). However, the type and duration of stressors used to elicit a stress response in mice were limited by the University Animal Care Committee, which did not approve more severe stressors such as predatory stress from another animal's bedding or physiological stress from lipopolysaccharide injection (Farooq et al., 2012). The use of a more severe CUS protocol may have elicited changes in regional Na⁺/K⁺-ATPase alpha isoform expression not observed under the current CUS protocol.

The transient MCAo model of stroke is limited by the morphological characteristics of rat cerebral vasculature. As a result of widespread variation in collaterals within the cerebral vasculature, as well as a particularly low infarction threshold compared to humans, up to 35% of rats do not experience any infarct despite ideal surgical technique and occlusion of the middle cerebral artery (Longo et al., 1989). Moreover, the majority of rats undergoing MCAo experience lesions restricted to the striatum, with only a fraction of rats also exhibiting cortical infarction. In the absence of infarction volume analysis by TTC staining or other methods, biochemical experiments of infarcted rats cannot assert with 100% confidence that the brain tissue being analyzed is indeed infarcted. Using a viable method for analyzing infarct volume that does not confound biochemical analyses, such as an immunohistochemical marker, would increase the validity of results and reduce the variation observed in immunoblotting experiments of supposedly infarcted neocortical samples.

4.6 Future Directions

This study investigated the impact of oxidative stress on regional Na⁺/K⁺-ATPase alpha isoform expression in mice, while the effect of ischemia on regional alpha isoform expression was studied in rats. In order to assess whether the results observed in infarcted rats is consistent among different species, this study should be replicated in a mouse stroke model. Furthermore, stroke models do not subject all brain areas to equivalent ischemic stress, rendering it difficult to assess ischemia-induced alterations in Na⁺/K⁺-ATPase alpha isoform expression in non-infarcted brain areas. The use of a transient MCA occlusion limits the infarct to the striatum with variable involvement of the neocortex (Longo et al., 1989). In order to fully appreciate and study selective vulnerability of different brain regions to anoxic depolarization and ischemia, future studies should employ a recoverable global ischemia model. This can be modelled using the four-vessel occlusion model, which involves transient occlusion of both vertebral and common carotid arteries to achieve uniform ischemic stress on the brain (Pulsinelli and Buchan, 1988; Li et al., 2000). Global ischemia can also be modelled by temporarily applying compression to the major cardiac vessels for 2-3 minutes until cardiac arrest occurs (Kawai et al., 1992). Subsequent resuscitation of mice will allow for some recovery and may induce changes in pump isoform expression in the entire central nervous system, including the spinal cord. α -motoneurons in spinal cord slices have been shown to generate strong anoxic depolarization when deprived of oxygen and glucose, and preferentially express Na⁺/K⁺-ATPase α 1 isoform mRNA based on gene data from the Allen Mouse Spinal Cord Bank (Nohda et al., 2007; Lein et al., 2007). Detecting ischemia-induced changes in pump isoform expression may suggest a mechanism underlying the increased resistance of the spinal cord to ischemic injury following ischemic preconditioning, whereby brief, non-

injurious periods of ischemia with subsequent reperfusion reduce neurological deficits and improve survival after spinal cord infarction (Zvara et al., 1999).

To determine if the $\alpha 3$ isoform of the Na^+/K^+ -ATPase truly confers a neuroprotective advantage against ischemic injury, future studies could develop a mouse knock-out model which only expresses the $\alpha 1$ isoform of the Na^+/K^+ -ATPase in neurons. This could also be achieved using an optogenetic approach in which the $\alpha 3$ isoform of the Na^+/K^+ -ATPase is functionally silenced in ischemia-resistant regions of the brain such as the brainstem. Subsequent experiments involving live brain slices under oxygen-glucose deprivation conditions, as well as *in vivo* models of stroke, may reveal an enhanced susceptibility of $\alpha 3$ isoform-dominant neurons and brain regions to ischemic injury.

Since the devastating impact of stroke has a significant impact on protein expression in infarcted regions, a 24 hour time point may not fully reveal all ischemia-relevant changes in Na^+/K^+ -ATPase alpha isoform expression. Therefore, the next phase of this study should sample infarcted tissue at all recovery time points which are relevant to spreading depolarization. Peri-infarct depolarizations (PIDs) in the penumbra recur over the hours and days following a stroke, thus investigating alpha isoform expression as early as six hours and as late as one week after ischemia-reperfusion is instrumental to documenting the time course of changes in Na^+/K^+ -ATPase isoform expression (Fabricius et al., 2005; Dohmen et al, 2008). Additional support for the Na^+/K^+ -ATPase alpha isoform theory of selective vulnerability to anoxic depolarization would allow further exploration of Na^+/K^+ -ATPase-related targets for molecular therapies that may promote neuronal survival and increase functional recovery after stroke.

Chapter 5

Conclusion

Stroke remains among the most challenging of human neurological diseases, due to limited therapeutic options and a narrow treatment window. Research investigating selective neuronal vulnerability to ischemic injury has focused predominantly on secondary ischemic injury mechanisms, with little focus on the divergent sensitivity of different brain regions to anoxic depolarization.

Failure of the Na⁺/K⁺-ATPase initiates anoxic depolarization in higher brain neurons, whereas brainstem neurons are intrinsically more resilient. This study proposes that differential regional expression of the Na⁺/K⁺-ATPase α 1 and α 3 isoforms may play a role in this phenomenon, based on evidence that these isoforms differ in efficiency under ischemic conditions. We expected that the α 1 isoform would be preferentially expressed in ischemia-vulnerable brain regions such as the neocortex and cerebellum, while the α 3 isoform would be more greatly expressed in the resilient brainstem. Consistent with this hypothesis, the α 1/ α 3 isoform ratio was found to be highest in the neocortex and cerebellum, and lowest in the brainstem. Interestingly, the hippocampus and striatum exhibited similar levels of both alpha isoforms, which may be due to a heterogeneous pattern of expression as suggested by pilot immunohistochemical studies.

This study proposed that Na⁺/K⁺-ATPase alpha isoform expression may be altered by elevated oxidative stress, chronic unpredictable stress, or ischemic injury. We hypothesized that the α 3 isoform would be upregulated in vulnerable brain regions following metabolic impairment. Compared to controls, no significant changes in Na⁺/K⁺-ATPase alpha isoform expression were detected in either *Aldh2*^{-/-} mice or chronically

stressed mice. However, pilot immunoblotting experiments on rats subjected to ischemia-reperfusion suggested an upregulation in the expression of both alpha isoforms in the infarcted striatum. The findings presented here imply Na⁺/K⁺-ATPase alpha isoform expression may play a role in the differential susceptibility of brain regions to anoxic depolarization, but not oxidative stress.

The encouraging results presented in this study should be replicated to confirm their validity. Future studies should employ a global ischemia model to investigate changes in Na⁺/K⁺-ATPase alpha isoform expression in brain regions not typically implicated in stroke models. Furthermore, protein expression of the Na⁺/K⁺-ATPase should be investigated over the hours and days following stroke to assess all changes during recurring peri-infarct depolarizations. Lastly, immunohistochemical experiments should be used to identify $\alpha 1$ and $\alpha 3$ -dominant regions within brain structures, which would improve immunoblotting experiments and identify targets for electrophysiological recordings. Identifying specific Na⁺/K⁺-ATPase isoform combinations that translate into regional resilience or susceptibility to ischemia would allow for the exploration of Na⁺/K⁺-ATPase related drug targets to promote survival of vulnerable brain regions after stroke.

References

- Abramov, A. Y., Scorziello, A., & Duchen, M. R. (2007). Three distinct mechanisms generate oxygen free radicals in neurons and contribute to cell death during anoxia and reoxygenation. *Journal of Neuroscience*, *27*(5), 1129-1138.
- Adibhatla, R. M., & Hatcher, J. F. (2010). Lipid oxidation and peroxidation in CNS health and disease: from molecular mechanisms to therapeutic opportunities. *Antioxidants & Redox Signaling*, *12*(1), 125-169.
- Arakawa, S., Wright, P. M., Koga, M., Phan, T. G., Reutens, D. C., Lim, I., ... & Zavala, J. (2006). Ischemic thresholds for gray and white matter: a diffusion and perfusion magnetic resonance study. *Stroke*, *37*(5), 1211-1216.
- Bandera, E., Botteri, M., Minelli, C., Sutton, A., Abrams, K. R., & Latronico, N. (2006). Cerebral blood flow threshold of ischemic penumbra and infarct core in acute ischemic stroke: a systematic review. *Stroke*, *37*(5), 1334-1339.
- Beal, C. C. (2010). Gender and stroke symptoms: a review of the current literature. *Journal of Neuroscience Nursing*, *42*(2), 80-87.
- Beal, M. F., Hyman, B. T., & Koroshetz, W. (1993). Do defects in mitochondrial energy metabolism underlie the pathology of neurodegenerative diseases?. *Trends in Neurosciences*, *16*(4), 125-131.
- Bederson, J. B., Pitts, L. H., Tsuji, M., Nishimura, M. C., Davis, R. L., & Bartkowski, H. (1986). Rat middle cerebral artery occlusion: evaluation of the model and development of a neurologic examination. *Stroke*, *17*(3), 472-476.
- Bernaudo, M., Nouvelot, A., MacKenzie, E. T., & Petit, E. (1998). Selective neuronal vulnerability and specific glial reactions in hippocampal and neocortical organotypic cultures submitted to ischemia. *Experimental Neurology*, *150*(1), 30-39.
- Betts, J., Jaros, E., Perry, R. H., Schaefer, A. M., Taylor, R. W., Abdel-All, Z., ... & Turnbull, D. M. (2006). Molecular neuropathology of MELAS: level of heteroplasmy in individual neurones and evidence of extensive vascular involvement. *Neuropathology and Applied Neurobiology*, *32*(4), 359-373.
- Blanco, G. (2005, September). Na, K-ATPase subunit heterogeneity as a mechanism for tissue-specific ion regulation. *Seminars in Nephrology*, *25*(5), 292-303.
- Blanco, G., & Mercer, R. W. (1998). Isozymes of the Na-K-ATPase: heterogeneity in structure, diversity in function. *American Journal of Physiology-Renal Physiology*, *275*(5), 633-650.
- Blanco, G., Sanchez, G., & Mercer, R. W. (1995). Comparison of the enzymic properties of the Na,K-ATPase alpha3beta1 and alpha3beta2 isoenzymes. *Biochemistry*, *34*(31), 9897-9903.

- Boldyrev, A. A. (2000). Na⁺,K⁺-ATPase: 40 years of investigations. *Membrane & Cell Biology*, 13(6), 715.
- Brines, M. L., & Robbins, R. J. (1993). Cell-type specific expression of Na⁺, K⁺-ATPase catalytic subunits in cultured neurons and glia: evidence for polarized distribution in neurons. *Brain Research*, 631(1), 1-11.
- Brisson, C. D., & Andrew, R. D. (2012). A neuronal population in hypothalamus that dramatically resists acute ischemic injury compared to neocortex. *Journal of Neurophysiology*, 108(2), 419-430.
- Brisson, C. D., Lukewich, M. K., & Andrew, R. D. (2013). A distinct boundary between the higher brain's susceptibility to ischemia and the lower brain's resistance. *PLoS One*, 8(11), 79589.
- Cameron, R., Klein, L., Shyjan, A. W., Rakic, P., & Levenson, R. (1994). Neurons and astroglia express distinct subsets of Na,K-ATPase α and β subunits. *Molecular Brain Research*, 21(3-4), 333-343.
- Carpenter, M. B. (1981). Anatomy of the corpus striatum and brain stem integrating systems. *Comprehensive Physiology*.
- Clausen, M. V., Hilbers, F., & Poulsen, H. (2017). The structure and function of the Na, K-ATPase isoforms in health and disease. *Frontiers in Physiology*, 8, 371.
- Chen, Q., Chopp, M., Bodzin, G., & Chen, H. (1993). Temperature modulation of cerebral depolarization during focal cerebral ischemia in rats: correlation with ischemic injury. *Journal of Cerebral Blood Flow & Metabolism*, 13(3), 389-394.
- Chung, C. Y., Seo, H., Sonntag, K. C., Brooks, A., Lin, L., & Isacson, O. (2005). Cell type-specific gene expression of midbrain dopaminergic neurons reveals molecules involved in their vulnerability and protection. *Human Molecular Genetics*, 14(13), 1709-1725.
- Church, A. J., & Andrew, R. D. (2005). Spreading depression expands traumatic injury in neocortical brain slices. *Journal of Neurotrauma*, 22(2), 277-290.
- Ciafaloni, E., Ricci, E., Shanske, S., Moraes, C. T., Silvestri, G., Hirano, M., ... & Martinuzzi, A. (1992). MELAS: clinical features, biochemistry, and molecular genetics. *Annals of Neurology*, 31(4), 391-398.
- Colella, A. D., Chegenii, N., Tea, M. N., Gibbins, I. L., Williams, K. A., & Chataway, T. K. (2012). Comparison of Stain-Free gels with traditional immunoblot loading control methodology. *Analytical Biochemistry*, 430(2), 108-110.
- Crambert, G., Hasler, U., Beggah, A. T., Yu, C., Modyanov, N. N., Horisberger, J. D., ... & Geering, K. (2000). Transport and pharmacological properties of nine different human Na, K-ATPase isozymes. *Journal of Biological Chemistry*, 275(3), 1976-1986.

- Davies, M. L., Kirov, S. A., & Andrew, R. D. (2007). Whole isolated neocortical and hippocampal preparations and their use in imaging studies. *Journal of Neuroscience Methods*, 166(2), 203-216.
- Dawson, V. L., & Dawson, T. M. (1998). Nitric oxide in neurodegeneration. *Progress in Brain Research*, 118, 215-229.
- Del Zoppo, G. J., & Hallenbeck, J. M. (2000). Advances in the vascular pathophysiology of ischemic stroke. *Thrombosis Research*, 98(3), 73-81.
- Dexter, D. T., Carter, C. J., Wells, F. R., Javoy-Agid, F., Agid, Y., Lees, A., ... & Marsden, C. D. (1989). Basal lipid peroxidation in substantia nigra is increased in Parkinson's disease. *Journal of Neurochemistry*, 52(2), 381-389.
- Dobretsov, M., & Stimers, J. R. (2005). Neuronal function and alpha3 isoform of the Na/K-ATPase. *Frontiers in Bioscience*, 10, 2373-2396.
- Dohmen, C., Sakowitz, O. W., Fabricius, M., Bosche, B., Reithmeier, T., Ernestus, R. I., ... & Graf, R. (2008). Spreading depolarizations occur in human ischemic stroke with high incidence. *Annals of Neurology*, 63(6), 720-728.
- Dreier, J. P. (2011). The role of spreading depression, spreading depolarization and spreading ischemia in neurological disease. *Nature Medicine*, 17(4), 439.
- Dreier, J. P., Major, S., Pannek, H. W., Woitzik, J., Scheel, M., Wiesenthal, D., ... & Speckmann, E. J. (2011). Spreading convulsions, spreading depolarization and epileptogenesis in human cerebral cortex. *Brain*, 135(1), 259-275.
- D'Souza, Y., Elharram, A., Soon-Shiong, R., Andrew, R. D., & Bennett, B. M. (2015). Characterization of Aldh2^{-/-} mice as an age-related model of cognitive impairment and Alzheimer's disease. *Molecular brain*, 8(1), 27.
- Duvernoy, H. M. (2005). The human hippocampus: functional anatomy, vascularization and serial sections with MRI. *Springer Science & Business Media*.
- Elharram, A., Czegledy, N. M., Golod, M., Milne, G. L., Pollock, E., Bennett, B. M., & Shchepinov, M. S. (2017). Deuterium-reinforced polyunsaturated fatty acids improve cognition in a mouse model of sporadic Alzheimer's disease. *The FEBS Journal*, 284(23), 4083-4095.
- Fabricius, M., Fuhr, S., Bhatia, R., Boutelle, M., Hashemi, P., Strong, A. J., & Lauritzen, M. (2005). Cortical spreading depression and peri-infarct depolarization in acutely injured human cerebral cortex. *Brain*, 129(3), 778-790.
- Farooq, R. K., Isingrini, E., Tanti, A., Le Guisquet, A. M., Arlicot, N., Minier, F., ... & Camus, V. (2012). Is unpredictable chronic mild stress (UCMS) a reliable model to study depression-induced neuroinflammation?. *Behavioural Brain Research*, 231(1), 130-137.

- Gadsby, D. C., Bezanilla, F., Rakowski, R. F., De Weer, P., & Holmgren, M. (2012). The dynamic relationships between the three events that release individual Na⁺ ions from the Na⁺/K⁺-ATPase. *Nature Communications*, 3, 669.
- Gilda, J. E., & Gomes, A. V. (2015). Western blotting using in-gel protein labeling as a normalization control: stain-free technology. *Proteomic Profiling: Methods and Protocols*, 381-391.
- Gottron, M. A., & Lo, D. C. (2010). The Na⁺/K⁺-ATPase as a Drug Target for Ischemic Stroke. *New Strategies in Stroke Intervention*, 129-151.
- Hacke, W., Kaste, M., Bluhmki, E., Brozman, M., Dávalos, A., Guidetti, D., ... & Schneider, D. (2008). Thrombolysis with alteplase 3 to 4.5 hours after acute ischemic stroke. *New England Journal of Medicine*, 359(13), 1317-1329.
- Hartings, J. A., Shuttleworth, C. W., Kirov, S. A., Ayata, C., Hinzman, J. M., Foreman, B., ... & Dahlem, M. A. (2017). The continuum of spreading depolarizations in acute cortical lesion development: examining Leão's legacy. *Journal of Cerebral Blood Flow & Metabolism*, 37(5), 1571-1594.
- Hashimoto, Y., Nakayama, T., Futamura, A., Omura, M., Nakarai, H., & Nakahara, K. (2002). Relationship between genetic polymorphisms of alcohol-metabolizing enzymes and changes in risk factors for coronary heart disease associated with alcohol consumption. *Clinical Chemistry*, 48(7), 1043-1048.
- Hinzman, J. M., Andaluz, N., Shutter, L. A., Okonkwo, D. O., Pahl, C., Strong, A. J., ... & Hartings, J. A. (2014). Inverse neurovascular coupling to cortical spreading depolarizations in severe brain trauma. *Brain*, 137(11), 2960-2972.
- Holm, T. H., & Lykke-Hartmann, K. (2016). Insights into the pathology of the $\alpha 3$ Na⁺/K⁺-ATPase ion pump in neurological disorders; lessons from animal models. *Frontiers in Physiology*, 7, 209.
- Intercollegiate Stroke Working Party (2012). National clinical guideline for stroke, 4th edition. *London: Royal College of Physicians*.
- Isse, T., Oyama, T., Kitagawa, K., Matsuno, K., Matsumoto, A., Yoshida, A., ... & Kawamoto, T. (2002). Diminished alcohol preference in transgenic mice lacking aldehyde dehydrogenase activity. *Pharmacogenetics and Genomics*, 12(8), 621-626.
- Jarvis, C. R., Anderson, T. R., & Andrew, R. D. (2001). Anoxic depolarization mediates acute damage independent of glutamate in neocortical brain slices. *Cerebral Cortex*, 11(3), 249-259.
- Ji, C., Rouzer, C. A., Marnett, L. J., & Pietenpol, J. A. (1998). Induction of cell cycle arrest by the endogenous product of lipid peroxidation, malondialdehyde. *Carcinogenesis*, 19(7), 1275-1283.

- Jiang, C. H. U. N., & Haddad, G. G. (1992). Differential responses of neocortical neurons to glucose and/or O₂ deprivation in the human and rat. *Journal of Neurophysiology*, 68(6), 2165-2173.
- Johnston, S. C. (2002). Transient ischemic attack. *New England Journal of Medicine*, 347(21), 1687-1692.
- Kawahara, N., Ruetzler, C. A., & Klatzo, I. (1995). Protective effect of spreading depression against neuronal damage following cardiac arrest cerebral ischaemia. *Neurological Research*, 17(1), 9-16.
- Kawai, K., Nitecka, L., Ruetzler, C. A., Nagashima, G., Joó, F., Mies, G., ... & Klatzo, I. (1992). Global cerebral ischemia associated with cardiac arrest in the rat: I. Dynamics of early neuronal changes. *Journal of Cerebral Blood Flow & Metabolism*, 12(2), 238-249.
- Kim, S. Y., Marx, K. A., & Wu, C. H. (1995). Involvement of the Na, K-ATPase in the induction of ion channels by palytoxin. *Naunyn-Schmiedeberg's Archives of Pharmacology*, 351(5), 542.
- Kitagawa, K., Kawamoto, T., Kunugita, N., Tsukiyama, T., Okamoto, K., Yoshida, A., ... & Nakayama, K. I. (2000). Aldehyde dehydrogenase (ALDH) 2 associates with oxidation of methoxyacetaldehyde; in vitro analysis with liver subcellular fraction derived from human and Aldh2 gene targeting mouse. *FEBS Letters*, 476(3), 306-311.
- Klann, E. (1998). Cell-permeable scavengers of superoxide prevent long-term potentiation in hippocampal area CA1. *Journal of Neurophysiology*, 80(1), 452-457.
- Kobayashi, S., Harris, V. A., & Welsh, F. A. (1995). Spreading depression induces tolerance of cortical neurons to ischemia in rat brain. *Journal of Cerebral Blood Flow & Metabolism*, 15(5), 7
- Kruman, I. I., & Mattson, M. P. (1999). Pivotal role of mitochondrial calcium uptake in neural cell apoptosis and necrosis. *Journal of Neurochemistry*, 72(2), 529-540.
- Lakhan, S. E., Kirchgessner, A., Tepper, D., & Aidan, L. (2013). Matrix metalloproteinases and blood-brain barrier disruption in acute ischemic stroke. *Frontiers in Neurology*, 4, 32.
- Leão, A. A. (1944). Spreading depression of activity in the cerebral cortex. *Journal of Neurophysiology*, 7(6), 359-390.
- Lee, K. W., Kim, J. B., Seo, J. S., Kim, T. K., Im, J. Y., Baek, I. S., ... & Han, P. L. (2009). Behavioral stress accelerates plaque pathogenesis in the brain of Tg2576 mice via generation of metabolic oxidative stress. *Journal of Neurochemistry*, 108(1), 165-175.
- Lee, W. C., Wong, H. Y., Chai, Y. Y., Shi, C. W., Amino, N., Kikuchi, S., & Huang, S. H. (2012). Lipid peroxidation dysregulation in ischemic stroke: plasma 4-HNE as a potential biomarker?. *Biochemical and Biophysical Research Communications*, 425(4), 842-847.

- Lein, E. S., Hawrylycz, M. J., Ao, N., Ayres, M., Bensinger, A., Bernard, A., ... & Chen, L. (2007). Genome-wide atlas of gene expression in the adult mouse brain. *Nature*, *445*(7124), 168-176.
- Li, J., Takeda, Y., & Hirakawa, M. (2000). Threshold of ischemic depolarization for neuronal injury following four-vessel occlusion in the rat cortex. *Journal of Neurosurgical Anesthesiology*, *12*(3), 247-254.
- Liu, S., Shi, H., Liu, W., Furuichi, T., Timmins, G. S., & Liu, K. J. (2004). Interstitial pO₂ in ischemic penumbra and core are differentially affected following transient focal cerebral ischemia in rats. *Journal of Cerebral Blood Flow & Metabolism*, *24*(3), 343-349.
- Liu, Y., Fiskum, G., & Schubert, D. (2002). Generation of reactive oxygen species by the mitochondrial electron transport chain. *Journal of Neurochemistry*, *80*(5), 780-787.
- Longa, E. Z., Weinstein, P. R., Carlson, S., & Cummins, R. (1989). Reversible middle cerebral artery occlusion without craniectomy in rats. *Stroke*, *20*(1), 84-91.
- Maas, M. B., Safdieh, J., & Maas, M. B. (2009). Ischemic Stroke: Pathophysiology and Principles of Stroke Localization. *Neurology*, *13*(1), 1.
- Madrigal, J. L., Olivenza, R., Moro, M. A., Lizasoain, I., Lorenzo, P., Rodrigo, J., & Leza, J. C. (2001). Glutathione depletion, lipid peroxidation and mitochondrial dysfunction are induced by chronic stress in rat brain. *Neuropsychopharmacology*, *24*(4), 420-429.
- Mattiasson, G., Shamloo, M., Gido, G., Mathi, K., Tomasevic, G., Yi, S., ... & Nikolich, K. (2003). Uncoupling protein-2 prevents neuronal death and diminishes brain dysfunction after stroke and brain trauma. *Nature Medicine*, *9*(8), 1062.
- Montagna, P., Gallassi, R., Medori, R., Govoni, E., Zeviani, M., Di Mauro, S., ... & Andermann, F. (1988). MELAS syndrome Characteristic migrainous and epileptic features and maternal transmission. *Neurology*, *38*(5), 751-751.
- Monteiro, S., Roque, S., de Sá-Calçada, D., Sousa, N., Correia-Neves, M., & Cerqueira, J. J. (2015). An efficient chronic unpredictable stress protocol to induce stress-related responses in C57BL/6 mice. *Frontiers in Psychiatry*, *6*, 6.
- Mozaffarian, D., Benjamin, E. J., Go, A. S., Arnett, D. K., Blaha, M. J., Cushman, M., ... & Howard, V. J. (2016). Heart disease and stroke statistics—2016 update: a report from the American Heart Association. *Circulation*, *133*(4), e38-e360.
- Munzer, J. S., Daly, S. E., Jewell-Motz, E. A., Lingrel, J. B., & Blostein, R. (1994). Tissue- and isoform-specific kinetic behavior of the Na, K-ATPase. *Journal of Biological Chemistry*, *269*(24), 16668-16676.
- Nanetti, L., Raffaelli, F., Vignini, A., Perozzi, C., Silvestrini, M., Bartolini, M., ... & Mazzanti, L. (2011). Oxidative stress in ischaemic stroke. *European Journal of Clinical Investigation*, *41*(12), 1318-1322.

- Niedernhofer, L. J., Daniels, J. S., Rouzer, C. A., Greene, R. E., & Marnett, L. J. (2003). Malondialdehyde, a product of lipid peroxidation, is mutagenic in human cells. *Journal of Biological Chemistry*, 278(33), 31426-31433.
- Nohda, K., Nakatsuka, T., Takeda, D., Miyazaki, N., Nishi, H., Sonobe, H., & Yoshida, M. (2007). Selective vulnerability to ischemia in the rat spinal cord: a comparison between ventral and dorsal horn neurons. *Spine*, 32(10), 1060-1066.
- Okun, E., Griffioen, K. J., Lathia, J. D., Tang, S. C., Mattson, M. P., & Arumugam, T. V. (2009). Toll-like receptors in neurodegeneration. *Brain Research Reviews*, 59(2), 278-292.
- Ouyang, Y. B., Voloboueva, L. A., Xu, L. J., & Giffard, R. G. (2007). Selective dysfunction of hippocampal CA1 astrocytes contributes to delayed neuronal damage after transient forebrain ischemia. *Journal of Neuroscience*, 27(16), 4253-4260.
- Papadakis, M., Hadley, G., Xilouri, M., Hoyte, L. C., Nagel, S., McMenamin, M. M., ... & Wood, M. J. (2013). Tsc1 (hamartin) confers neuroprotection against ischemia by inducing autophagy. *Nature Medicine*, 19(3), 351.
- Pavlakis, S. G., Phillips, P. C., DiMauro, S., De Vivo, D. C., & Rowland, L. P. (1984). Mitochondrial myopathy, encephalopathy, lactic acidosis, and strokelike episodes: a distinctive clinical syndrome. *Annals of Neurology*, 16(4), 481-488.
- Pulsinelli, W. A., Brierley, J. B., & Plum, F. (1982). Temporal profile of neuronal damage in a model of transient forebrain ischemia. *Annals of Neurology*, 11(5), 491-498.
- Pulsinelli, W. A., & Buchan, A. M. (1988). The four-vessel occlusion rat model: method for complete occlusion of vertebral arteries and control of collateral circulation. *Stroke*, 19(7), 913-914.
- Reivich, M., Kuhl, D., Wolf, A., Greenberg, J., Phelps, M. A., Ido, T., ... & Som, P. (1979). The [¹⁸F] fluorodeoxyglucose method for the measurement of local cerebral glucose utilization in man. *Circulation research*, 44(1), 127-137.
- Rezkalla, S. H., & Kloner, R. A. (2002). No-reflow phenomenon. *Circulation*, 105(5), 656-662.
- Richard, D., Clavel, S., Huang, Q., Sanchis, D., & Ricquier, D. (2001). Uncoupling protein 2 in the brain: distribution and function. *Biochemical Society Transactions*, 29(6), 812.
- Rizzuto, R., Pinton, P., Ferrari, D., Chami, M., Szabadkai, G., Magalhaes, P. J., ... & Pozzan, T. (2003). Calcium and apoptosis: facts and hypotheses. *Oncogene*, 22(53), 8619.
- Rotig, A. D. L. P., Lonlay, P. D., Chretien, D., Foury, F., Koenig, M., Sidi, D., ... & Rustin, P. (1997). Aconitase and mitochondrial iron-sulphur protein deficiency in Friedreich ataxia. *Nature Genetics*, 17(2), 215-217.
- Sapolsky, R. M., & Pulsinelli, W. A. (1985). Glucocorticoids potentiate ischemic injury to neurons: therapeutic implications. *Science*, 229(4720), 1397-1400.

- Sapolsky, R. M., Krey, L. C., & McEwen, B. S. (1986). The Neuroendocrinology of Stress and Aging: The Glucocorticoid Cascade Hypothesis. *Endocrine Reviews*, 7(3), 284-301.
- Saver, J. L. (2006). Time is brain—quantified. *Stroke*, 37(1), 263-266.
- Schaur, R. J. (2003). Basic aspects of the biochemical reactivity of 4-hydroxynonenal. *Molecular Aspects of Medicine*, 24(4-5), 149-159.
- Schmidt-Kastner, R., & Freund, T. F. (1991). Selective vulnerability of the hippocampus in brain ischemia. *Neuroscience*, 40(3), 599-636.
- Shichita, T., Sugiyama, Y., Ooboshi, H., Sugimori, H., Nakagawa, R., Takada, I., ... & Iwakura, Y. (2009). Pivotal role of cerebral interleukin-17-producing $\gamma\delta$ T cells in the delayed phase of ischemic brain injury. *Nature Medicine*, 15(8), 946.
- Sieber, F. E., Palmon, S. C., Traystman, R. J., & Martin, L. J. (1995). Global incomplete cerebral ischemia produces predominantly cortical neuronal injury. *Stroke*, 26(11), 2091-2096.
- Siesjö, B. K., & Siesjö, P. (1996). Mechanisms of secondary brain injury. *European Journal of Anaesthesiology*, 13(3), 247-268.
- Siow, R. C., Ishii, T., & Mann, G. E. (2007). Modulation of antioxidant gene expression by 4-hydroxynonenal: atheroprotective role of the Nrf2/ARE transcription pathway. *Redox Report*, 12(1-2), 11-15.
- Sokoloff, L. (1977). Relation between physiological function and energy metabolism in the central nervous system. *Journal of Neurochemistry*, 29(1), 13-26.
- Stoll, G., Jander, S., & Schroeter, M. (1998). Inflammation and glial responses in ischemic brain lesions. *Progress in Neurobiology*, 56(2), 149-171.
- Tanaka, E., Yamamoto, S., Kudo, Y., Mihara, S., & Higashi, H. (1997). Mechanisms underlying the rapid depolarization produced by deprivation of oxygen and glucose in rat hippocampal CA1 neurons in vitro. *Journal of Neurophysiology*, 78(2), 891-902.
- Testai, F. D., & Gorelick, P. B. (2010). Inherited metabolic disorders and stroke part 1: Fabry disease and mitochondrial myopathy, encephalopathy, lactic acidosis, and strokelike episodes. *Archives of Neurology*, 67(1), 19-24.
- Therien, A. G., Karlish, S. J., & Blostein, R. (1999). Expression and functional role of the γ subunit of the Na, K-ATPase in mammalian cells. *Journal of Biological Chemistry*, 274(18), 12252-12256.
- Thiels, E., Urban, N. N., Gonzalez-Burgos, G. R., Kanterewicz, B. I., Barrionuevo, G., Chu, C. T., ... & Klann, E. (2000). Impairment of long-term potentiation and associative memory in mice that overexpress extracellular superoxide dismutase. *Journal of Neuroscience*, 20(20), 7631-7639.

- Toni, D., Fiorelli, M., Bastianello, S., Sacchetti, M. L., Sette, G., Argentino, C., ... & Bozzao, L. (1996). Hemorrhagic transformation of brain infarct Predictability in the first 5 hours from stroke onset and influence on clinical outcome. *Neurology*, *46*(2), 341-345.
- Tuttolomondo, A., Di Raimondo, D., di Sciacca, R., Pinto, A., & Licata, G. (2008). Inflammatory cytokines in acute ischemic stroke. *Current Pharmaceutical Design*, *14*(33), 3574-3589.
- Wang, X., & Michaelis, E. K. (2010). Selective neuronal vulnerability to oxidative stress in the brain. *Frontiers in Aging Neuroscience*, *2*, 12.
- Wang, X., Pal, R., Chen, X. W., Kumar, K. N., Kim, O. J., & Michaelis, E. K. (2007). Genome-wide transcriptome profiling of region-specific vulnerability to oxidative stress in the hippocampus. *Genomics*, *90*(2), 201-212.
- Wang, Q., Tang, X. N., & Yenari, M. A. (2007). The inflammatory response in stroke. *Journal of Neuroimmunology*, *184*(1), 53-68.
- Wang, J., Wang, H., Hao, P., Xue, L., Wei, S., Zhang, Y., & Chen, Y. (2011). Inhibition of aldehyde dehydrogenase 2 by oxidative stress is associated with cardiac dysfunction in diabetic rats. *Molecular Medicine*, *17*(3), 172.
- Witter, M. P. (2009). Hippocampal formation. *Encyclopedia of Neuroscience*, Springer Berlin Heidelberg. 1840-1845.
- Woodruff, T. M., Thundyil, J., Tang, S. C., Sobey, C. G., Taylor, S. M., & Arumugam, T. V. (2011). Pathophysiology, treatment, and animal and cellular models of human ischemic stroke. *Molecular Neurodegeneration*, *6*(1), 11.
- Wytrzes, L. M., Chatrian, G. E., Shaw, C. M., & Wirch, A. L. (1989). Acute failure of forebrain with sparing of brain-stem function. Electroencephalographic, multimodality evoked potential, and pathologic findings. *Archives of Neurology*, *46*(1), 93.
- Yanamoto, H., Hashimoto, N., Nagata, I., & Kikuchi, H. (1998). Infarct tolerance against temporary focal ischemia following spreading depression in rat brain. *Brain Research*, *784*, 239-249.
- Ying, W., Han, S. K., Miller, J. W., & Swanson, R. A. (1999). Acidosis potentiates oxidative neuronal death by multiple mechanisms. *Journal of Neurochemistry*, *73*(4), 1549-1556.
- Zhang, R., Lahens, N. F., Ballance, H. I., Hughes, M. E., & Hogenesch, J. B. (2014). A circadian gene expression atlas in mammals: implications for biology and medicine. *Proceedings of the National Academy of Sciences*, *111*(45), 16219-16224.
- Zhao, Y., & Wang, C. (2015). Glu504Lys single nucleotide polymorphism of aldehyde dehydrogenase 2 gene and the risk of human diseases. *BioMed Research International*, 2015.
- Zvara, D. A., Colonna, D. M., Deal, D. D., Vernon, J. C., Gowda, M., & Lundell, J. C. (1999). Ischemic preconditioning reduces neurologic injury in a rat model of spinal cord ischemia. *The Annals of Thoracic Surgery*, *68*(3), 874-880.

Appendix

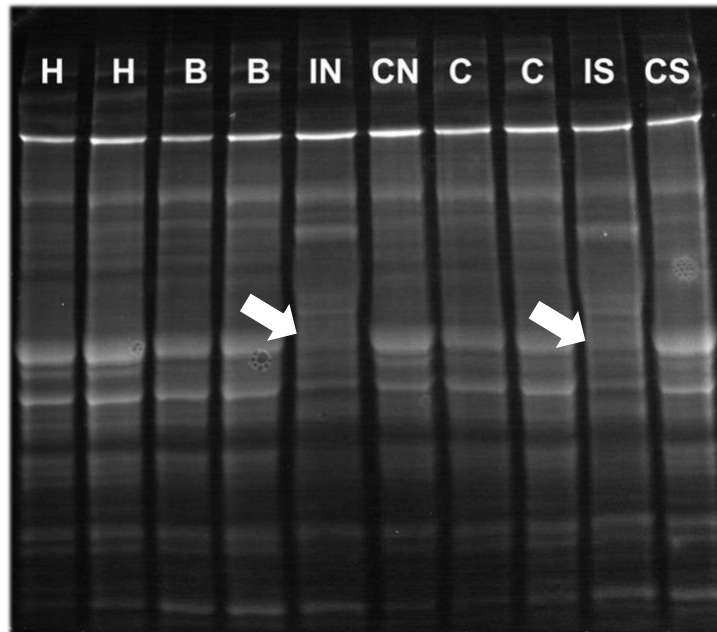


Figure 28. Total protein activation showing loss of distinct bands in infarcted tissue.

Total protein images acquired by UV302 reveal loss of distinct bands of protein in the infarcted neocortex (IN) compared to the control neocortex (CN) as well as the infarcted striatum (IS) compared to the control striatum (CS). This likely represents degradation of proteins by hydrolytic enzymes released from lysosomes following tissue infarction. Non-infarcted brain regions such as the hippocampus (H), brainstem (B), and cerebellum (C) do not exhibit similar loss of protein bands.